NATIONAL ADVISORY COMMITTEE FOR AERONAUTICS

TECHNICAL NOTE 3381

HEAT-LOSS CHARACTERISTICS OF HOT-WIRE ANEMOMETERS AT VARIOUS DENSITIES IN TRANSONIC AND SUPERSONIC FLOW

By W. G. Spangenberg

National Bureau of Standards

Washington
May 1955

1M

NATIONAL ADVISORY COMMITTEE FOR AERONAUTICS

TECHNICAL NOTE 3381

HEAT-LOSS CHARACTERISTICS OF HOT-WIRE ANEMOMETERS AT VARIOUS DENSITIES IN TRANSONIC AND SUPERSONIC FLOW

By W. G. Spangenberg

SUMMARY

An experimental investigation was made of the heat-loss characteristics of heated fine wires suitable for use as anemometers in turbulence research. Speeds ranged from low subsonic to Mach number 1.9. Density and temperature loading were varied over wide limits, and wire diameters ranged from 0.00005 to 0.0015 inch. The effects of each of the several variables on the heat-loss characteristics of both normally oriented and swept wires were measured. The characteristics were found to depend on Reynolds number, Mach number, temperature loading, and the ratio of wire diameter to the molecular mean free path of the air. Dependence on the last caused marked departures from King's law, even at low speeds. Mach number effects were found to be larger in the subsonic than in the supersonic range. Temperature-loading effects were found to cause large sensitivity differences between constant-temperature and constant-current operation. Possible applications of these instruments, utilizing the displayed characteristics to measure the contributions of each of the various fluctuating quantities contributing to turbulence in compressible flow, are discussed.

INTRODUCTION

Recent applications of hot-wire anemometers at supersonic speeds have shown that the hot-wire promises to be a useful tool at high speeds as well as at low speeds. It is too early to predict whether the hot-wire in the hands of a competent experimenter will contribute the same information about turbulence in high-speed flow as it has at low speeds. There is, of course, an urgent need for such information, especially since the phenomena associated with turbulence are considerably more complicated in compressible flow than they are at low speeds.

At low speeds velocity fluctuations and their characteristics are alone sufficient to define turbulence. At high speeds, by virtue of the

fact that compressibility cannot be neglected, densities and temperatures fluctuate along with the velocity. In high-speed wind tunnels large amounts of power are expended, and temperature fluctuations may be disproportionately high. These, while not uniquely related to turbulence, are associated phenomena contributing to the composite effect of fluctuations on aerodynamic phenomena, such as transition in boundary layers. Because of these factors much more is demanded of the hot-wire at high speeds than at low speeds.

The hot-wire produces a signal in response to fluctuations only in proportion to its temperature change. This in turn rests on its thermal capacity and changes in its rate of cooling when it is employed as an anemometer. In order to respond to the high frequencies associated with turbulent fluctuations the thermal capacity must be exceedingly low, and wire diameters must therefore be small. In fact, one of the major problems is how to make and operate an instrument with the finest possible wire.

The purpose of the present investigation was to make known the heat-loss characteristics of fine wires over the widest possible range of variables. The equipment available permitted the Mach number to be varied from 0.05 to 1.9, the free-stream pressure to be varied from 1/6 atmosphere to $2\frac{1}{2}$ atmospheres, and the stagnation temperature to be varied from 80° to 140° F. Wire diameters ranged from 0.00005 to 0.0015 inch. Most of the wires were run with their axes perpendicular to the wind. A few were run at various angles of inclination in order to find the effect of "sweep" on heat-loss characteristics. While these conditions do not cover all that are likely to be met in practice, they at least fill in the previously existing gap between the subsonic and supersonic regimes.

A thorough coverage of the transonic regime, together with some overlap with previous results, has been made to close the wide gap existing between the well-known low-speed characteristics and certain supersonic characteristics recently found by Kovásznay and Törmarck (ref. 1) and Lowell (ref. 2). A systematic investigation of density effects apart from velocity effects was conducted in view of the fact that the mass-flow dependence given by King's law (ref. 3) appears not to have been checked, even at low speeds. This matter takes on special significance at high speeds where density and velocity fluctuations may coexist. It is also a factor in a calibration procedure introduced early into hot-wire work at supersonic speeds. In the first attempt by the National Bureau of Standards to measure turbulence at supersonic speeds conducted by Schubauer and Klebanoff in 1946 in the Aberdeen Bomb Tunnel, wires were calibrated by varying only the density of the air. The same procedure was repeated by the same investigators in 1947 when more detailed measurements were attempted at Mach number 1.9 in the 9-inch supersonic tunnel of the National Advisory Committee for Aeronautics at Langley

Field. These results were not published because of the lack of information on heat-loss characteristics needed to interpret the observations. This early work did, however, demonstrate that the hot-wire had possibilities and emphasized the desirability of such detailed studies as have since been carried out here and in other laboratories.

This investigation was conducted at NBS under the sponsorship and with the financial assistance of the NACA. The author wishes to acknowledge the active guidance and assistance given by Dr. G. B. Schubauer throughout this investigation. Acknowledgment is also extended to Messrs. J. E. Kelly and K. Tidstrom who assisted in carrying out the experimental program and did much of the detailed processing of data.

SYMBOLS

a, b	constants
c_p	specific heat at constant pressure
d	diameter, cm
H	heat loss from wire
h_m	resistance ratio based on measured values, $\Delta R/R_o$
h_∞	ideal resistance ratio if wire had been infinitely long
i	current, amps
K	thermal conductivity of wire material
k	thermal conductivity of air
l	length, cm
R	resistance, ohms
ΔR	increase in wire resistance caused by ΔT
T	temperature, ^oK
ΔT	temperature difference, $T_w - T_r$
t	temperature, ^oC
V	velocity, cm/sec
M	Mach number

Nu	Nusselt number
Nu_m	Nusselt number as measured without wire end-loss corrections
Nu_∞	Nusselt number with wire end-loss corrections applied
Pr	Prandtl number
Re	Reynolds number
α	first-order resistivity coefficient
β	second-order resistivity coefficient
γ	ratio of specific heats
Δ	difference
θ	angle measured from stream axis, deg
λ	molecular mean free path, cm
μ	viscosity, poises
ρ	density, gm/cm^3
$\sigma = h_m/h_\infty$	
Subscripts:	
o	at 0° C
1,2,3...n	various temperature loadings
a	average or mean condition; in particular, average between free-stream temperature and that behind a normal shock
m	measured value without correction for end losses
r	recovery, refers to temperature indicated by unheated wire immersed in free stream
s	stagnation
w	wire
II	computed condition behind normal shock
∞	based on infinitely long wire

If no subscript, free-stream conditions.

TEST APPARATUS AND CALIBRATIONS

Tunnel

The tunnel used for these tests is shown diagrammatically in figure 1 and by the photograph of the test section with wire probe in place in figure 2. The tunnel is of the continuously operating, variable-density type, with a 3- by 4-inch test section. The compressor is driven through step-up gearing with a 400-horsepower induction motor. The stagnation pressure may be varied from $\frac{1}{3}$ atmosphere to $2\frac{1}{2}$ atmospheres, and the stagnation temperature can be regulated at all speeds and pressures from about 80° to 140° F.

The particular nozzle blocks used for the supersonic data were designed for $M = 1.99$, and parallel blocks of short test section to stabilize the flow near sonic speed (spread slightly to compensate for boundary-layer growth) were used for most of the subsonic data. Some subsonic data were, however, run in the throat of the supersonic nozzle blocks.

The subsonic speeds were obtained by a combination of throttling and bypassing the entire tunnel. These speeds were set by means of a reference pressure taken from a wall orifice. These pressure readings were related to the static pressures at the wire position by direct calibration, using a static-pressure tube with a sharp conical tip. Different supersonic speeds were obtained by using various stations on the tunnel axis in the expanding section between the throat and maximum section of the supersonic nozzle. The Mach numbers at the various stations were predetermined with the aid of the special conical-tipped static-pressure probe shown in figure 3.

The calibrations showed that the Mach number variation along the stream center line was a function of the free-stream density. This was apparently caused by a shift of the effective throat location as the boundary-layer thickness changed with density. Separate calibrations were therefore made for each free-stream density. The axial calibration of the supersonic nozzle blocks for a free-stream density of 0.0006 gram per cubic centimeter is shown in figure 4.

The wires were run in the blocks designed for $M = 1.99$ to a speed of only $M = 1.90$ because a shock wave originating on the nozzle walls caused a disturbance at about $M = 1.92$, resulting in a slight discontinuity in the axial Mach number distribution. The condition of the flow in the expanding section of the nozzle where the measurements were made is shown in the schlieren photograph of the flow in the test section with the wire probe in place (fig. 5).

Experimental Requirements

King's formula, which for many years has been used to express the forced convective heat loss from fine wires with axes normal to the wind, is usually written in the form

$$H = \Delta T l \left(ak + b\sqrt{kc_p \rho V d}\right) \qquad (1)$$

where a and b are constants which are usually determined by experiment. In terms of electrical quantities,

$$H = i^2 R$$

and

$$\Delta T = \frac{\Delta R}{R_o \alpha}$$

At low speeds where V is usually the only independent variable, it is customary, for a particular instrument, to express relation (1) in the form of a linear calibration curve obtained by plotting $i^2R/\Delta R$ against $\sqrt{V}$.

When there are more variables involved, it is desirable to express relation (1) in the following nondimensional form

$$\frac{H}{\pi l k \Delta T} = a + b\sqrt{\frac{\rho V d}{\mu} \frac{\mu c_p}{k}} \qquad (2)$$

or, in terms of the symbols for dimensionless quantities,

$$Nu = a + b\sqrt{Re}\sqrt{Pr} \qquad (3)$$

The form of equation (3) suggests that Nusselt number depends only on Reynolds number and Prandtl number. However, in compressible flow Mach number must be recognized as an additional flow parameter. Hence a more complete expression, written in functional form, is

$$Nu = f\ (Re, Pr, M) \qquad (4)$$

Relation (4) includes all of the dimensionless parameters that may be anticipated in advance and around which an experimental program would be planned in the absence of additional information. It was known from the work of Kovásznay and Tőrmarck (ref. 1) that H is not exactly proportional to ΔT. In other words, there exists what has come to be

known as a "temperature-loading effect." Thus there is a ΔT parameter, usually expressed as $\Delta T/T_s$, in addition to those in relation (4), requiring some attention.

With regard to the importance of the parameters, it was known that the Prandtl number changes but little within the range of conditions obtainable in the tunnel. There was evidence from reference 1 that little dependence on Mach number was to be expected in the supersonic range. Hence the investigation was begun with the assumption that Reynolds number was probably the important parameter, with the implication that density, velocity, and wire diameter were equivalent physical variables. It soon became evident, however, that density and velocity changes affected the heat loss from the wires in different ways, particularly in subsonic flow. This indicated the presence of a Mach number effect that strangely persisted into the very low subsonic region where compressibility effects were expected to disappear.

Based on these preliminary observations the experiment was designed to vary the free-stream density and velocity and the wire diameter independently over the widest possible range so that the role of each in heat loss could be evaluated. The limitations of the equipment did not permit the velocity to be varied independently of the free-stream temperature; hence the effects of Mach number, free-stream viscosity, and conductivity could not be evaluated independently of velocity. To reduce the number of variables, all data were run at a constant stagnation temperature.

The values of free-stream density, Mach number, viscosity, and conductivity were computed for supersonic flow from the measured stagnation pressure and temperature, assuming isentropic expansion, and for subsonic flow from stagnation pressure, pressure differential between stagnation and test-section conditions, and stagnation temperature.

The pressures and pressure differentials were measured with either vertical or inclined manometers, depending upon their magnitude, and temperature was measured with a mercury-in-glass thermometer with 0.2° C graduations. Wire lengths were measured to the nearest 0.01 millimeter with a traveling microscope. No accurate means were available to measure wire diameters directly because they ranged in size down to about 2 wave lengths of yellow light. The manufacturer's stated diameters were used in the calculations.

The evaluation of the heat loss from wires required the accurate measurement of wire resistance and current. The unheated resistance was found by using a bridge current sufficiently small to avoid heating the wire significantly. The temperature rise ΔT of the heated wire was determined from the resistance change and the temperature coefficient of the metal.

Electrical Instruments

The electrical circuit used to make the current and resistance measurements was of the conventional type commonly used in hot-wire work. A Wheatstone bridge was used for the resistance determinations and a direct-current potentiometer was used to measure the voltage drop across a standard resistor in the bridge circuit for the current determinations. The schematic diagram is shown in figure 6. A sensitive galvanometer ($2\mu V$ per millimeter deflection) was used to balance both the bridge and potentiometer. Since the wires tested were of such a wide range of resistance and their heating currents varied so widely ($0.7 \text{ ohm} < R < 850 \text{ ohms}$ and $0.004 \text{ ampere} < i < 1.4 \text{ amperes}$), the standard resistors were changed in the bridge from time to time to accommodate the particular wire being tested. Resistances and currents were read to four significant figures for all wires, resulting in reading accuracies ranging from 0.1 to 0.01 percent. To obtain sufficiently small bridge current when unheated resistance determinations were being made, a variable resistance of the order of 16,000 ohms was introduced. This resistance was increased until no evidence of heating could be detected with the wire in still air. Sufficient bridge sensitivity remained after this adjustment to detect resistance differences in the fourth significant figure with certainty.

Probe Design and Wires

Several designs of hot-wire probes were tried, ranging from machined steel wedges for supporting the prongs to various plastics. The design finally adopted for the tests was of the form shown in figure 7. This consisted of honed sewing needles 0.018 inch in diameter butt brazed to electrical leads embedded in hard rubber. This type of probe was used because of its ease of fabrication. The spacing of the needles was usually selected to accommodate a wire about 3 millimeters long to minimize the end-loss correction. Holders of this design were sufficiently rigid to withstand the stresses and vibrational forces encountered while running in the transonic-speed region and during the passage of the shock wave while starting and stopping the tunnel. These holders were held by a chuck attached to a three-directional traversing shaft extending forward into the test section from a diamond-shaped strut farther downstream.

The wire materials used were platinum, tungsten, and an alloy of platinum with 10 percent rhodium with diameters ranging from 0.00005 to 0.0015 inch. The largest size was about five times the diameter normally used for turbulence measurements. The larger sizes were introduced at a later stage of the investigation to extend the range of diameter after it became apparent that the smaller diameters were showing a large influence of the slip-flow regime. For example, air at a pressure of 760 millimeters of mercury and 15° C has a molecular mean free path of about

2.5×10^{-6} inch. The smallest wire (0.00005-inch diameter) was only about 5 molecular mean free paths in diameter when operated at a free-stream density of 1/4 atmosphere, and the largest commonly used for turbulence measurements (0.0003-inch diameter) was only about 30 mean free paths in diameter at the same density. At a free-stream density corresponding to $2\frac{1}{2}$ atmospheres this figure reaches 300, which is in the boundary between continuum and slip flow. The 0.0015-inch diameter made it possible to enter the continuum condition.

The values of the temperature coefficient of resistance of samples of each of the several wires used were predetermined with the aid of an electric furnace and a calibrated thermocouple for measuring temperature. It was found that the resistance of none of the wires followed a strictly linear relationship with temperature and also that the value of the resistance coefficient varied from sample to sample. To correct for the slight deviation of the resistance-temperature relationship from a straight line the experimental determinations were fitted to a curve of the type

$$R = R_o\left(1 + \alpha t + \beta t^2\right) \tag{5}$$

The values for α and β used in the computations are shown in table I, along with the handbook value of the unit resistivity for the various wire materials. Since the sensitivity of a given wire in terms of voltage signal produced by a fluctuation in rate of cooling is given approximately by $\alpha\sqrt{R_o}$, it is advantageous to have α and resistivity as high as possible. It will be noted from a comparison of the properties of the several materials that platinum is the superior material in this respect and that tungsten and platinum-rhodium alloy follow in that order.

The data from which the temperature coefficients were derived are shown plotted in figure 8. These curves are representative of several samples of each kind of wire tested. To show the variation for samples from the same spool, figure 8 also includes the temperature-resistance relationship for two presumably identical samples of the 0.0003-inch-diameter platinum wire.

In the case of the platinum-alloy wires containing 10 percent rhodium it was found that R_o, α, β, and consequently R would all change depending on the highest temperature to which the sample was subjected in the oven. This phenomenon is illustrated by the resistance-temperature curve of figure 9, which shows that when starting with a cold wire as received, an α of about 0.0014 is indicated up to a temperature of about 450° to 500° C, at which point the resistance increases at an abnormally high rate with temperature change and continues to do so until the maximum temperature is attained in the oven. Readings taken as the oven

cooled showed higher values for both α and R_o than originally indicated. The magnitude of the change in all samples tested was dependent upon the highest oven temperature reached. The annealing of the wires therefore became of paramount importance. It was found by successive trials that, if the larger wires (0.0001- and 0.00015-inch diameter) were preheated electrically so that their heated resistances were about 2.05 times their resistances at room temperature and then the current was gradually increased over a period ranging from 3 to 5 minutes to increase the resistance to about 2.3 times the original cold resistance, the values of R_o, α, and β would become stabilized up to a furnace temperature of 700° to 750° C. This exact annealing procedure was adopted for all wires of this alloy. Departure from this procedure resulted in unstable wires at the higher temperature loadings and a permanent increase in R_o each time these temperatures were reached. Too rapid an increase of resistance ratio from 2.05 to 2.3 caused them to burn off. High-temperature loadings of the 0.00005-inch-diameter alloy wire could not be attained because of an apparent lack of uniformity along the wire. Observation during the preliminary annealing showed localized heating over lengths of about 0.1 to 0.2 millimeter spaced at 1- to 3-millimeter distances along the wire, with resultant destruction of the wires if they were heated electrically to an average resistance corresponding to a temperature above 400° to 450° C. These wires were therefore not annealed but were heated electrically to the maximum resistance anticipated while under close observation under a microscope to detect localized heating indicated by red glowing in spots along the wire. Those showing such nonuniformity were discarded. Since these wires were not annealed at the same high temperatures as the larger wires, the value of the temperature coefficient was much lower. No great change was noted in the form of the temperature-resistance curve for wires of platinum and tungsten with the oven temperature attained, which was about 400° C for the tungsten and 750° C for the platinum.

In all tests the identical wire was used for all the data shown unless otherwise noted. It was found that the variation in Nusselt number obtained with samples of wire from the same spool was as great as the variation obtained with wires of different materials; that is, two samples from the same spool of tungsten wire may have as great a difference in heat loss as samples of the same diameter of tungsten and platinum. From this observation it was verified that individual wires need individual calibrations. No general calibration will describe all samples.

Most of the wires were run with their axes normal to the wind. Some wires with their axes at an angle to the stream were, however, included. In the initial stages of the investigation it was found that wires normal to the wind would not withstand the wind loadings to which they were subjected if they were applied too taut on the needles. Computations showed that if a catenary shape (uniformly loaded cable) was assumed for the wire, a sag of from 0.2 to 0.3 millimeter was necessary in a 3-millimeter length to keep the unit stress to a resonable value. All normally oriented wires

were therefore applied so that when loaded they had a sag of about this magnitude. The sag of course depended on the length of the wire, becoming almost imperceptible for wires 1 millimeter in length. The wires placed slantwise to the wind were run taut because of the reduced wind loading resulting from their smaller projected area. In addition to this structural detail, great care was taken in starting and stopping the tunnel because of the violent action of the shock wave passing over the wire. This action did not adversely affect the stronger wires when the stagnation density was atmospheric or below. For wires of less than 0.00015-inch diameter, the tunnel was evacuated to about 1/2-atmosphere stagnation pressure for the starting and stopping operation. No particular precaution was taken with the angled wires.

The question of "strain-gage effect" (an increase in resistance with wind loading) was also investigated. It was observed that when the wires were stressed by wind loading to such a point that any strain-gage effect was observed they either failed in tension or they were so stretched that a permanent increase was shown in their cold resistance. During these tests no wire withstood a wind loading sufficient to show strain-gage effect without permanent distortion.

The presence of dirt or dust in the tunnel caused numerous wire failures. Even the dust entering from the room when the test section was opened for an appreciable time would cause trouble. Precautions were therefore taken to prevent any dust from entering the tunnel, first by successive filtering of all air which was added to the tunnel and second by leaving the test section open only long enough to change the instruments. With these precautions the wires could be run over a period of weeks without failure. For example, two wires were each run over a period covering about 2 weeks at speeds up to $M = 1.05$, after which they were removed from the tunnel and stored in a dessicator for several months and then replaced in the tunnel and run for another week at supersonic speeds. Only a slight change in cold resistance (about 2 percent) occurred over this period. One of these wires was tungsten loaded to a mean temperature in excess of 400° C, and the other was 0.0003-inch-diameter platinum.

It was further found that the tensile strength of the platinum and platinum-rhodium-alloy wires decreased so rapidly with temperature loading that the maximum temperature had to be limited in order for them to withstand the higher wind speeds. The highest average temperature to which the wires could be loaded was also a function of the wire length and wire diameter. Since the temperature at the center of a short wire is greater than that for a long wire at the same mean temperature, the short wires could not be loaded to the same mean temperatures without failure due to loss of strength. The maximum average temperatures and wind loads to which the various wires were subjected are shown in table II. The maximum dynamic pressure attainable in the tunnel was

887 grams per square centimeter which occurred at a Mach number of 1.25 with a free-stream density of 0.0012 gram per cubic centimeter. Those wires loaded to this value may have withstood even greater wind loadings.

In the case of the tungsten wire, failure due to loss of strength with temperature was not a factor. If these wires are heated much above these maximum values observed, rapid deterioration due to oxidation of the wires results, causing a large increase in the cold resistance. Data concerning the oxidation of tungsten wires at the higher temperature loadings are included in reference 2. No deterioration attributable to oxidation was observed in any of the samples of platinum or platinum-alloy wire containing 10 percent rhodium tested.

All the platinum and platinum-rhodium-alloy wires were attached to the probes with soft solder, with the exception of the 0.0015-inch-diameter platinum wire. At the maximum temperature loading for this wire, the heat loss to the needles was sufficient to melt the soft solder. This wire was therefore electric-arc welded to the probe.

Various methods of attaching tungsten wires to the probes were tried. Some samples were copper plated at the ends and soft soldered as described in reference 4. A "strike" nickel plating was applied to the ends of others to permit soldering to the prongs. The results from nickel plating compared favorably with those from the copper plating. The method of attachment found the most suitable for producing stable and strong connections was a simple electric-arc welding technique, which is illustrated schematically in figure 10. The process consists of applying the wire at the point of the needle, then striking it with the electrode. Welding electrodes of various diameters and of different materials were tried, including copper, platinum, iron, and silver. The silver or copper electrodes of small diameter (0.005 inch) proved the most satisfactory. Since the wires were applied manually, expert manipulation of the electrode was essential. No flux was used for the process. Microscopic examination of the welds showed that material had been transferred from the electrode to the needle to embed the wire. These welded wires were exceptionally stable over long periods. The wires were not annealed after welding, and there was some indication of embrittlement of the 0.00015-inch-diameter wire near the welded ends. Furnace annealing in an inert atmosphere may prove beneficial to eliminate possible embrittlement.

Test Procedure

The preparation of a wire sample consisted of mounting it on a holder like that shown in figure 7, annealing it (if not tungsten), and then exposing it to extreme wind loading at maximum temperature loading. The last of these produced many wire casualties and was done deliberately to eliminate defective wires before effort was expended on detailed measurements.

The temperature loading ΔT and stagnation temperature to be maintained during a run were adjusted with the tunnel in operation with air dried to a dew point below about -30° F. It will be noted that a constant ΔR was maintained on the wires which corresponded to a nearly constant temperature-loading operation rather than constant-temperature operation. In this case the wire temperature decreased with increasing Mach number because of the decrease of T_r as shown in figure 11. The stagnation temperature was usually 30° C and was held constant to $\pm 1/2^{\circ}$ C by manual adjustment of the tunnel cooling water. For selected free-stream densities, series of observations of i, R, and R_r were made at the various wire positions in the supersonic nozzle corresponding to the fixed Mach numbers determined by the static-pressure calibration of the nozzle. The stagnation pressure was adjusted to keep the free-stream density the same at each position. Since the stream temperature varied with Mach number, its value was computed, assuming isentropic expansion with $\gamma = 1.4$, in order to ascertain the values of μ and k for the free stream.

While it was possible to pass nearly continuously to subsonic speeds with the supersonic nozzle by moving the wire upstream through the throat, this was not attempted. All the subsonic work was done either with subsonic nozzle blocks or in the throat of the supersonic nozzle. The subsonic speeds were varied by throttling the tunnel.

End-Loss Corrections

In all cases there exists an unavoidable flow of heat from a wire to the supports. The amount lost in this way becomes a larger proportion of the total as the wire is made shorter or its diameter is increased. Ordinarily this is not objectionable, but in comparing the performance of wires of different diameter it is an extraneous effect tending to confuse the points at issue. For the present purposes corrections were applied which removed this effect and yielded values of Nusselt number corresponding to infinitely long wires.

Since no means were available to obtain the temperature attained by the supporting needles, the end-loss corrections were based on the assumption that the needles attained the same temperature in the air stream as the unheated wire; that is, the temperature-recovery ratio was the same for both the wire and its support. This also involved the assumption that the support was not heated by the flow of heat from the wire. Because of the uncertainty arising from this approximation and because the end-loss corrections were of such small magnitude, it was assumed that the linear corrections (assuming heat loss proportional to temperature difference) as proposed by King (ref. 3) were adequate. The more complicated nonlinear corrections worked out by Betchov (ref. 5) were not considered necessary.

The linear corrections of King were put in a nondimensional form by Kovásznay and Törmarck (ref. 1) who proposed the following relationships which were used in these computations:

$$Nu_\infty/Nu_m = F = \left(\sigma + h_m\right)\Big/\left(1 + h_m\right) \tag{6}$$

The quantity σ can be determined from the transcendental equation

$$\sigma = 1 - (S/\sqrt{\sigma}) \tanh (\sqrt{\sigma}/S) \tag{7}$$

in which

$$S = (d/l)\sqrt{(1 + h_m)K/Nu_o k_o} \tag{8}$$

and

$$h_m = \Delta R/R_o = \Delta T\left[\alpha + \beta\left(t_w + t_r\right)\right] \tag{9}$$

The handbook values of K used in equation (8) were corrected for the heated wire temperature (ref. 6).

Three graphical determinations were made in the processing of the data to apply these end-loss corrections. First, S was determined from a logarithmic plot of $S = f\left(Nu_o\right)$ described by equation (8); second, the value of σ was read from a graph of the transcendental equation (7); and, third, the Nusselt number ratio described by equation (6) was read from the straight-line function $F = f(\sigma)$. All other computations were made numerically.

The minimum Nusselt number ratios (maximum end-loss corrections) occurred at the lower temperature loadings and lower Nusselt numbers. The variations of the end-loss corrections with temperature and Nusselt number are shown graphically in figure 12.

In making the computations, Nu_{om} was first determined by using the expression

$$Nu_{om} = 0.2389\ i^2R/\pi l k_o \Delta T \tag{10}$$

where 0.2389 is used to convert watts to calories per second to make the variables dimensionally consistent. This quantity Nu_{om} was necessary for the end-loss corrections as applied. After the measured values of the Nusselt numbers based on free-stream conditions were determined by multiplying equation (10) by the factor k_o/k, the correction factor F was applied to yield the corrected Nusselt numbers shown in the data presented.

RESULTS FOR WIRES NORMAL TO WIND

As mentioned in the section entitled "Experimental Requirements," it appears to be desirable in the face of numerous variables to take advantage of dimensionless groupings of physical variables. This also appears to be the best way to generalize hot-wire behavior and show in a broad way the possibilities for applications.

At first hand it appears that the observations should be used to show the functional relations between the parameters in equation (4). This in fact will be done, but there is a need for first discovering whether there are sufficient parameters. Furthermore there is a certain arbitrariness in connection with the choice of μ and k. For these reasons the results are presented first in the more elementary form showing as far as possible the dependence of Nusselt number on the more elementary variables. These turn out to be the Mach number and density of the stream and the diameter of the wire. This will introduce the new, and physically significant, parameter d/λ. Later the Reynolds number will be introduced along with a discussion of the basis for evaluating μ and k. Following this, the effect of temperature loading will be treated.

Since the Prandtl number appearing in equations (3) and (4) could not be varied independently, and since it changed relatively little and only with Mach number under the conditions of the experiment, it was decided to allow such effects as might be present to be combined with effects of Mach number. For a fixed stagnation temperature of 30° C the Prandtl number ranges from 0.748 at zero speed to 0.707 at a Mach number of 1.9 - a change of about 6 percent.

It did not appear desirable to eliminate a parameter containing viscosity by forming the Peclet number, which results from the product of Reynolds number and Prandtl number. This of course leads to some disadvantage in checking a theory such as Tchen's (ref. 7) in which Peclet number is used. Actually Reynolds number is a fair substitute for Peclet number, except for numerical value.

Temperature Recovery

When a wire is subjected to the impact of a high-speed stream, it attains a temperature above that of the free stream because of aerodynamic heating. This is termed the recovery temperature and denoted by T_r. The recovery temperatures observed for various wire samples are shown together with other published data in figure 11 in terms of T_r/T_s as a function of Mach number. No consistent change in T_r was observed with d or ρ, which implies that T_r is independent of Reynolds number. A slight variation of T_r (about 5° C maximum) was observed among the various wire samples.

Since it is obvious that the wire can lose heat to the stream only when heat is added to raise its temperature above T_r, the temperature loading ΔT was taken to be $T_w - T_r$. A reasonable assumption, as indicated by formula (1), is that the rate of heat loss is directly proportional to ΔT. Actually this is not the case, and the departures are treated separately in some detail in the section entitled "Effect of Temperature Loading."

In the plotted curves discussed in the next two sections all data are based on the lowest temperature loading at which the wires were tested. This was a ΔT of approximately 67° C which corresponds to a temperature-loading ratio $\Delta T/T_s$ of about 0.22.

Dependence of Heat Loss on Mach Number, Density, and Wire Diameter

An examination of the data from all of the wires tested showed that of the three principal parameters, M, ρ, and d, the wires responded differently to changes in M from the way they did to changes in ρ or d. This was the case even at low speeds where a dependence on M amounted to dependence on V. The response to change in ρ, however, was identical to the response to change in d within the limits of the repeatability of the measurements. These facts made it apparent that the ρd product played a separate role apart from being a constituent of Reynolds number. The most natural dimensionless parameter derivable from ρd was d/λ. The conversion involved the assumption, customary in elementary kinetic theory, that $\rho\lambda$ could be regarded as constant. Taking $\lambda = 6.32 \times 10^{-6}$ centimeter at a density corresponding to 760 millimeters of mercury and 15° C (ref. 6), the product becomes 7.748×10^{-9} gram per square centimeter.

It must be made clear that the parameter d/λ was introduced for physical clarity rather than from necessity. The ratio Re/M might have been used instead, since this ratio may be shown to be proportional to d/λ by elementary kinetic theory. It must be pointed out also that the use of either quantity in place of ρd disregards the change of collision cross section of the molecule with temperature. The error really amounts to assuming an idealized λ rather than the true one. Since d/λ is given by

$$\frac{d}{\lambda} = \frac{\rho d}{7.748 \times 10^{-9}}$$

it is exactly proportional to ρd, and in describing effects the two may be used interchangeably.

The dependence of Nu_∞ on M and d/λ is shown in figures 13, 14, 15, and 16. It should be borne in mind that the velocity of sound is so nearly constant for $M < 0.4$ that the independent variable here becomes V. The temperature-loading ratio $\Delta T/T_s$ is constant throughout.

Figure 13 shows the variation of Nu_∞ with Mach number for various chosen values of d/λ and figure 14 shows the same data plotted logarithmically. The wire diameters are indicated in the figures. The value of λ is based on the density of the free stream. From figure 13 it can be seen that the slope of the curves is greatest at the low Mach numbers and decreases with increasing Mach number up to the speed of sound, at which point the slope increases abruptly. Complete insensitivity to changes in M is shown over a considerable range for a d/λ of 6.5, but as this parameter increases a greater sensitivity to change in M is shown.

The logarithmic plot (fig. 14) shows that the Nusselt number is not a simple function involving a constant power of M in either the subsonic- or supersonic-speed region. The curves show a point of inflection in the subsonic region and also change from concave downward to concave upward at $M = 1.0$. Plots using velocity as the independent variable, rather than Mach number, do not alter the basic picture shown in these figures.

Figures 15 and 16 show a cross plot of the same data presented in figures 13 and 14. These plots show Nu_∞ as a function of free-stream d/λ with M as curve parameter. Returning now to the interchangeability of d/λ and ρd, the curves of figure 15 indicate that as the Mach number increases the wire becomes more sensitive to changes in density. They show further that the wires are more sensitive to change in density in the low density or small-wire-diameter region, in contrast with the insensitivity to Mach number in the same region.

Since King's law would indicate that the curves of figure 15 would be a family of parabolas, they are replotted in figure 16 as a function of the square root of d/λ with Mach number as a parameter. This plot shows that straight lines result for all wires shown. Other wires tested showed the same characteristics. Only slight variations exist among the various lines describing the several wires of different diameters. These variations are of the same order of magnitude as those shown from presumably identical samples of the same wire and so may be attributed to sample variation. The slopes of these lines increase with increasing Mach number as would be expected by King's law; but, contrary to King's law, their intercepts decrease. This combination of decreasing intercept with increasing slope results in a nearly common point of intersection for all subsonic lines and a second nearly common intersecting point for the lines of constant supersonic Mach numbers. These points of intersection appear in all cases in the first quadrant, that is, where both Nu_∞ and d/λ are positive.

It is noted that, in considering only the subsonic portion of the curves of figure 14, the slope does not approach 1/2 as indicated by King's law. For example, at the lower Mach numbers with a density near that for atmospheric pressure, the slopes of the lines of figure 14 vary from 0.3 to 0.4, depending upon the wire diameter and density. This shows that Nusselt number varies at one rate with Mach number and at another with density, even at velocities as low as about 50 feet per second. This discrepancy continues throughout the entire velocity range to $M = 1.9$. In the supersonic region the slopes are approximately unity.

Effect of Reynolds Number

One of the most troublesome features of compressible flow concerns the choice of conditions at which the physical properties of the air surrounding the wire are to be evaluated.

It is to be noted that the figures discussed in the section entitled "Dependence of Heat Loss on Mach Number, Density, and Wire Diameter" show the measured data when the conductivity factor of the Nusselt number is based on the free-stream temperature. If, rather than free stream, other conditions had been assumed for the ambient air, different characteristics and sensitivities of the wires to changes in Mach number and density would have been indicated. These differences will become more obvious in the present section where the effects of Reynolds number on heat-loss characteristics are to be illustrated.

Some investigators have suggested that the stream properties should be evaluated at some mean film temperature between the recovery temperature and heated-wire temperature, or between the temperature of the heated wire and the free stream. Any such average must be arbitrary because the temperature field around the wire is unknown. Trial computations based upon air properties evaluated at various mean temperatures between those of the heated wire and the air failed to clarify the test data. No virtue was exhibited by any manipulation involving the heated-wire temperature. From these trials it was concluded that at the velocities encountered in these tests the thermal boundary layer around the wire was so thin that the viscosity and conductivity of the air within this layer did not control the heat losses to any great extent.

Other possible conditions upon which the physical properties of the stream may be evaluated would be either stagnation or free-stream conditions, or the condition T_r indicated by the wire itself, which lies between the stagnation and free-stream temperatures. Of these possible conditions, the recovery temperature would exist adjacent to the wire only in its unheated state. With the wire heated, the gradient causing heat flow would be determined by the difference in temperature between the heated wire and the free stream. If the inference is correct that

the thermal layer surrounding the wire is so thin that its conductivity and viscosity have little influence on the heat loss, only the free-stream temperature remains as a definitive condition upon which to base the physical properties of the air. This reasoning can be applied only to subsonic flow. In the supersonic regime, a blunt object such as a wire will create a shock wave behind which the wire will lie. It appears that the condition of the air in the vicinity of the wire would be about the same as that behind a normal shock because that portion of the detached shock wave immediately in front of the wire is approximately normal. If the physical properties of the air are to be evaluated at the ambient conditions outside the thermal layer, it appears that in supersonic flow the condition of the ambient air is that attained by the free stream after having passed through a normal shock.

To illustrate these observations the data for one wire have been plotted using each of the three conditions T, T_s, and T_{II} to evaluate the air properties so that a direct comparison may be made. Figure 17 shows these data. In these plots Nusselt number is shown as a function of Reynolds number with M and d/λ as parameters. It will be noted that, since the mass flow given by ρV is a constant for all cross sections of the stream, viscosity is the only quantity causing the Reynolds number to be different for each of the three assumed conditions. Likewise k, the other quantity defining air properties, is the only factor causing Nusselt number to differ for the three conditions. In addition to these three separate conditions assumed for the ambient air, figure 17 also includes a plot basing the air properties on a fourth condition, to be discussed later, which yields an apparently better correlation of the supersonic data.

In figure 17(a), the conductivity and viscosity are based on free-stream conditions; figure 17(b) shows the same data based on the estimated ambient conditions at the wire; that is, the subsonic data are based on free-stream conditions, and the supersonic data are based on the condition behind a normal shock; and in figure 17(c) the identical data are shown with the physical properties of the air evaluated at stagnation conditions.

By a comparison of these curves it is seen that under no condition is the dependence on any one dimensionless parameter eliminated. In all three cases separate straight lines result for each Mach number as the density varies and separate curved lines describe the variation in Mach number when the density is held constant. These plots show further that the indicated sensitivity of the wire to changes in Mach number or density at a particular Reynolds number depends upon the condition which is selected to evaluate the physical properties of the air.

If these properties are evaluated at stagnation conditions (fig. 17(c)) the wire has approximately equal sensitivity to changes in velocity and density in the supersonic-speed region above $M = 1.25$ because of the smallness of the dependence on Mach number. In the subsonic-speed region there is no such effect, except possibly in a region to be discussed later, where the Mach number is low and d/λ is large. As the speed increases, the slope of the curves with d/λ constant decreases, showing a decreased sensitivity to change in Mach number or velocity. This effect is greatest at the lower values of d/λ, as, for example, at a d/λ of 20 the wires show complete insensitivity to change in velocity at $M = 0.8$ and a negative slope in the region $0.8 < M < 1.0$.

When the air properties are based upon free-stream conditions in the subsonic region (figs. 17(a) and 17(b)), zero and negative slopes do not occur, but a decreasing slope of the constant-density curves with an increasing Mach number persists. At the lowest Mach numbers, the curves are identical to those based on stagnation conditions because the free-stream temperature is essentially stagnation. In the remainder of the subsonic region approximately the same sensitivity to change in density is indicated throughout because the lines of constant Mach number are nearly parallel.

The supersonic data of figure 17(a) show an increasing heat loss with increasing Mach number (holding Re constant), which is just the reverse of the phenomena shown at the subsonic speeds. The plot shows further that, as the Mach number increases above unity, the slopes of the constant Mach number lines also increase.

The supersonic data of figure 17(b), based on the conditions behind a normal shock, show lines of constant Mach number having approximately the same slope as those in the subsonic region, indicating that at a fixed Reynolds number the same dependence on density obtains throughout the entire range of Mach numbers. Separate curves are obtained for different Mach numbers, but there is less dependence on Mach number above $M = 1.5$ than shown in figure 17(a).

The work of Kovásznay and Törmarck (ref. 1) showed that basing μ and k on conditions behind a normal shock (or stagnation which is a near equivalent) virtually eliminated the effect of Mach number in the supersonic range covered in their investigation ($1 < M < 2$ approximately). Accordingly, it might be surmised that compressibility effects merely reflect the effect of temperature on the properties of the air. It is highly significant therefore that the results obtained in the present investigation show that this choice of μ and k reduces but does not eliminate the Mach number effect in the supersonic range and at the same time increases the effect in the subsonic range. It must be concluded therefore that no basic significance can be attributed to this choice

of μ and k and that, lacking further information, the choice may be made a matter of convenience or may be made to conform to the assumed variation of properties in any particular application.

Since it would evidently be advantageous to approximate independence of Mach number, if only in a limited region, it is worth while to see whether this is possible. Obviously nothing can be done in the subsonic region; in fact, basing μ and k on anything but the free-stream condition would appear to be unwarranted. Detailed study of the supersonic data from normal wires showed that μ and k based on a temperature 60 percent of the way from free stream to the temperature behind a normal shock (varying somewhat from sample to sample) resulted in the minimum Mach number effect. This was arbitrarily rounded off to an arithmetic mean of the temperature of the free stream and that behind a normal shock to give the results shown in figure 17(d). It is a matter of some interest, and perhaps of some significance, that the data for swept wires, to be discussed later in the section entitled "Test Results With Swept Wires," fell in line with the data for wires of normal incidence when this convention was adopted.

In figure 18 data are presented for four wires covering the full range of diameter, plotted with subsonic data based on free-stream conditions and supersonic data based on the arithmetic mean of the temperature of the free stream and that behind a normal shock. The particular conditions chosen do not materially affect this figure. The feature to which attention is drawn is the change in the character of the curves with changing d/λ. Each of the four plots in this figure covers the range of d/λ made possible by varying the air density for a wire of a particular diameter, the four different diameters giving a range of d/λ from 6.5 to 590.

Attention should be focused on the difference in the character of the lines of constant Mach number a, b, c, and so forth and the lines of constant d/λ. In figure 18(a) where d/λ is small the two sets of curves have radically different slopes, and the lines of constant d/λ bend over markedly followed by a sharp upturn into the supersonic region as the Reynolds number increases. It will be noted that the bending decreases as d/λ increases. This trend continues as d/λ gets progressively larger in going to parts (b), (c), and (d) of figure 18. At the same time the difference in the slopes of the two sets of lines becomes less and less in the subsonic region and they approach one another at the lower Mach numbers.

While the curvature of the lines of constant d/λ decreases with increasing d/λ, the curvature remains pronounced for $M > 0.4$. Coupled with this is the separation of the two families: M constant and d/λ constant. This is the manner in which Mach number effect manifests itself in the subsonic region. The source of this effect is a stronger

dependence of Nusselt number on density than on velocity. The phenomenon is intimately connected with d/λ, becoming larger as d/λ decreases. For example, when $d/\lambda = 6.5$, the dependence of Nusselt number on velocity becomes small above a Mach number of 0.4 and actually ceases around $M = 0.8$. This is a very significant feature, for it means a vanishing sensitivity to velocity.

Figure 19 is a composite plot of the same data given in figure 18 with the addition of the straight line derived from King's law. The fact that this line does not agree with the observations is unimportant, for the constants are not usually checked by experiment, but it is worth noting in this comparison that a King's law type of behavior is being approached with increasing d/λ and decreasing M. The evidence from this investigation is that departures from linearity and differences in response to density and velocity have existed for the conditions under which most hot-wires have been used in the past but did not become apparent because of the limited range of variables. For example, for atmospheric densities and wire sizes normally used, the departure from linearity is only 5 percent over speeds ranging from near 0 to 200 feet per second. A not uncommon scatter of $\pm 2\frac{1}{2}$ percent is sufficient to mask a departure of this magnitude.

Effect of Temperature Loading

Magnitude and direction of effect.- While King's law states that the rate of heat loss from a heated wire is proportional to its temperature rise, the present investigation and other recent work conducted at high speeds show that deviations occur. In short, Nusselt number is found to depend on the temperature loading.

The temperature loading, given by $T_w - T_r$ and denoted by ΔT, is the temperature rise produced by the heat generated electrically in the wire, this rise being just sufficient to make the rate of heat loss equal to the rate of heat input under the given external conditions. A rate of loss which is other than proportional to the temperature loading must be attributed to some external effect produced by the heating. In reference 1 it is pointed out that the ratio $\Delta T/T_s$ is a good measure of the distortion of the flow around the wire caused by the addition of heat. In reference 7, where the recovery temperature of the wire is assumed to be T_s, the difference $T_w - T_s$ is used as a measure of the perturbation caused by the introduction of heat. Aerodynamic effects associated with heat input to the stream are therefore recognized and probably account for the effects about to be discussed.

Reference 1 reports a decreasing slope of the curve obtained by plotting rate of heat loss against $\Delta T/T_s$ at supersonic speeds. No

dependence of this effect on Mach number or Reynolds number was observed. The theory of reference 7 predicts such an effect at supersonic speeds but the reverse at subsonic speeds. The present measurements show that effects do exist in both the subsonic and supersonic regions but that the magnitude and direction are a function of other variables.

Since the data taken for each wire in this investigation included from three to five different temperature loadings, covering a wide temperature range at each density and speed, sufficient observations were available to show a temperature-loading effect dependent on both M and ρ. As far as could be ascertained the effects of temperature loading were not influenced by Reynolds number. Since, however, the difference in heat loss caused by temperature loading is a second-order effect, a possible influence of Reynolds number may have been masked by the experimental uncertainty associated with scatter and the normal sample variation associated with the different wires. No simple correlation could be found to cover all of the effects observed.

Figure 20 shows the data from a single wire plotted for each of three different temperature loadings, with a ΔT of 67°, 204°, and 511° C, respectively. By reference to this figure it is seen that lines of constant Mach number are always straight when Nusselt number is plotted against Reynolds number, but a different line results for each constant temperature loading. A decrease of Nusselt number results as the temperature loading is increased, except at the lower Mach numbers, where Nusselt number may either increase or decrease with temperature loading depending upon the density.

In the subsonic region the lines of constant Mach number show an increasing slope as the temperature loading increases, indicating a greater sensitivity to change in density at the higher temperatures. Conversely, a decreased sensitivity to change in Mach number is indicated as the temperature loading is increased.

The combination of unit heat loss and slope among the various conditions is such that the $M = 0.05$ lines intersect near the point where the free-stream density is near that for standard atmospheric pressure, so that no change in heat loss with temperature loading at this density and Mach number would be indicated. At lower densities, a decreasing Nusselt number with increased temperature loading is indicated, and at densities above atmospheric increased Nusselt numbers result from increased temperature loadings. Because of the peculiar combination of contributing factors, similar phenomena may occur at other combinations of Mach number and density.

In the supersonic region, a different type of characteristic is indicated. As the temperature loading is increased the Nusselt number decreases, as was the case in the subsonic region for the higher Mach

numbers within the density limits of the tests, but the slopes of the constant Mach number lines decrease as the temperature loading is increased. The change from increasing to decreasing slope with temperature loading apparently occurs near $M = 1$; that is, the lines of constant ΔT are parallel near sonic speed. No combination of factors was encountered in the supersonic region where an increased Nusselt number resulted from increased temperature loading, but an extrapolation of the lines of constant Mach number indicates that this could occur at very low densities.

After various unsuccessful attempts to illustrate the observed phenomena in a simple manner, it was found that the temperature-loading effects could best be shown by a system of nondimensional ratios involving the temperature loading, Mach number, density, and Nusselt number. In this system the Nusselt number corresponding to the lowest temperature loading ($\Delta T = 67^\circ$ C and $\Delta T/T_s = 0.22$) was taken as a standard from which deviations at the higher temperature loadings could be based.

If $Nu_{\Delta T_1}$ denotes Nusselt number measured at the lowest temperature loading, and $Nu_{\Delta T_n}$ denotes that at any temperature loading, the ratio $Nu_{\Delta T_n}/Nu_{\Delta T_1}$ will show the effect of temperature loading. When these ratios are plotted against Mach number with density and $\Delta T/T_s$ as parameters, variations of the ratio with Mach number, density, and $\Delta T/T_s$ will be shown, as in figure 21.

This figure indicates that at the lower Mach numbers the Nusselt numbers may be greater or less than or equal to that at the lowest temperature loading, depending upon M, ρ, and $\Delta T/T_s$. It further shows, in general, that, as M increases, a decrease in $Nu_{\Delta T_n}/Nu_{\Delta T_1}$ results up to $M = 1.0$. The maximum effect of temperature loading always occurs at $M = 1.0$, but the exact value is somewhat indeterminate. For values of M greater than unity, the Mach number effect tends to disappear, but variations with density and $\Delta T/T_s$ persist.

A cross plot of figure 21, with $Nu_{\Delta T_n}/Nu_{\Delta T_1}$ as a function of $\Delta T_n/T_s$, is shown in figure 22 for two different densities. These plots show that at the lower Mach numbers either an increasing or decreasing heat loss may result, depending upon $\Delta T/T_s$, density, and M; hence no general statement may be made describing the exact effect of temperature loading. At the higher Mach numbers ($M > 0.4$) increased temperature loading in general results in a lower Nusselt number at an air density approximating that of a standard atmosphere ($\rho = 0.0012$ gram per cubic centimeter), but here again the rate of decrease is dependent upon M, ρ, and $\Delta T/T_s$. The heat loss may even increase with temperature loading at this Mach number when densities are higher than those shown in the figure. In general, it may be said that the departure of the Nusselt

number ratio from unity is less for the higher densities than for the lower; that is, as the density increases, temperature loading has less effect on Nusselt number. No systematic investigation of effect of wire diameter was made in this connection, but in figure 22 the trend with diameter appears to be similar to that of density, indicating a d/λ dependence. It is pointed out, however, that the second-order resistivity coefficient β enters into these Nusselt number ratios. Any deviation of β from the measured values used in the heat-loss computations will alter the values of the Nusselt number ratios and may cause sufficient dispersion from wire to wire to mask differences attributable to diameter.

Practical aspects of temperature loading.- Because the temperature-loading effect is large under many conditions, it has an important bearing on hot-wire applications. In the measurement of fluctuations the circuit is usually arranged to maintain constant current, and the wire temperature varies as the heat loss fluctuates. There are systems, known as constant-temperature systems, in which a nearly constant wire temperature is maintained by electronic regulation of the current, but these have so far found little application at high speeds because of their relatively high noise level. The temperature-loading effect comes into play in different ways in these two methods of operation.

Figures 23, 24, and 25 were prepared to illustrate the different Nusselt number variations, with constant temperature on the one hand and with constant current on the other. The Nusselt number Nu_{om} is here simply the observed heat loss without end corrections divided by $\pi l k_o \Delta T$, where k_o is a constant thermal conductivity, selected arbitrarily at 0° C. Similarly, Re_o in figure 25 is a Reynolds number based on the viscosity at 0° C. Accordingly, figures 23 and 24 may be regarded as ordinary calibration curves, in one case for density varying and in the other case for Mach number varying.

It will be seen in figure 23 that the character of the curves for a constant i is markedly different from that for a constant ΔT and that this difference depends on the Mach number. As would be expected, the differences are very significant when the Mach number is high. It is obviously not permissible to carry over into high-speed work the practice sometimes followed at low speeds, namely, calibrating at constant ΔT and then maintaining constant current in fluctuation measurements. In short, the wire must be calibrated under the conditions at which it will be used. The effect is not so striking in figure 24, but the same argument applies.

One of the important features of constant-current operation shown in figure 23 is the extreme sensitivity to density at the higher Mach numbers. It will be seen that curves such as d and e become very steep in certain ranges, depending on the current, density, and Mach

number. The region of steepness occurs at different temperature loadings under different conditions. When this condition is met during operation, it appears as a near instability. The observer has difficulty in taking readings, and his first reaction is that something has gone wrong with the equipment. In fact, this effect was encountered in some of the early work in 1946 and 1947 when, during adjustments of the heating current, a slight increase in the current would sometimes throw the temperature out of bounds and burn out the wire.

A comparison of figures 23 and 24 will show that this extreme characteristic does not carry over to Mach number dependence. The sensitivity to Mach number (or velocity) fluctuations is different for a constant i from that for a constant ΔT, but the differences are not nearly so marked as they are for density fluctuations. Figure 24 shows that the looping over, which gives rise to triple-valued Nusselt numbers and a region of insensitivity, is accentuated in the constant-current curves.

Figure 25 is a diagram of Nusselt number against Reynolds number in which both constant ΔT and constant i curves have been placed. Again the characteristic effects just discussed will be noted. The loop in the heavy solid lines for ρ and constant i and the discontinuity around $M = 1$ are again very pronounced, particularly at the lower values of d/λ.

TEST RESULTS WITH SWEPT WIRES

Probes with single slant wires or with two wires arranged in the form of an "X" have been in general use at low speeds for measuring shearing stresses and cross-stream velocity fluctuations. Since it is obviously desirable to extend such applications to high speeds, the characteristics of the inclined wire must be known. Investigations were therefore conducted with single-wire probes with the wire at various angles to the stream. As was the case with the normal wires, data were taken at several different temperature loadings and the plotted curves represent the observed data at a constant temperature loading, $\Delta T/T_s = 0.22$. Temperature-loading effect was found to be similar to that for normal wires.

In the low-speed range, where the characteristics of slanted wires are known, the heat loss depends on the normal component of the flow for angles ranging from 90° to about 20° (ref. 8). One question that naturally arises is whether the same dependence extends into the high-speed range. Another question concerns shock-wave effects, both from the wave created by the leading support prong and from the wave created by the wire itself. When the Mach angle corresponds to the angle of the wire, the wire lies in the shock wave created by the leading probe tip. For lower supersonic speeds the wire lies behind the wave, and for higher speeds it lies ahead. Furthermore, the flow is effectively subsonic when the Mach angle is

greater than the angle of the wire and supersonic when it is less. Coincidence of the wire angle and Mach angle would therefore appear to be a critical condition.

A comparison of the data for a single swept wire based on various assumed conditions for the ambient air is shown in figure 26. This figure is similar to figure 17 for a normal wire in that the identical assumptions were made concerning the temperature of the air surrounding the wire for the evaluation of the conductivity and viscosity factors. By a comparison of the four plots of figure 26 it is again seen that the best correlation of the supersonic data results when the ambient air is assumed at a temperature midway between that of the free stream and that behind the normal shock induced by the wire (fig. 26(d)). In this case the shock strength was computed from the normal component of the Mach number. The dotted line represents the Mach number for which the Mach angle is equal to the measured angle of the wire. This represents the dividing line between subsonic and supersonic flow of the component of velocity normal to the wire. It is to be noted that no shock wave will be induced by a swept wire until the Mach angle of the flow is less than the angle of the wire.

A comparison of figures 26 and 17 shows a marked similarity between them in both the subsonic and the supersonic regions, except for the region of figure 26 which lies between sonic free-stream velocity and sonic normal component of flow to the wire. This range in the swept-wire data is a region of comparative insensitivity.

It will be noted that the values of the Nusselt number and the shapes of the curves in this insensitive region are dependent upon the conditions assumed for the ambient air. In figure 26(c) with the air temperature assumed at stagnation, a decreasing Nusselt number is indicated between free-stream velocities corresponding to $M = 0.9$ and 1.4, the higher of which corresponds to Mach number unity for the component perpendicular to the wire. After $M \sin \theta$ is increased above unity (free stream $M = 1.40$) an increasing heat loss with increasing free-stream Mach number occurs. These phenomena indicate that the wire is insensitive to velocity or Mach number changes near an $M \sin \theta$ of unity.

On the other hand, if free-stream conditions are assumed for evaluating the properties of the ambient air in this Mach number range (fig. 26(d)), this insensitivity to Mach number or velocity occurs near a free-stream Mach number of 1.25, and the region of insensitivity is reduced greatly. The shift in the point of insensitivity may be of assistance in a turbulence measurement in that it will tell whether or not fluctuations in air properties are present. If, for example, the signal disappears at $M = 1.4$, only velocity fluctuations are present. If, on the other hand, the signal disappears at $M = 1.25$, Mach number fluctuations are present along with the accompanying changes in temperature which influence the properties of the air.

To test whether the heat losses from swept wires are determined by the component of velocity (or Mach number) perpendicular to the wire over any great range of speeds, several swept wires were tested and compared with a normal wire. Pertinent results are shown in figure 27.

A direct comparison of performance of the various wires was difficult because of the inherent variation among the several samples. To make a direct comparison, with sample dispersion removed, the Nusselt numbers of each of the swept-wire samples were multiplied by a factor to bring them into agreement with normal-wire data in the subsonic range below a Mach number of 0.6. It will be seen from the factors listed in the figure that the adjustments do not exceed 5 percent.

From this figure it can be seen that the sensitivity to density is independent of wire angles and that, as the velocity changes, identical correlation exists at the higher supersonic speeds. In the range of speeds between that at which the Mach number of normal flow to the wire and that at which the free-stream Mach number are unity the heat loss is somewhat indeterminate, and the curves show a region relatively insensitive to Mach number, or velocity, changes.

It is to be noted that these curves are based on free-stream temperatures for values of $M \sin \theta$ less than unity and on the average temperature midway between those temperatures behind a normal shock and those of the free stream for $M \sin \theta$ greater than unity. No such correlation exists, except at the lowest speeds, if any other temperatures are assumed for the ambient air, such as stagnation, free stream, or the computed condition behind a normal shock. It is felt that the character of the indeterminate region shown on the curves may be caused by differences in the shapes of the wind-loaded wires, the effect of the shock waves created by the holder, and other mechanical factors difficult to control.

In an attempt to find some correlation between the heat-loss characteristics and the positions of the shock wave from the holder, schlieren photographs were taken of one sample. This series of pictures is shown in figure 28. This is the identical wire and holder for which the data are shown in figures 26 and 27.

When this wire was applied, it appeared taut when not loaded. The photograph shows that when under wind loading, the wire is not straight but has a definite curvature caused by the wind, with the result that the component of velocity normal to the wire varies throughout its length. This condition would exist even if the wire were applied with initial tension. The shape of the wire near the short needle is such that it is nearly normal to the stream, whereas near the longer needle the wire approaches a direction parallel with the flow. These photographs show that the shape of the wire is such that for this range of Mach numbers it always lies within the shock cone created by the longer needle. The

region of insensitivity and points of inflection shown on the curves of figure 26 cannot be associated with the position of this shock cone relative to the wire. At higher Mach numbers where the shock wave must pass over the wire, no irregularity in the data is indicated. Tests on a single wire attached well back from the tip of both a sharp and blunted long needle showed only a difference in level of Nusselt number above free-stream sonic speed.

Wire calibrations over a range of temperature loadings indicated the same type of performance as was shown by the normal wires provided that the effective velocity on the wire was assumed to be that of the component of the free-stream velocity perpendicular to the wire. Nusselt numbers were governed by a combination of Mach number, density, and temperature loading, and the sensitivity to velocity and density at constant heating current depended upon the temperature loading taken by the wire at the conditions of operation.

POSSIBLE APPLICATIONS OF HOT-WIRES

In the foregoing sections an attempt has been made to set forth the basic characteristics of the hot-wire. It is believed that this kind of information forms the foundation on which to construct techniques of measurement. With a knowledge of what can be done, what limitations exist, and how the response of the wire can be varied at will, the technique and probe form most likely to accomplish the desired measurement can be selected. Once this selection has been made, the probe must be calibrated in terms of the variables concerned.

At first sight hot-wire performance looks forbiddingly formidable and complex. The behavior of a hot-wire definitely is not simple, but the very fact that it shows so many behavior patterns is evidence of versatility. It is also true that turbulence phenomena themselves are complex; hence the observer must be well informed about the capabilities of his instrument and clear about the objectives of his measurements. Fortunately the hot-wire exhibits most of its complexities in the subsonic region where turbulence phenomena are not yet greatly complicated by compressibility effects. The supersonic performance is not reducible to a single curve and is therefore not so simple as it was originally thought to be (ref. 1) yet is not so complex as to exclude the possibility of applying the methods of reference 9. In order to apply any of the established methods above Mach number 0.2, the temperature loading must not exceed something in the neighborhood of 200° C.

In addition to the ordinary uses of probes containing slanting wires, the swept wire offers the possibility of moving subsonic behavior into the supersonic range. Particular reference is made to the utility of

the "dead spots" (regions of zero slope) when it is desired to eliminate a variable. Unfortunately the prospect of reaching much above the low supersonic range is dim because of practical limitations on the inclination and straightness of the wire. However, it is felt that the possibilities of swept wires have not been fully covered in this investigation.

The author is fully cognizant of the fact that a reader interested in some particular aspect of hot-wire performance may wish to use methods of plotting not found in the figures given here. For this reason some of the results are summarized in tables III to XIII. Here Nusselt numbers, with end-loss corrections applied, are given on the basis of free-stream conditions. Since for practical applications end-loss corrections would not ordinarily be applied, figure 12 is included as an adjunct to the tables, giving the curves of the conversion factors which were applied to the measured data to apply the end-loss corrections. In order to convert the corrected Nusselt numbers presented in the tables to the measured values without end-loss corrections applied, the tabulated Nu_∞ must first be multiplied by the factor k/k_o, values of which are tabulated in table XIV, to eliminate the variable conductivity included in the corrected Nusselt numbers. This converts the tabulated Nusselt numbers to Nusselt numbers for an ambient air temperature of 0° C and thus eliminates a function of Mach number which is not included in the end-loss correction. An application of the Nusselt number ratio determined from figure 12 to the tabulated Nusselt numbers yields values as measured without end-loss correction.

CONCLUSIONS

The following conclusions were derived from an investigation of the heat-loss characteristics of hot-wire anemometers at various densities in transonic and supersonic flow:

1. It was found that King's law did not correctly express the rate of heat loss from fine wires under any conditions of the present investigation. The conditions of validity of this law are approached in the incompressible-flow range as the wire diameter and air density are increased. The governing parameters in the incompressible range are Reynolds number and ρd, or its equivalent, d/λ, where ρ is the density, d is the wire diameter, and λ is the molecular mean free path.

2. In the subsonic range, large differences occur in the response to velocity and density. The parameters governing this behavior are Mach number M, d/λ, and temperature difference ΔT. Fine wires, in general, exhibit low sensitivity to velocity, again depending on d/λ and M.

3. In the supersonic range $1.2 < M < 1.9$, near independence of Mach number may be obtained at a constant temperature loading by evaluating viscosity μ and the thermal conductivity of air k at a temperature midway between that of free stream and that behind a normal shock. No data were obtained above Mach number 1.9 because of tunnel limitations.

4. Temperature-loading effects in the compressible-flow region become very important above loadings of 200° to 300° C and cause large differences between the response of the wire for constant temperature and for constant current.

5. On swept wires, the rate of heat loss was found to depend on the component of flow normal to the wire for the angle range covered in the investigation ($90^{\circ} \geq \theta \geq 36^{\circ}$ where θ is the angle measured from the stream axis).

6. Swept wires ($\theta < 90^{\circ}$) do not exhibit supersonic characteristics until the Mach angle is less than θ. When the Mach angle exceeds θ, the wires show little or no sensitivity to velocity, or Mach number, change.

National Bureau of Standards,
Washington, D. C., February 18, 1954.

REFERENCES

1. Kovásznay, Leslie S. G., and Törmarck, Sven I. A.: Heat Loss of Hot Wires in Supersonic Flow. Bumblebee Rep. No. 127, Dept. Aero., The Johns Hopkins Univ., Apr. 1950.

2. Lowell, Herman H.: Design and Applications of Hot-Wire Anemometers for Steady-State Measurements at Transonic and Supersonic Airspeeds. NACA TN 2117, 1950.

3. King, Louis Vessot: On the Convection of Heat From Small Cylinders in a Stream of Fluid: Determination of the Convection Constants of Small Platinum Wires With Applications to Hot-Wire Anemometry. Phil. Trans. Roy. Soc. (London), ser. A, vol. 214, no. 14, Nov. 12, 1914, pp. 373-432.

4. Schubauer, G. B. and Klebanoff, P. S.: Theory and Application of Hot-Wire Instruments in the Investigation of Turbulent Boundary Layers. NACA WR W-86, 1946. (Formerly ACR 5K27.)

5. Betchov, R.: Théorie non-linéaire de l'anémomètre à fil chaud. Verhand. Kon. Ned. Acad. Wetensch. (Amsterdam), vol. LII, no. 3, 1949, pp. 195-207.

6. Anon.: Smithsonian Physical Tables. Smithsonian Institution,

7. Tchen, Chan-Mou: Heat Delivery in a Compressible Flow and Applications to Hot-Wire Anemometry. NACA TN 2436, 1951.

8. Weske, John R.: Methods of Measurement of High Air Velocities by the Hot-Wire Method. NACA TN 880, 1943.

9. Kovásznay, Leslie S. G.: Turbulence in Supersonic Flow. Jour. Aero. Sci., vol. 20, no. 10, Oct., 1953, pp. 657-674, 682.

TABLE I

TEMPERATURE COEFFICIENTS AND RESISTIVITIES OF WIRES

Material	Diameter, in.	α	β	Resistivity (handbook value), micro-ohms/cm^3 at 20° C
Tungsten	0.00015	4.220×10^{-3}	7.299×10^{-7}	5.5
Tungsten	.0003	3.944	7.510	
Platinum	.0003	3.808	-6.220	10.6
Platinum	.00152	3.769	-8.405	
Platinum with 10 percent rhodium	.00005	1.418	0	19.0
Platinum with 10 percent rhodium	.0001	1.596	-2.149	
Platinum with 10 percent rhodium	.00015	1.544	-1.498	

TABLE II

MAXIMUM WIND LOADING OF WIRES

Material	Diameter, in.	Length, mm	Maximum temperature, °C	Maximum $\frac{1}{2}\rho V^2$, gm/cm^2	Tensile strength (handbook value) lb/sq in.	
					Annealed	Hard drawn
Tungsten	0.00015	2.82	374	887	230,000	590,000
Tungsten	.0003	2.66	404	887		
Platinum	.0003	2.82	496-626	887-450	18,000-22,000	30,000-36,000
Platinum	.00152	9.12	361	781		
Platinum with 10 percent rhodium	.00005	2.72	397	771	47,000	84,000
Platinum with 10 percent rhodium	.00005	.73	350	887		
Platinum with 10 percent rhodium	.0001	2.86	539	887		
Platinum with 10 percent rhodium	.00015	2.80	694-544	570-887		
Platinum with 10 percent rhodium	.00015	.68	534	887		

TABLE III

NUSSELT NUMBERS Nu_∞ FOR INFINITELY LONG PLATINUM WIRE CONTAINING 10 PERCENT RHODIUM WITH d = 0.00005 INCH, l = 0.73 MILLIMETER, R_o = 117.9 OHMS, AND T_g = 308° K

(a) ΔT = 61.70° C; ΔR = 10.32 ohms; $\Delta T/T_g$ = 0.200; $\Delta R/R_o$ = 0.08737

M	Nu_∞ at free-stream density, gm/cm^3, of -								
	0.0002	0.0003	0.0004	0.0006	0.0008	0.0010	0.0012	0.0016	0.0024
0.05			0.6154	0.6946	0.7901	0.8935	0.8927		1.205
.10			.6730	.8144	.9020	1.022	1.088		1.508
.20			.7826	.9610	1.115	1.250	1.370		
.40			.9211	1.167	1.365	1.535	1.713		
.60			.9957	1.283	1.544	1.708	1.919		
.80			1.036	1.346	1.639	1.869	2.006		
.90			1.027	1.369	1.666	1.881	2.103		
.95			1.036	1.357	1.642	1.903	2.128		
1.05		0.9256	1.097	1.478	1.716	1.965	2.205		
1.25		1.005	1.240	1.548	1.855	2.160	2.412		
1.50		1.214	1.442	1.828	2.162				
1.75		1.397	1.665	2.109					
1.90		1.532	1.813	2.378					

(b) ΔT = 185° C; ΔR = 30.95 ohms; $\Delta T/T_g$ = 0.601; $\Delta R/R_o$ = 0.2624

M	Nu_∞ at free-stream density, gm/cm^3, of -								
	0.0002	0.0003	0.0004	0.0006	0.0008	0.0010	0.0012	0.0016	0.0024
0.05			0.6263	0.7158	0.8038	0.8751	0.9239		1.270
.10			.6783	.8206	.9372	1.068	1.127		1.561
.20			.7875	.9714	1.135	1.277	1.391		
.40			.9130	1.164	1.367	1.559	1.726		
.60			.9830	1.273	1.525	1.735	1.932		
.80			1.020	1.330	1.608	1.836	2.057		
.90			1.009	1.339	1.645	1.863	2.082		
.95			1.012	1.333	1.627	1.874	2.091		
1.05		0.8949	1.080	1.408	1.687	1.942	2.173		
1.25		.9812	1.190	1.539	1.838	2.081	2.313		
1.50		1.161	1.397	1.792	2.127				
1.75		1.363	1.628	2.104					
1.90		1.482	1.767	2.306					

(c) ΔT = 315° C; ΔR = 52.64 ohms; $\Delta T/T_g$ = 1.020; $\Delta R/R_o$ = 0.4463

M	Nu_∞ at free-stream density, gm/cm^3, of -								
	0.0002	0.0003	0.0004	0.0006	0.0008	0.0010	0.0012	0.0016	0.0024
0.05			0.6164	0.7261	0.8259	0.7933	0.9754		1.316
.10			.6721	.8208	.9511	1.073	1.161		1.618
.20			.7614	.9553	1.128	1.285	1.412		
.40			.8795	1.133	1.337	1.547	1.720		
.60			.9437	1.236	1.475	1.722	1.915		
.80			.9176	1.293	1.576	1.822	2.030		
.90			.9491	1.293	1.612	1.839	2.055		
.95			.9689	1.287	1.583	1.839	2.056		
1.05		0.8303	.9955	1.319	1.594	1.857	2.094		
1.25		.9132	1.111	1.429	1.728	2.023	2.203		
1.50		1.078	1.309	1.683	2.014				
1.75		1.271	1.577	1.983					
1.90		1.443	1.658	2.153					

TABLE IV

NUSSELT NUMBERS Nu_∞ FOR INFINITELY LONG PLATINUM WIRE CONTAINING 10 PERCENT RHODIUM WITH d = 0.00015 INCH, l = 2.80 MILLIMETERS, R_o = 48.61 OHMS, AND T_s = 303° K

(a) ΔT = 66.8° C; ΔR = 4.99 ohms; $\Delta T/T_s$ = 0.221; $\Delta R/R_o$ = 0.1026

M	Nu_∞ at free-stream density, gm/cm³, of -								
	0.0002	0.0003	0.0004	0.0006	0.0008	0.0010	0.0012	0.0016	0.0020
0.05			1.014	1.140	1.300	1.349	1.416	1.606	1.758
.10			1.224	1.444	1.589	1.737	1.842	2.073	2.296
.20			1.544	1.820	2.003	2.186	2.383	2.689	3.004
.40			1.900	2.322	2.593	2.822	3.069	3.501	
.60			2.138	2.642	2.962	3.263	3.594	4.142	
.80			2.294	2.868	3.258	3.635	4.018		
.90			2.298	2.951	3.338	3.771	4.148		
.95			2.315	2.977	3.368	3.778	4.230		
1.05		1.986	2.390	3.098	3.624	4.205	4.606		
1.25		2.188	2.620	3.375	4.076	4.627	5.092		
1.50	2.015	2.591	3.055	3.922	4.723				
1.75	2.330	3.014	3.584	4.636					
1.90	2.548	3.286	3.976	5.121					

(b) ΔT = 204° C; ΔR = 14.76 ohms; $\Delta T/T_s$ = 0.672; $\Delta R/R_o$ = 0.3036

M	Nu_∞ at free-stream density, gm/cm³, of -								
	0.0002	0.0003	0.0004	0.0006	0.0008	0.0010	0.0012	0.0016	0.0020
0.05			0.9921	1.166	1.313	1.373	1.456	1.647	1.795
.10			1.215	1.416	1.585	1.723	1.861	2.106	2.315
.20			1.485	1.757	1.988	2.182	2.374	2.718	3.010
.40			1.845	2.224	2.524	2.789	3.034	3.484	
.60			2.046	2.519	2.871	3.198	3.524	4.080	
.80			2.190	2.797	3.133	3.514	3.892		
.90			2.164	2.825	3.189	3.631	4.021		
.95			2.148	2.824	3.205	3.632	4.075		
1.05		1.884	2.274	2.955	3.494	4.026	4.423		
1.25		2.067	2.483	3.235	3.870	4.400	4.885		
1.50	1.848	2.399	2.924	3.764	4.442				
1.75	2.150	2.844	3.384	4.396					
1.90	2.361	3.122	3.761	4.848					

(c) ΔT = 344° C; ΔR = 24.76 ohms; $\Delta T/T_s$ = 1.135; $\Delta R/R_o$ = 0.5094

M	Nu_∞ at free-stream density, gm/cm³, of -								
	0.0002	0.0003	0.0004	0.0006	0.0008	0.0010	0.0012	0.0016	0.0020
0.05			0.9653	1.128	1.306	1.389	1.489	1.703	1.861
.10			1.184	1.356	1.545	1.742	1.888	2.154	2.373
.20			1.416	1.658	1.895	2.182	2.391	2.747	3.039
.40			1.714	2.042	2.450	2.739	2.987	3.492	
.60			1.862	2.267	2.826	3.183	3.501	4.071	
.80			1.966	2.537	3.078	3.472	3.837		
.90			1.957	2.593	3.115	3.541	3.964		
.95			2.024	2.510	3.029	3.498	3.997		
1.05		1.710	2.089	2.844	3.417	3.796	4.119		
1.25		1.883	2.296	3.122	3.550	4.213	4.701		
1.50	1.657	2.236	2.764	3.617	4.265				
1.75	1.969	2.684	3.249	4.123					
1.90	2.171	2.993	3.469	4.623					

TABLE IV.- Concluded

NUSSELT NUMBERS Nu_∞ FOR INFINITELY LONG PLATINUM WIRE CONTAINING 10 PERCENT RHODIUM WITH d = 0.00015 INCH, l = 2.80 MILLIMETERS, R_o = 48.61 OHMS, AND T_s = 303° K

(d) ΔT = 514° C; ΔR = 35.97 ohms; $\Delta T/T_s$ = 1.696; $\Delta R/R_o$ = 0.7400

M	Nu_∞ at free-stream density, gm/cm³, of -								
	0.0002	0.0003	0.0004	0.0006	0.0008	0.0010	0.0012	0.0016	0.0020
0.05			0.9165	1.110	1.272	1.336	1.472	1.706	1.867
.10			1.060	1.313	1.437	1.625	1.829	2.118	2.346
.20			1.246	1.564	1.738	1.994	2.270	2.662	2.973
.40			1.472	1.878	2.115	2.451	2.826	3.356	
.60			1.589	2.075	2.347	2.783	3.238	3.861	
.80			1.654	2.177	2.556	3.076	3.533		
.90			1.612	2.190	2.597	3.170	3.681		
.95			1.579	2.176	2.612	3.174	3.716		
1.05		1.541	1.893	2.530	3.043	3.222	3.604		
1.25		1.718	2.101	2.794	3.190	3.632	4.205		
1.50	1.525	2.044	2.506	3.260	3.778				
1.75	1.796	2.405	2.897	3.641					
1.90	1.982	2.654	3.065	4.064					

(e) ΔT = 664° C; ΔR = 46.15 ohms; $\Delta T/T_s$ = 2.192; $\Delta R/R_o$ = 0.9494

M	Nu_∞ at free-stream density, gm/cm³, of -								
	0.0002	0.0003	0.0004	0.0006	0.0008	0.0010	0.0012	0.0016	0.0020
0.05			0.9201	1.126	1.291	1.347	1.493	1.742	1.914
.10			1.058	1.323	1.418	1.608	1.820	2.134	2.371
.20			1.229	1.550	1.694	1.965	2.244	2.660	2.968
.40			1.417	1.841	2.028	2.388	2.760	3.317	
.60			1.561	2.017	2.242	2.679	3.130		
.80			1.582	2.112	2.390	2.906	3.386		
.90			1.555	2.116	2.445	3.020			
.95			1.539	2.105	2.448	3.174			

TABLE V

NUSSELT NUMBERS Nu_∞ FOR INFINITELY LONG PLATINUM WIRE CONTAINING 10 PERCENT RHODIUM WITH d = 0.00015 INCH, l = 0.68 MILLIMETER, R_o = 11.09 OHMS, AND T_s = 303° K

(a) ΔT = 66.8° C; ΔR = 1.14 ohms; $\Delta T/T_s$ = 0.221; $\Delta R/R_o$ = 0.1028

M	Nu_∞ at free-stream density, gm/cm³, of -								
	0.0002	0.0003	0.0004	0.0006	0.0008	0.0010	0.0012	0.0016	0.0020
0.05			0.9590	1.054	1.143	1.264	1.333	1.505	1.646
.10			1.103	1.287	1.485	1.610	1.729	1.939	2.124
.20			1.356	1.648	1.901	2.077	2.217	2.516	2.772
.40			1.686	2.060	2.432	2.632	2.842	3.254	3.605
.60			1.876	2.369	2.732	3.056	3.330	3.862	
.80			2.067	2.592	3.042	3.372	4.047		
.90			2.096	2.698	3.148	3.508	3.910		
.95			2.130	2.787	3.170	3.599	4.020		
1.05		1.808	2.174	2.812	3.293	3.762	4.122		
1.25		2.055	2.501	3.178	3.723	4.252	4.694		
1.50		2.466	2.934	3.723	4.430				
1.75		2.791	3.369	4.321					
1.90		3.086	3.751	4.763					

(b) ΔT = 199° C; ΔR = 3.37 ohms; $\Delta T/T_s$ = 0.657; $\Delta R/R_o$ = 0.3039

M	Nu_∞ at free-stream density, gm/cm³, of -								
	0.0002	0.0003	0.0004	0.0006	0.0008	0.0010	0.0012	0.0016	0.0020
0.05			0.9748	1.088	1.188	1.319	1.386	1.588	1.732
.10			1.099	1.332	1.498	1.634	1.767	2.031	2.216
.20			1.355	1.667	1.903	2.068	2.278	2.585	2.893
.40			1.697	2.068	2.405	2.551	2.859	3.322	3.666
.60			1.814	2.339	2.719	3.056	3.365	3.905	
.80			1.983	2.551	2.955	3.339	3.686		
.90			1.997	2.570	3.037	3.460	3.840		
.95			1.982	2.609	3.091	3.515	3.926		
1.05		1.592	2.174	2.812	3.123	3.584	3.975		
1.25		2.055	2.261	2.928	3.554	4.079	4.544		
1.50		2.466	2.696	3.506	4.202				
1.75		2.544	3.144	4.152					
1.90		2.801	3.474	4.544					

(c) ΔT = 339° C; ΔR = 5.65 ohms; $\Delta T/T_s$ = 1.119; $\Delta R/R_o$ = 0.5095

M	Nu_∞ at free-stream density, gm/cm³, of -								
	0.0002	0.0003	0.0004	0.0006	0.0008	0.0010	0.0012	0.0016	0.0020
0.05			0.9362	1.079	1.197	1.300	1.400	1.599	1.761
.10			1.068	1.302	1.467	1.593	1.732	2.015	2.213
.20			1.278	1.580	1.851	1.961	2.173	2.521	2.847
.40			1.532	1.927	2.310	2.390	2.668	3.169	3.525
.60			1.696	2.138	2.494	2.837	3.214	3.767	
.80			1.804	2.347	2.693	3.052	3.463		
.90			1.799	2.350	2.719	3.147	3.618		
.95			1.777	2.329	2.779	3.183	3.668		
1.05		1.399	1.696	2.233	2.797	3.312	3.698		
1.25		1.583	1.961	2.541	3.263	3.767	4.268		
1.50		1.893	2.376	3.133	3.861				
1.75		2.266	2.773	3.832					
1.90		2.469	3.126	4.212					

(d) ΔT = 501° C; ΔR = 8.21 ohms; $\Delta T/T_s$ = 1.653; $\Delta R/R_o$ = 0.7403

M	Nu_∞ at free-stream density, gm/cm³, of -								
	0.0002	0.0003	0.0004	0.0006	0.0008	0.0010	0.0012	0.0016	0.0020
0.05			0.9069	1.055	1.190	1.299	1.410	1.615	1.783
.10			1.016	1.241	1.424	1.570	1.727	1.983	2.214
.20			1.159	1.467	1.720	1.908	2.102	2.459	2.762
.40			1.360	1.750	2.071	2.297	2.569	3.036	3.446
.60			1.468	1.930	2.298	2.597	2.899	3.455	
.80			1.575	2.031	2.415	2.780	3.132		
.90			1.551	2.056	2.488	2.847	3.233		
.95			1.554	2.064	2.478	2.872	3.280		
1.05		1.277	1.553	2.030	2.489	2.902	3.268		
1.25		1.451	1.793	2.315	2.841	3.321	3.785		
1.50		1.759	2.104	2.771	3.427				
1.75		2.025	2.451	3.305					
1.90		2.192	2.712	3.668					

TABLE VI

NUSSELT NUMBERS Nu_∞ FOR INFINITELY LONG TUNGSTEN WIRE

WITH d = 0.00015 INCH, l = 2.82 MILLIMETERS,

R_o = 14.51 OHMS, AND T_s = 303° K

(a) ΔT = 64.9° C; ΔR = 4.06 ohms; $\Delta T/T_s$ = 0.214; $\Delta R/R_o$ = 0.2798

M	Nu_∞ at free-stream density, gm/cm^3, of -							
	0.0002	0.0003	0.0004	0.0006	0.0008	0.0010	0.0012	0.0016
0.05			0.8954	1.028	1.171	1.263	1.354	
.10			1.110	1.288	1.451	1.593	1.746	
.20			1.352	1.652	1.873	2.062	2.253	
.40			1.711	2.095	2.402	2.673	2.932	
.60			1.919	2.380	2.778	3.100	3.439	
.80			2.072	2.626	3.044	3.418	3.811	
.90			2.105	2.702	3.186	3.600	3.960	
.95			2.142	2.723	3.227	3.662	4.023	
1.05		1.809	2.192	2.782	3.331	3.768	4.144	
1.25		2.066	2.487	3.211	3.768	4.284	4.758	
1.50	1.890	2.477	2.935	3.759	4.469			
1.75	2.189	2.857	3.429	4.405				
1.90	2.394	3.132	3.768	4.834				

(b) ΔT = 196° C; ΔR = 12.51 ohms; $\Delta T/T_s$ = 0.647; $\Delta R/R_o$ = 0.8622

M	Nu_∞ at free-stream density, gm/cm^3, of -							
	0.0002	0.0003	0.0004	0.0006	0.0008	0.0010	0.0012	0.0016
0.05			0.9018	1.058	1.176	1.280	1.381	
.10			1.072	1.289	1.458	1.600	1.742	
.20			1.328	1.618	1.843	2.046	2.232	
.40			1.651	2.042	2.348	2.607	2.869	
.60			1.853	2.318	2.712	3.027	3.318	
.80			1.974	2.505	2.955	3.337	3.649	
.90			1.993	2.571	3.063	3.462	3.782	
.95			1.999	2.579	3:095	3.521	3.883	
1.05		1.655	2.011	2.625	3.124	3.588	3.977	
1.25		1.932	2.322	3.011	3.596	4.105	4.571	
1.50	1.748	2.278	2.762	3.562	4.222			
1.75	2.026	2.676	3.212	4.162				
1.90	2.230	2.927	3.531	4.585				

(c) ΔT = 334° C; ΔR = 21.82 ohms; $\Delta T/T_s$ = 1.102; $\Delta R/R_o$ = 1.504

M	Nu_∞ at free-stream density, gm/cm^3, of -							
	0.0002	0.0003	0.0004	0.0006	0.0008	0.0010	0.0012	0.0016
0.05			0.8917	1.062	1.178	1.286	1.374	
.10			1.035	1.272	1.446	1.590	1.718	
.20			1.269	1.573	1.805	2.005	2.186	
.40			1.548	1.952	2.268	2.529	2.761	
.60			1.728	2.188	2.578	2.896	3.199	
.80			1.833	2.345	2.788	3.163	3.498	
.90			1.830	2.385	2.857	3.273	3.616	
.95			1.811	2.376	2.877	3.301	3.650	
1.05		1.493	1.869	2.430	2.914	3.376	3.765	
1.25		1.775	2.151	2.799	3.407	3.913	4.365	
1.50	1.571	2.083	2.553	3.353	3.991			
1.75	1.849	2.474	2.986	3.900				
1.90	2.028	2.712	3.317	4.316				

TABLE VII

NUSSELT NUMBERS Nu_∞ FOR INFINITELY LONG TUNGSTEN WIRE

WITH d = 0.0003 INCH, l = 2.67 MILLIMETERS,

R_o = 3.349 OHMS, AND T_s = 303° K

(a) ΔT = 64.5° C; ΔR = 0.88 ohms; $\Delta T/T_s$ = 0.213; $\Delta R/R_o$ = 0.261

M	Nu_∞ at free-stream density, gm/cm^3, of -								
	0.0002	0.0003	0.0004	0.0006	0.0008	0.0010	0.0012	0.0016	0.0020
0.05			1.210	1.424	1.599	1.755	1.881	2.118	2.305
.10			1.541	1.830		2.246		2.781	
.20			1.969		2.722		3.191		4.053
.40			2.556	3.188	3.517	3.950	4.261	4.994	5.733
.60			2.893		4.119		5.121		6.254
.80			3.149		4.602		5.693		
.90			3.242	4.192		5.424			
.95			3.186	4.132	4.934	5.473	5.998		
1.05		3.305	3.447	4.476	5.216	5.899	6.697		
1.25		3.714	4.214	5.346	6.261	6.773	7.770		
1.50	3.421	4.210	4.959	6.232	7.364				
1.75	3.771	4.869	5.850	7.389					
1.90	4.151	5.333	6.387	8.144					

(b) ΔT = 207° C; ΔR = 2.89 ohms; $\Delta T/T_s$ = 0.682; $\Delta R/R_o$ = 0.862

M	Nu_∞ at free-stream density, gm/cm^3, of -								
	0.0002	0.0003	0.0004	0.0006	0.0008	0.0010	0.0012	0.0016	0.0020
0.05			1.236	1.453	1.622	1.790	1.936	2.189	2.419
.10			1.546	1.844		2.295		2.809	
.20			1.952		2.689		3.202		4.020
.40			2.491	3.017	3.462	3.842	4.160	4.948	5.561
.60			2.797		4.024		4.983		6.107
.80			2.993		4.518		5.547		
.90			3.051	3.999		5.346			
.95			3.029	3.946	4.649	5.313	5.864		
1.05		2.953	3.236	4.258	5.020	5.775	6.375		
1.25		3.406	4.018	5.041	6.017	6.617	7.364		
1.50	3.128	3.990	4.730	6.046	7.087				
1.75	3.562	4.658	5.609	7.094					
1.90	3.976	5.151	6.145	7.844					

(c) ΔT = 374° C; ΔR = 5.35 ohms; $\Delta T/T_s$ = 1.234; $\Delta R/R_o$ = 1.586

M	Nu_∞ at free-stream density, gm/cm^3, of -								
	0.0002	0.0003	0.0004	0.0006	0.0008	0.0010	0.0012	0.0016	0.0020
0.05			1.246	1.450	1.624	1.791	1.952	2.205	2.418
.10			1.534	1.810		2.264		2.812	
.20			1.910		2.622		3.162		4.013
.40			2.380	2.894	3.357	3.732	4.054	4.734	5.358
.60			2.697		3.862		4.778		5.942
.80			2.822		4.273		5.359		
.90			2.860	3.736		5.019			
.95			2.781	3.646	4.330	4.961	5.589		
1.05		2.722	2.995	3.938	4.671	5.342	6.211		
1.25		3.175	3.673	4.754	5.722	6.451	7.174		
1.50	2.893	3.652	4.358	5.675	6.652				
1.75	3.281	4.234	5.201	6.617					
1.90	3.558	4.720	5.735	7.398					

TABLE VIII

NUSSELT NUMBERS Nu_∞ FOR INFINITELY LONG PLATINUM WIRE

WITH d = 0.0003 INCH, l = 2.82 MILLIMETERS,

R_0 = 5.63 OHMS, AND T_s = 303° K

(a) ΔT = 68.5° C; ΔR = 1.43 ohms; $\Delta T/T_s$ = 0.226; $\Delta R/R_0$ = 0.254

M	Nu_∞ at free-stream density, gm/cm^3, of -								
	0.0002	0.0003	0.0004	0.0006	0.0008	0.0010	0.0012	0.0016	0.0024
0.05			1.501	1.708	1.879	2.110	2.244	2.442	2.988
.10			1.839	2.169		2.670		3.163	3.801
.20			2.392		3.148		3.690		
.40			2.992		4.100		4.882		7.140
.60			3.430		4.857		5.926		
.80			3.808		5.413		6.652		
.90			3.948	4.877		6.258			
.95			4.021	4.985	5.864	6.502	7.036		
1.05		3.550	4.162	5.246	6.075	6.735	7.225		
1.25		4.037	4.649	5.879	6.854	7.658			
1.50	3.710	4.704	5.491	7.088	7.914				
1.75	4.314	5.501	6.386	7.877					
1.90	4.706	5.911	6.940	8.732					

(b) ΔT = 200° C; ΔR = 4.11 ohms; $\Delta T/T_s$ = 0.658; $\Delta R/R_0$ = 0.730

M	Nu_∞ at free-stream density, gm/cm^3, of -								
	0.0002	0.0003	0.0004	0.0006	0.0008	0.0010	0.0012	0.0016	0.0024
0.05			1.525	1.752	1.939	2.144	2.294	2.526	3.074
.10			1.849	2.186		2.712		3.240	3.897
.20			2.328		3.147		3.722		
.40			2.915		4.037		4.793		7.118
.60			3.327		4.716		5.805		
.80			3.630		5.281		6.440		
.90			3.792	4.734		6.264			
.95			3.790	4.843	5.679	6.299	6.953		
1.05		3.418	4.098	5.183	5.966	6.677	7.279		
1.25		3.863	4.596	5.732	6.675	7.438			
1.50	3.543	4.597	5.347	6.688	7.697				
1.75	4.142	5.273	6.209	7.799					
1.90	4.506	5.740	6.812	8.506					

(c) ΔT = 334° C; ΔR = 6.71 ohms; $\Delta T/T_s$ = 1.102; $\Delta R/R_0$ = 1.192

M	Nu_∞ at free-stream density, gm/cm^3, of -								
	0.0002	0.0003	0.0004	0.0006	0.0008	0.0010	0.0012	0.0016	0.0024
0.05			1.541	1.790	2.018	2.205	2.360	2.620	3.184
.10			1.848	2.201		2.763		3.314	3.981
.20			2.281		3.143		3.747		
.40			2.808		3.970		4.747		7.100
.60			3.177		4.588		5.685		
.80			3.454		5.132		6.338		
.90			3.559	4.536		6.010			
.95			3.575	4.588	5.429	6.173	6.800		
1.05		3.216	3.969	5.036	5.778	6.552	7.212		
1.25		3.690	4.416	5.538	6.525	7.280			
1.50	3.336	4.374	5.181	6.562	7.499				
1.75	3.922	5.028	6.148	7.574					
1.90	4.300	5.481	6.573	8.220					

TABLE VIII.- Concluded

NUSSELT NUMBERS Nu_∞ FOR INFINITELY LONG PLATINUM WIRE

WITH $d = 0.0003$ INCH, $l = 2.82$ MILLIMETERS,

$R_o = 5.63$ OHMS, AND $T_s = 303^\circ$ K

(d) $\Delta T = 470^\circ$ C; $\Delta R = 9.27$ ohms; $\Delta T/T_s = 1.551$; $\Delta R/R_o = 1.647$

M	Nu_∞ at free-stream density, gm/cm^3, of -								
	0.0002	0.0003	0.0004	0.0006	0.0008	0.0010	0.0012	0.0016	0.0024
0.05			1.540	1.815	2.053	2.240	2.398	2.671	3.252
.10			1.835	2.212		2.782		3.355	4.038
.20			2.242		3.130		3.751		
.40			2.732		3.917		4.711		7.007
.60			3.041		4.482		5.511		
.80			3.328		4.939		6.178		
.90			3.361	4.278		5.818			
.95			3.349	4.335	5.191	6.004	6.600		
1.05		2.912	3.623	4.548	5.421	6.233	6.901		
1.25		3.336	4.030	5.087	6.148	6.892	7.571		
1.50	3.011	3.938	4.728	6.068	7.175				
1.75	3.744	4.578	5.637	7.044					
1.90	3.881	5.021	6.075	7.779					

(e) $\Delta T = 596^\circ$ C; $\Delta R = 11.47$ ohms; $\Delta T/T_s = 1.968$; $\Delta R/R_o = 2.038$

M	Nu_∞ at free-stream density, gm/cm^3, of -								
	0.0002	0.0003	0.0004	0.0006	0.0008	0.0010	0.0012	0.0016	0.0024
0.05			1.545	1.833	2.082	2.275	2.436	2.704	3.274
.10			1.848	2.212		2.791		3.394	4.098
.20			2.213		3.119		3.767		
.40			2.693		3.873		4.689		
.60			2.970		4.387		5.363		
.80			3.222		4.804		5.966		
.90			3.265	4.146		5.622			
.95			3.237	4.205	5.036				
1.05			3.391	4.400	5.277				

TABLE IX

NUSSELT NUMBERS Nu_∞ FOR INFINITELY LONG PLATINUM WIRE

WITH d = 0.00152 INCH, l = 9.12 MILLIMETERS,

R_o = 0.812 OHMS, AND T_s = 303° K

(a) ΔT = 68.2° C; ΔR = 0.201 ohms; $\Delta T/T_s$ = 0.225; $\Delta R/R_o$ = 0.248

M	Nu_∞ at free-stream density, gm/cm^3, of -							
	0.0002	0.0003	0.0004	0.0006	0.0008	0.0010	0.0012	0.0016
0.05			2.613	2.855	3.202	3.502	3.738	4.088
.10			3.280	3.635		4.752		5.840
.20			4.185		5.805		7.283	
.40			5.694		8.132		9.830	
.60			6.707		9.554		11.67	
.80			7.340		10.44		12.67	
.90			7.620	9.396		12.23		
.95			7.859	9.323	11.02	12.34		
1.05		6.983	8.142	9.776	11.35	13.02	14.15	
1.25		8.051	8.490	11.41	13.05	14.62		
1.50	7.395	9.312	10.64	13.01	14.98			
1.75	8.720	10.67	12.52	15.50				
1.90	9.731	11.80	13.58	16.67				

(b) ΔT = 199° C; ΔR = 0.573 ohms; $\Delta T/T_s$ = 0.658; $\Delta R/R_o$ = 0.706

M	Nu_∞ at free-stream density, gm/cm^3, of -							
	0.0002	0.0003	0.0004	0.0006	0.0008	0.0010	0.0012	0.0016
0.05			2.814	2.939	3.282	3.476	3.814	4.196
.10			3.349	3.728		4.583		5.774
.20			4.173		5.766		7.202	
.40			5.472		8.060		9.937	
.60			6.512		9.529		11.65	
.80			7.188		10.54		12.78	
.90			7.548	9.329		12.20		
.95			7.758	9.391	11.11	12.39		
1.05		7.100	7.975	9.830	11.56	12.91	14.25	
1.25		7.782	8.419	11.30	13.08	14.78		
1.50	7.364	9.071	10.78	13.27	15.17			
1.75	8.477	10.57	12.51	15.66				
1.90	9.329	11.51	13.69	16.96				

(c) ΔT = 331° C; ΔR = 0.924 ohms; $\Delta T/T_s$ = 1.093; $\Delta R/R_o$ = 1.138

M	Nu_∞ at free-stream density, gm/cm^3, of -							
	0.0002	0.0003	0.0004	0.0006	0.0008	0.0010	0.0012	0.0016
0.05			2.888	2.986	3.336	3.594	3.824	4.212
.10			3.362	3.717		4.647		5.763
.20			4.170		5.657		7.119	
.40			5.435		7.921		9.745	
.60			6.227		9.286		11.58	
.80			7.009		10.30		13.03	
.90			7.264	9.154		12.06		
.95			7.561	9.255	10.90	12.24		
1.05		6.845	7.535	9.711	11.44	12.84	14.05	
1.25		7.486	8.174	11.03	12.96	14.53		
1.50	7.120	8.793	10.38	13.02	14.36			
1.75	8.419	9.895	12.13	15.38				
1.90	9.180	11.11	13.45	16.63				

TABLE X

NUSSELT NUMBERS Nu_∞ FOR INFINITELY LONG PLATINUM WIRE CONTAINING 10 PERCENT RHODIUM WITH d = 0.00015 INCH, AN ANGLE OF 54.5°, l = 3.48 MILLIMETERS, R_0 = 59.65 OHMS, AND T_s = 308° K

(a) ΔT = 68.5° C; ΔR = 6.12 ohms; $\Delta T/T_s$ = 0.222; $\Delta R/R_0$ = 0.1026

M	Nu_∞ at free-stream density, gm/cm^3, of -						
	0.0003	0.0004	0.0006	0.0008	0.0010	0.0012	0.0024
0.05		0.8741	0.9662	1.065		1.241	1.563
.10		1.004	1.179	1.328		1.579	2.076
.20		1.230	1.486	1.697		2.047	
.40		1.539	1.888	2.178		2.643	
.60		1.746	2.171	2.507		3.053	
.80		1.901	2.381	2.768		3.381	
.90		1.961	2.468	2.894		3.527	
.95		2.003	2.522	2.925		3.612	
1.05	1.710	2.038	2.550	2.968	3.340	3.582	
1.10	1.673	1.959	2.497	2.969	3.338	3.649	
1.20	1.656	1.975	2.557	3.011	3.406	3.790	
1.25	1.688	2.029	2.592	3.128	3.504	3.935	
1.30	1.750	2.076	2.692	3.185	3.627	4.000	
1.40	1.861	2.208	2.862	3.373	3.806		
1.50	1.968	2.364	3.034	3.590			
1.60	2.089	2.536	3.256	3.826			
1.70	2.204	2.649	3.428				
1.80	2.320	2.804	3.612				
1.90	2.460	2.973	3.829				

(b) ΔT = 202° C; ΔR = 18.11 ohms; $\Delta T/T_s$ = 0.656; $\Delta R/R_0$ = 0.3036

M	Nu_∞ at free-stream density, gm/cm^3, of -						
	0.0003	0.0004	0.0006	0.0008	0.0010	0.0012	0.0024
0.05		0.9047	1.020	1.144		1.323	1.667
.10		1.034	1.224	1.389		1.661	2.211
.20		1.252	1.527	1.752		2.126	
.40		1.546	1.923	2.227		2.724	
.60		1.749	2.196	2.555		3.138	
.80		1.889	2.394	2.799		3.470	
.90		1.942	2.469	2.903		3.629	
.95		1.977	2.512	2.954		3.733	
1.05	1.668	2.010	2.542	2.998	3.383	3.668	
1.10	1.632	1.905	2.480	2.972	3.349	3.697	
1.20	1.607	1.927	2.517	3.031	3.425	3.820	
1.25	1.645	1.997	2.568	3.102	3.503	3.919	
1.30	1.691	2.037	2.658	3.168	3.599	4.019	
1.40	1.810	2.160	2.817	3.351	3.822		
1.50	1.913	2.316	2.993	3.545			
1.60	2.038	2.484	3.205	3.794			
1.70	2.148	2.598	3.366				
1.80	2.278	2.748	3.562				
1.90	2.410	2.905	3.795				

(c) ΔT = 342° C; ΔR = 30.39 ohms; $\Delta T/T_s$ = 1.111; $\Delta R/R_0$ = 0.5094

M	Nu_∞ at free-stream density, gm/cm^3, of -						
	0.0003	0.0004	0.0006	0.0008	0.0010	0.0012	0.0024
0.05		0.8954	1.034	1.166		1.370	1.737
.10		1.012	1.223	1.406		1.686	2.267
.20		1.203	1.489	1.735		2.121	
.40		1.462	1.859	2.170		2.652	
.60		1.625	2.098	2.455		3.050	
.80		1.742	2.264	2.699		3.424	
.90		1.792	2.335	2.789		3.570	
.95		1.810	2.374	2.827		3.671	
1.05	1.576	1.914	2.425	2.890	3.302	3.601	
1.10	1.533	1.805	2.383	2.861	3.282	3.624	
1.20	1.506	1.818	2.398	2.890	3.324	3.751	
1.25	1.542	1.870	2.447	2.963	3.409	3.829	
1.30	1.579	1.907	2.499	3.024	3.470	3.921	
1.40	1.685	2.004	2.634	3.223	3.686		
1.50	1.777	2.153	2.828	3.398			
1.60	1.891	2.317	3.053	3.644			
1.70	2.000	2.431	3.217				
1.80	2.126	2.552	3.399				
1.90	2.261	2.771	3.636				

TABLE XI

NUSSELT NUMBERS Nu_∞ FOR INFINITELY LONG PLATINUM WIRE CONTAINING 10 PERCENT RHODIUM WITH d = 0.00015 INCH, AN ANGLE OF 45.5°, l = 3.23 MILLIMETERS, R_0 = 51.44 OHMS, AND T_s = 308° K

(a) ΔT = 68.5° C; ΔR = 5.28 ohms; $\Delta T/T_s$ = 0.222; $\Delta R/R_0$ = 0.1026

M	Nu_∞ at free-stream density, gm/cm^3, of -								
	0.0002	0.0003	0.0004	0.0006	0.0008	0.0010	0.0012	0.0016	0.0024
0.05			0.7562	0.9106	1.013	1.093	1.177	1.301	1.521
.10			.9301	1.122	1.258		1.502		1.987
.20			1.159	1.412	1.615		1.934		2.604
.40			1.460	1.802	2.049		2.483		
.60			1.676	2.074	2.400		2.920		
.80			1.820	2.290	2.649		3.216		
.90			1.892	2.379	2.796		3.393		
.95			1.925	2.410	2.821		3.484		
1.05		1.682	2.015	2.545	2.941	3.309	3.621		
1.10		1.698	1.986	2.549	3.003	3.346	3.657		
1.20		1.700	2.019	2.585	3.059	3.405	3.786		
1.25		1.715	2.073	2.618	3.096	3.468			
1.30		1.739	2.079	2.654	3.143	3.508			
1.40		1.800	2.142	2.746	3.246	3.690			
1.50		1.883	2.253	2.866	3.398				
1.60		1.981	2.394	3.027	3.554				
1.70		2.078	2.457	3.169					
1.80		2.174	2.580	3.331					
1.90		2.287	2.747	3.503					

(b) ΔT = 202° C; ΔR = 15.62 ohms; $\Delta T/T_s$ = 0.656; $\Delta R/R_0$ = 0.3036

M	Nu_∞ at free-stream density, gm/cm^3, of -								
	0.0002	0.0003	0.0004	0.0006	0.0008	0.0010	0.0012	0.0016	0.0024
0.05			0.8336	0.9681	1.080	1.171	1.259	1.396	1.623
.10			.9928	1.174	1.327		1.579		2.088
.20			1.219	1.466	1.668		2.011		2.770
.40			1.505	1.826	2.099		2.579		
.60			1.706	2.092	2.427		2.992		
.80			1.852	2.292	2.675		3.352		
.90			1.910	2.378	2.793		3.512		
.95			1.933	2.404	2.836		3.611		
1.05		1.647	1.988	2.528	2.974	3.361	3.671		
1.10		1.653	1.949	2.537	3.006	3.386	3.727		
1.20		1.677	1.975	2.569	3.064	3.459	3.832		
1.25		1.680	2.017	2.601	3.098	3.505			
1.30		1.690	2.029	2.637	3.140	3.545			
1.40		1.767	2.082	2.727	3.239	3.707			
1.50		1.816	2.186	2.850	3.375				
1.60		1.905	2.345	2.991	3.537				
1.70		1.996	2.407	3.127					
1.80		2.082	2.518	3.300					
1.90		2.203	2.672	3.463					

(c) ΔT = 342° C; ΔR = 26.20 ohms; $\Delta T/T_s$ = 1.111; $\Delta R/R_0$ = 0.5094

M	Nu_∞ at free-stream density, gm/cm^3, of -								
	0.0002	0.0003	0.0004	0.0006	0.0008	0.0010	0.0012	0.0016	0.0024
0.05	-		0.8075	0.9473	1.058	1.147	1.236	1.373	1.593
.10			.9528	1.137	1.298		1.538		2.054
.20			1.156	1.391	1.604		1.937		2.656
.40			1.419	1.733	2.000		2.457		
.60			1.591	1.976	2.272		2.822		
.80			1.726	2.180	2.536		3.206		
.90			1.777	2.249	2.655		3.348		
.95			1.796	2.279	2.699		3.423		
1.05		1.503	1.812	2.335	2.838	3.295	3.566		
1.10		1.512	1.777	2.371	2.913	3.354	3.636		
1.20		1.497	1.800	2.411	2.951	3.391	3.759		
1.25		1.496	1.832	2.424	2.981	3.370			
1.30		1.510	1.824	2.452	3.024	3.500			
1.40		1.535	1.851	2.551	3.141	3.552			
1.50		1.598	1.933	2.639	3.164				
1.60		1.699	2.085	2.728	3.321				
1.70		1.738	2.119	2.874					
1.80		1.804	2.211	3.037					
1.90		1.920	2.331						

TABLE XII

NUSSELT NUMBERS Nu_∞ FOR INFINITELY LONG PLATINUM WIRE CONTAINING 10 PERCENT RHODIUM WITH d = 0.00015 INCH, AN ANGLE OF 38.5°, l = 4.87 MILLIMETERS, R_o = 80.94 OHMS, AND T_s = 308° K

(a) ΔT = 68.1° C; ΔR = 8.30 ohms; $\Delta T/T_s$ = 0.222; $\Delta R/R_o$ = 0.1026

M	Nu_∞ at free-stream density, gm/cm^3, of -								
	0.0002	0.0003	0.0004	0.0006	0.0008	0.0010	0.0012	0.0016	0.0024
1.05		1.741	2.110	2.629	3.042	3.387	3.644		
1.10		1.787	2.099	2.642	3.072	3.453	3.691		
1.20		1.782	2.109	2.692	3.148	3.496	3.785		
1.25		1.779	2.159	2.703	3.175	3.555			
1.30		1.804	2.142	2.740	3.191	3.537			
1.40		1.835	2.173	2.787	3.283				
1.50		1.905	2.261	2.892	3.369				
1.60		1.957	2.371	3.013	3.478				
1.70		2.015	2.400	3.115					
1.80		2.065	2.488	3.223					
1.90		2.174	2.590						

(b) ΔT = 202° C; ΔR = 24.57 ohms; $\Delta T/T_s$ = 0.656; $\Delta R/R_o$ = 0.3036

M	Nu_∞ at free-stream density, gm/cm^3, of -								
	0.0002	0.0003	0.0004	0.0006	0.0008	0.0010	0.0012	0.0016	0.0024
1.05		1.674	2.003	2.503	2.935	3.283	3.564		
1.10		1.676	1.970	2.522	2.964	3.318	3.622		
1.20		1.671	1.982	2.556	3.015	3.360	3.689		
1.25		1.671	2.018	2.569	3.033	3.480			
1.30		1.677	2.000	2.585	3.058	3.418			
1.40		1.709	2.036	2.651	3.125				
1.50		1.762	2.110	2.722	3.214				
1.60		1.829	2.223	2.833	3.328				
1.70		1.868	2.245	2.928					
1.80		1.918	2.322	3.037					
1.90		2.009	2.426						

(c) ΔT = 342° C; ΔR = 41.23 ohms; $\Delta T/T_s$ = 1.111; $\Delta R/R_o$ = 0.5094

M	Nu_∞ at free-stream density, gm/cm^3, of -								
	0.0002	0.0003	0.0004	0.0006	0.0008	0.0010	0.0012	0.0016	0.0024
1.05		1.603	1.948	2.449	2.874	3.205	3.540		
1.10		1.609	1.907	2.450	2.903	3.282	3.598		
1.20		1.601	1.911	2.467	2.952	3.338	3.672		
1.25		1.605	1.948	2.477	2.960	3.374			
1.30		1.612	1.931	2.495	2.981	3.358			
1.40		1.631	1.957	2.556	3.070				
1.50		1.692	2.025	2.614	3.146				
1.60		1.748	2.119	2.726	3.271				
1.70		1.782	2.124	2.831					
1.80		1.817	2.211	2.941					
1.90		1.891	2.310						

TABLE XIII

NUSSELT NUMBERS Nu_∞ FOR INFINITELY LONG PLATINUM WIRE CONTAINING 10 PERCENT RHODIUM WITH d = 0.00015 INCH, AN ANGLE OF 36°, l = 5.07 MILLIMETERS, R_o = 83.28 OHMS, AND T_s = 308° K

(a) ΔT = 65.1° C; ΔR = 8.54 ohms; $\Delta T/T_s$ = 0.222; $\Delta R/R_o$ = 0.1026

M	Nu_∞ at free-stream density, gm/cm^3, of -								
	0.0002	0.0003	0.0004	0.0006	0.0008	0.0010	0.0012	0.0016	0.0024
0.05			0.8298	0.9504	1.039		1.208		1.449
.10			.9679	1.145	1.292		1.537		1.905
.20			1.215	1.451	1.645		1.975		
.40			1.488	1.847	2.089		2.535		
.60			1.709	2.123	2.436		2.967		
.80			1.892	2.363	2.721		3.302		
.90			1.985	2.463	2.838		3.479		
.95			2.011	2.508	2.906				
1.05		1.641	2.044	2.551					
1.10		1.658	2.000	2.524					
1.20		1.705	2.016	2.553					
1.25		1.723	2.040	2.556					
1.30		1.724	2.036	2.596					
1.40		1.759	2.077						
1.50		1.813	2.157						
1.60		1.878	2.247						
1.70		1.920	2.265						
1.80		1.987							
1.90		2.054							

(b) ΔT = 202° C; ΔR = 25.28 ohms; $\Delta T/T_s$ = 0.656; $\Delta R/R_o$ = 0.3036

M	Nu_∞ at free-stream density, gm/cm^3, of -								
	0.0002	0.0003	0.0004	0.0006	0.0008	0.0010	0.0012	0.0016	0.0024
0.05			0.8130	0.9301	1.040		1.202		1.466
.10			.9441	1.122	1.263		1.495		1.928
.20			1.149	1.394	1.579		1.896		
.40			1.411	1.748	2.003		2.429		
.60			1.606	1.997	2.300		2.813		
.80			1.756	2.209	2.577		3.127		
.90			1.835	2.299	2.668		3.289		
.95			1.858	2.329	2.719				
1.05		1.496	1.863	2.331					
1.10		1.507	1.813	2.346					
1.20		1.546	1.815	2.362					
1.25		1.541	1.858	2.516					
1.30		1.544	1.829	2.409					
1.40		1.574	1.865						
1.50		1.604	1.934						
1.60		1.669	2.034						
1.70		1.718	2.075						
1.80		1.769							
1.90		1.854							

(c) ΔT = 342° C; ΔR = 42.42 ohms; $\Delta T/T_s$ = 1.111; $\Delta R/R_o$ = 0.5094

M	Nu_∞ at free-stream density, gm/cm^3, of -								
	0.0002	0.0003	0.0004	0.0006	0.0008	0.0010	0.0012	0.0016	0.0024
0.05			0.8014	0.9393	1.069		1.231		1.529
.10			.9189	1.115	1.277		1.506		1.983
.20			1.096	1.355	1.574		1.866		
.40			1.326	1.693	1.950		2.394		
.60			1.485	1.933	2.243		2.763		
.80			1.601	2.131	2.483		3.095		
.90			1.691	2.208	2.581		3.255		
.95			1.722	2.224	2.626				
1.05		1.323	1.747	2.182					
1.10		1.361	1.645	2.187					
1.20		1.389	1.645	2.182					
1.25		1.397	1.684	2.310					
1.30		1.392	1.664	2.311					
1.40		1.440	1.669						
1.50		1.444	1.754						
1.60		1.493	1.817						
1.70		1.521	1.966						
1.80		1.565							
1.90		1.644							

TABLE XIV

THERMAL CONDUCTIVITY OF DRY AIR AS A FUNCTION OF M FOR $T_s = 303^\circ$ K

$\left[k_o = 5.770 \times 10^{-5} \text{ cal/cm/sec/}^\circ\text{K}\right]$

M	T, $^\circ$K	k/k_o
0.05	302.8	1.096
.10	302.4	1.095
.20	300.6	1.089
.40	293.6	1.066
.60	282.6	1.031
.80	268.6	.9847
.90	260.8	.9588
.95	256.7	.9450
1.05	248.3	.9166
1.25	230.9	.8574
1.50	209.0	.7811
1.75	187.9	.7063
1.90	176.0	.6635

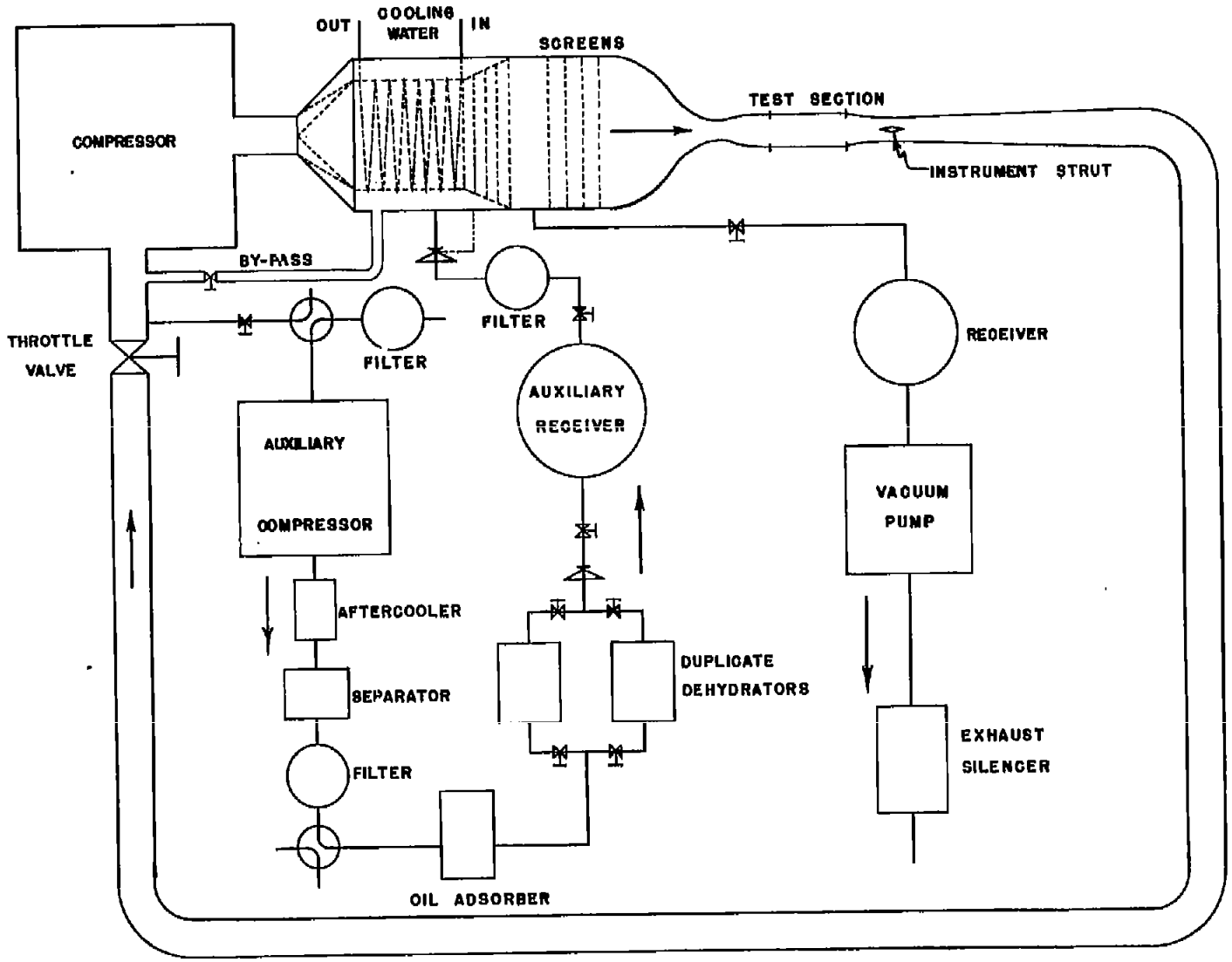

Figure 1.- Diagrammatic sketch of supersonic wind tunnel.

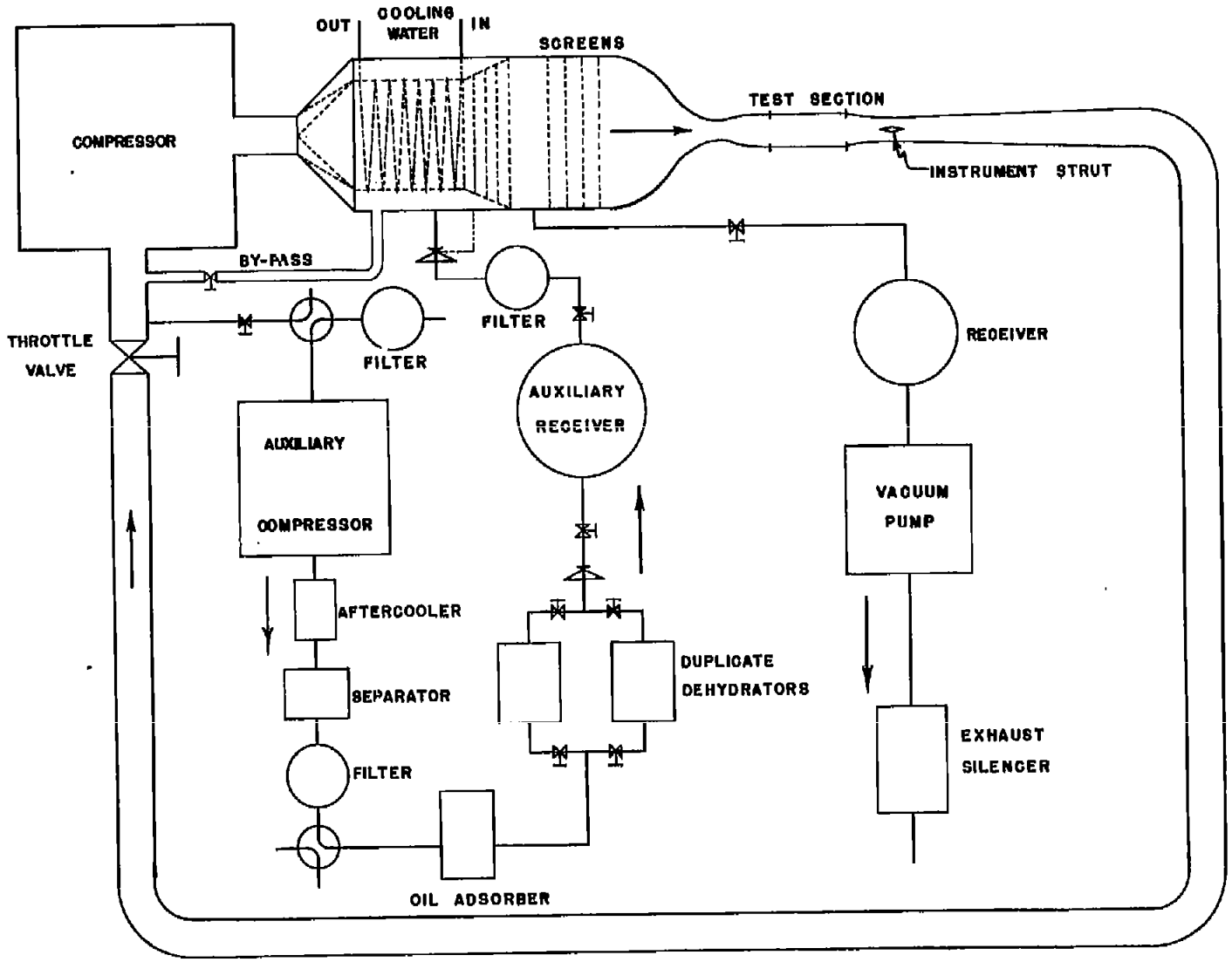

Figure 1.- Diagrammatic sketch of supersonic wind tunnel.

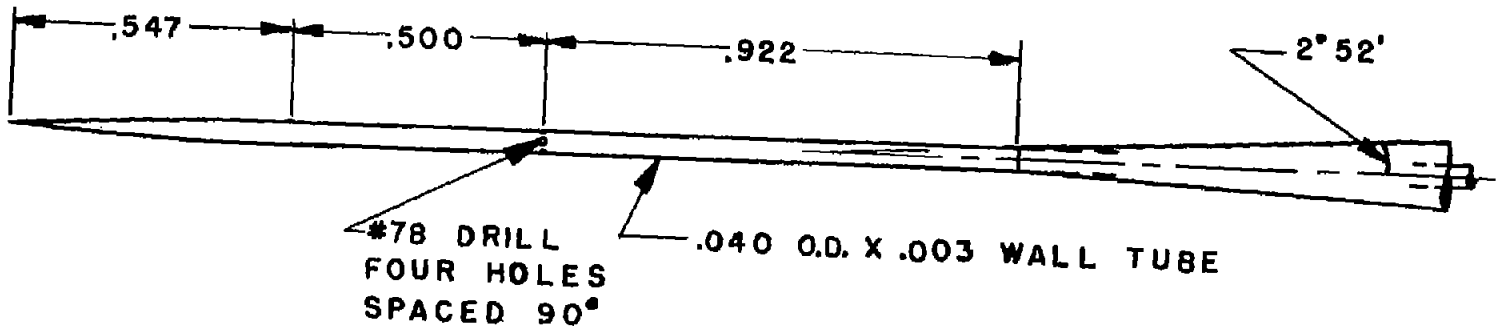

Figure 3.- Static-pressure probe. Dimensions are in inches.

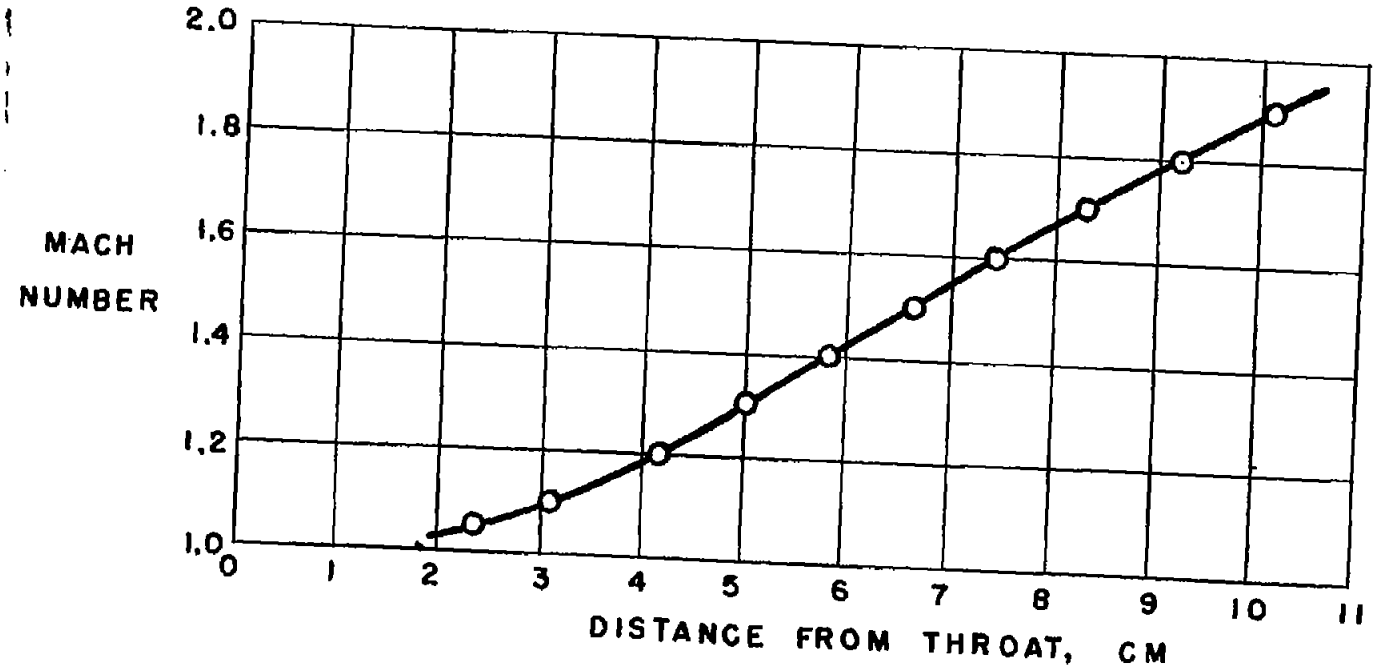

Figure 4.- Calibration curve for supersonic nozzle. ρ = 0.0006 gram per cubic centimeter.

L-87569

Figure 5.- Schlieren photograph of hot-wire probe in supersonic nozzle.

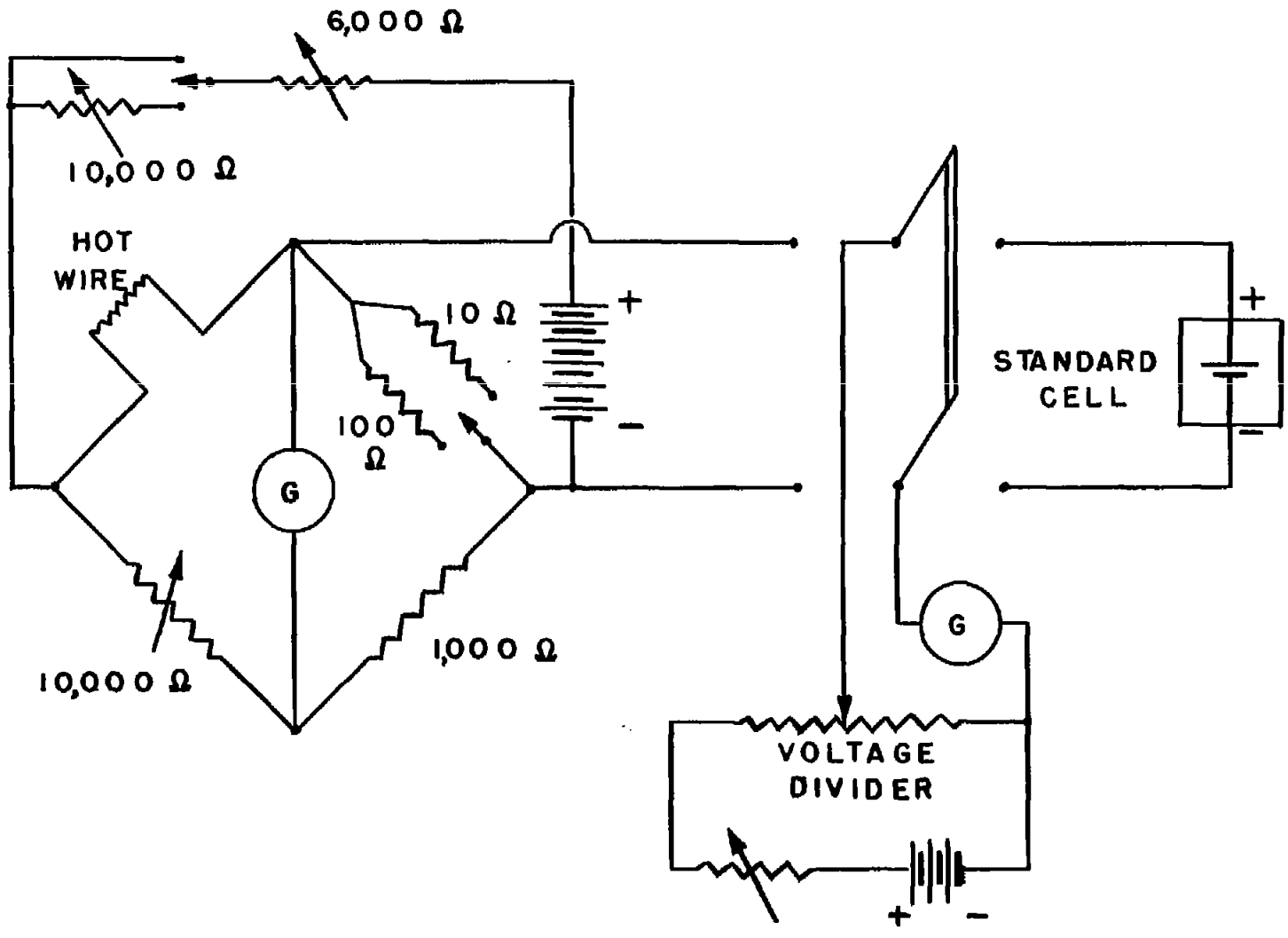

Figure 6.- Electrical circuit.

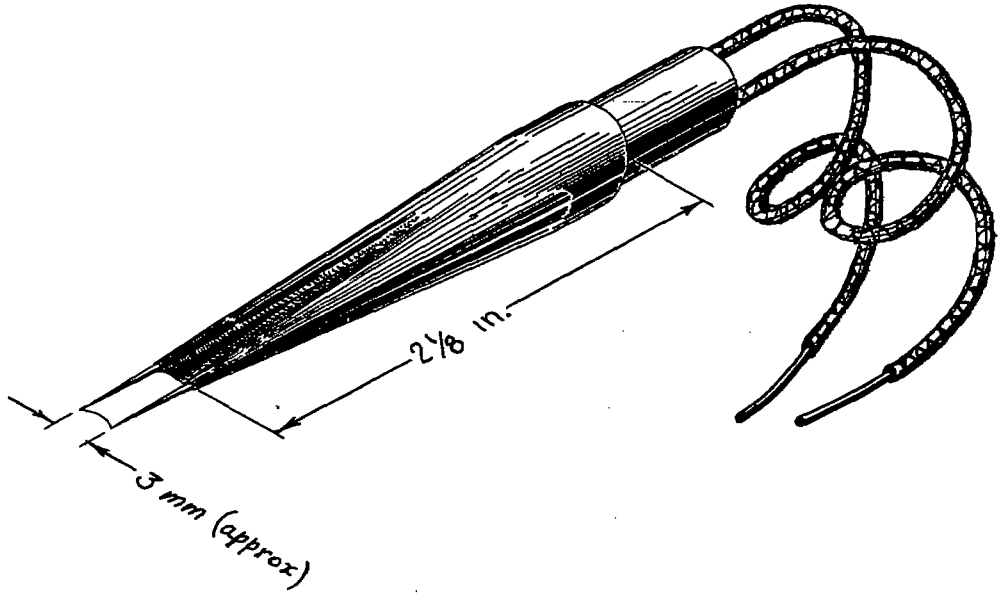

Figure 7.- Hot-wire probe. Included angle between vertical faces is 4° and that between horizontal faces is 8°.

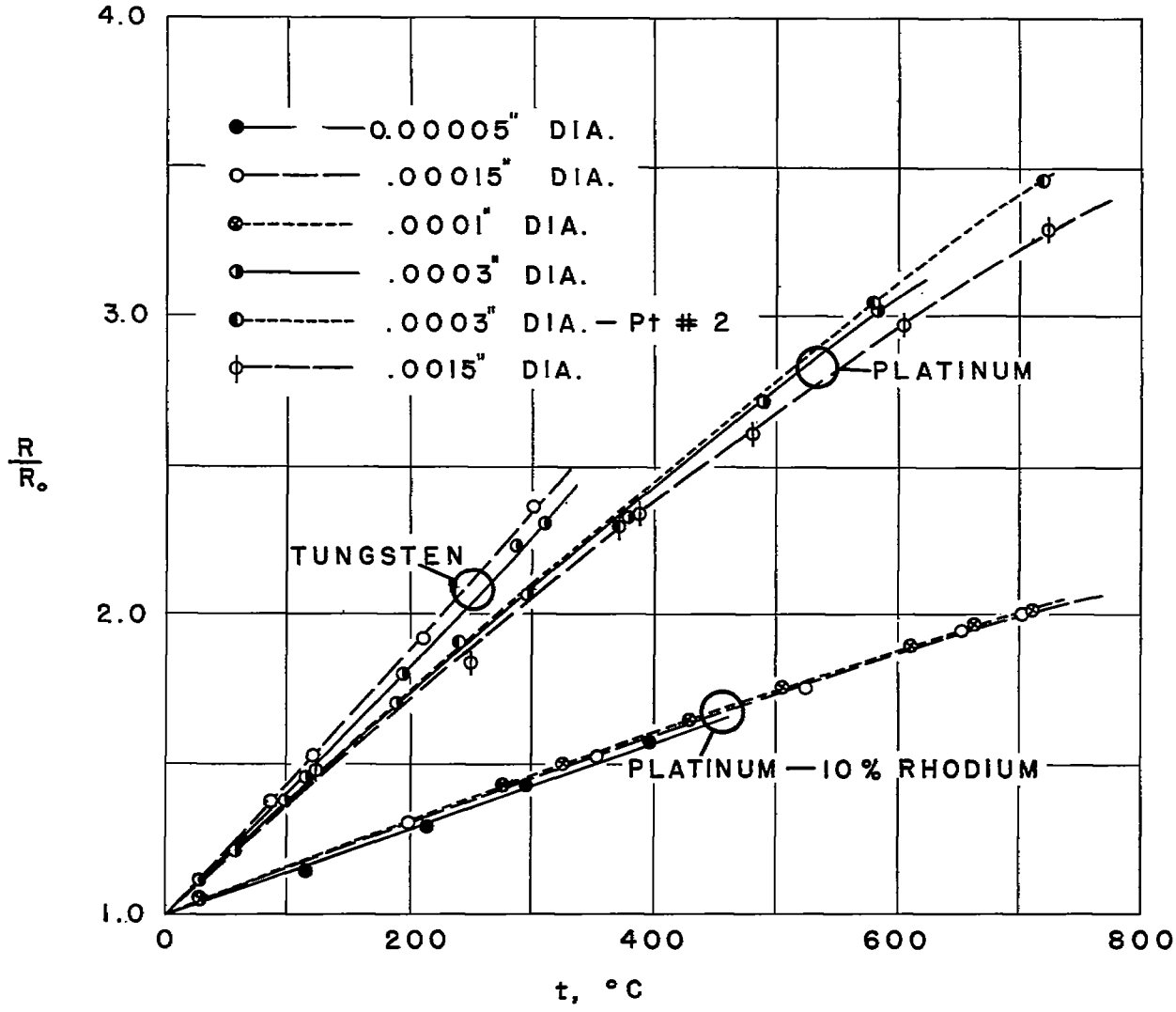

Figure 8.- Temperature-resistance relationship for various wires.

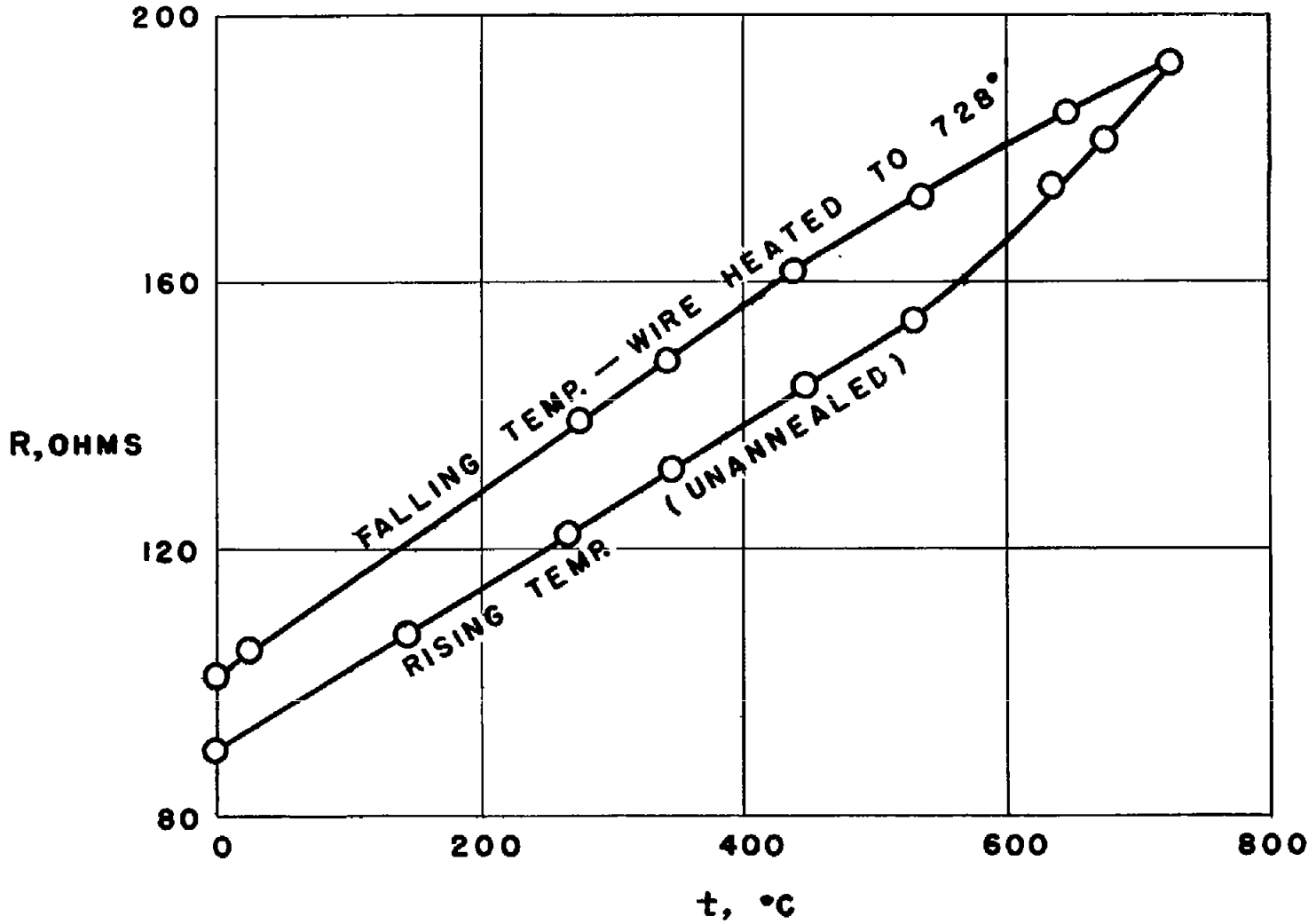

Figure 9.- Effect of annealing 0.00015-inch-diameter platinum wire containing 10 percent rhodium.

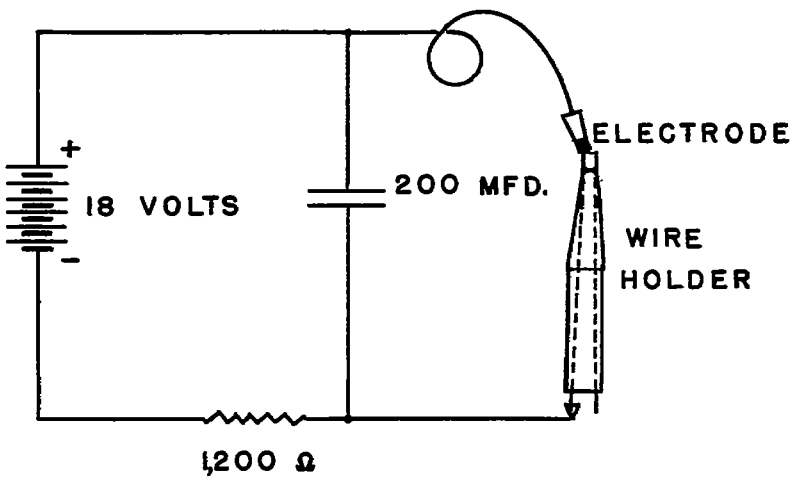

Figure 10.- Electric-arc welding circuit.

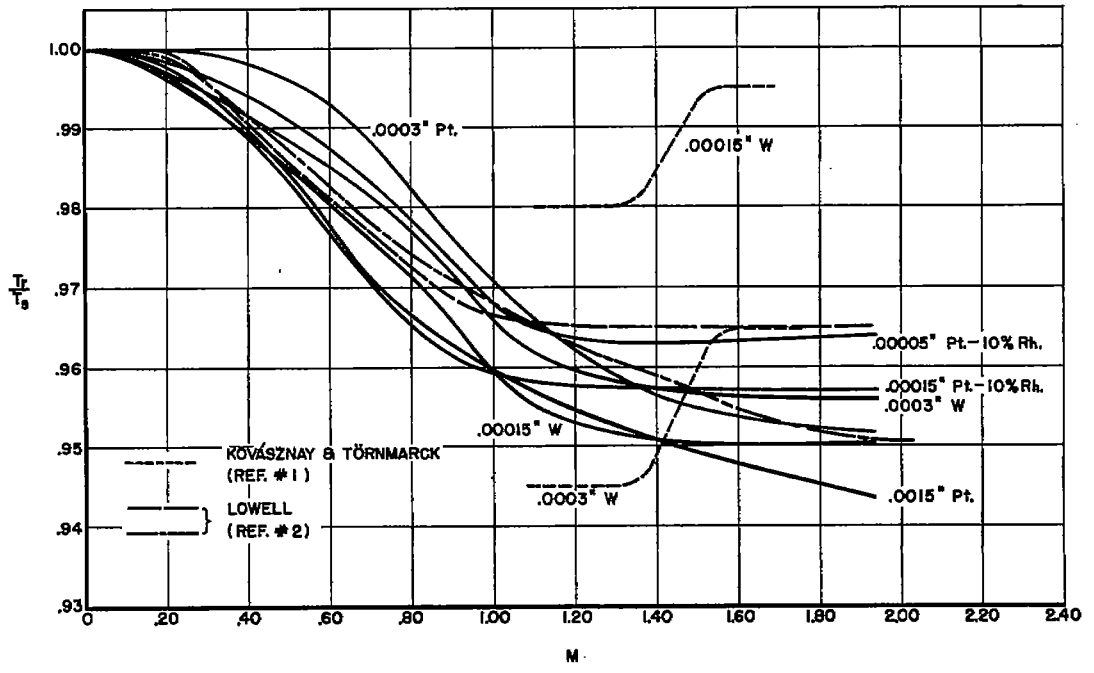

(a) Various wires, all normal to wind.

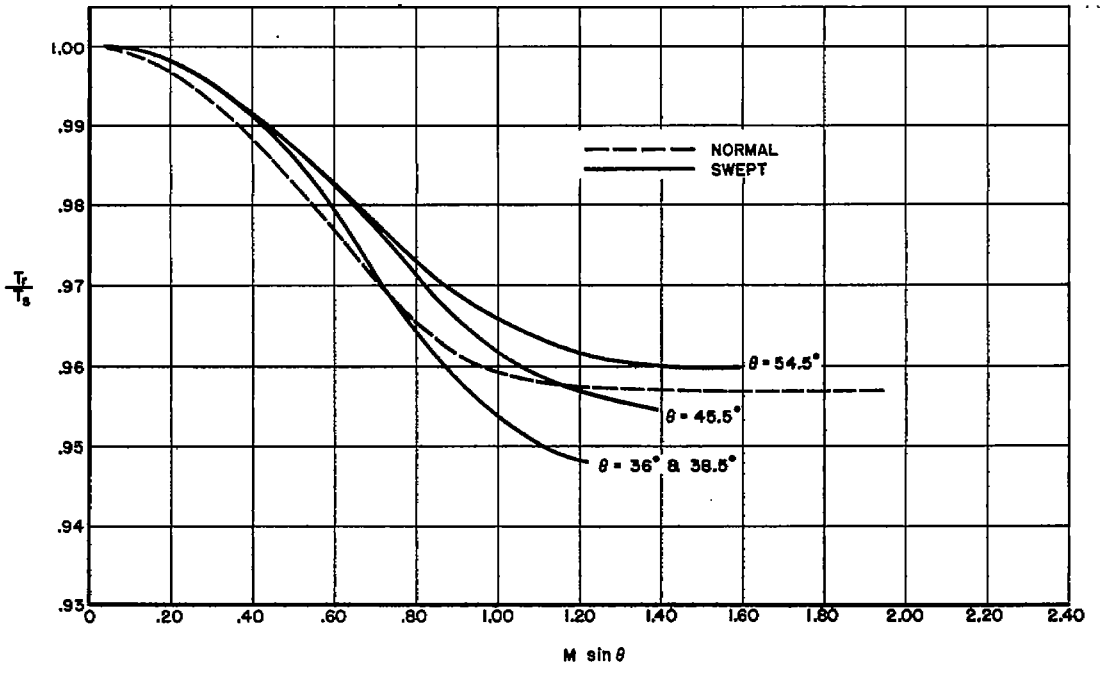

(b) 0.00015-inch-diameter platinum wire containing 10 percent rhodium both normal to wind and swept.

Figure 11.- Temperature-recovery ratio for various wires.

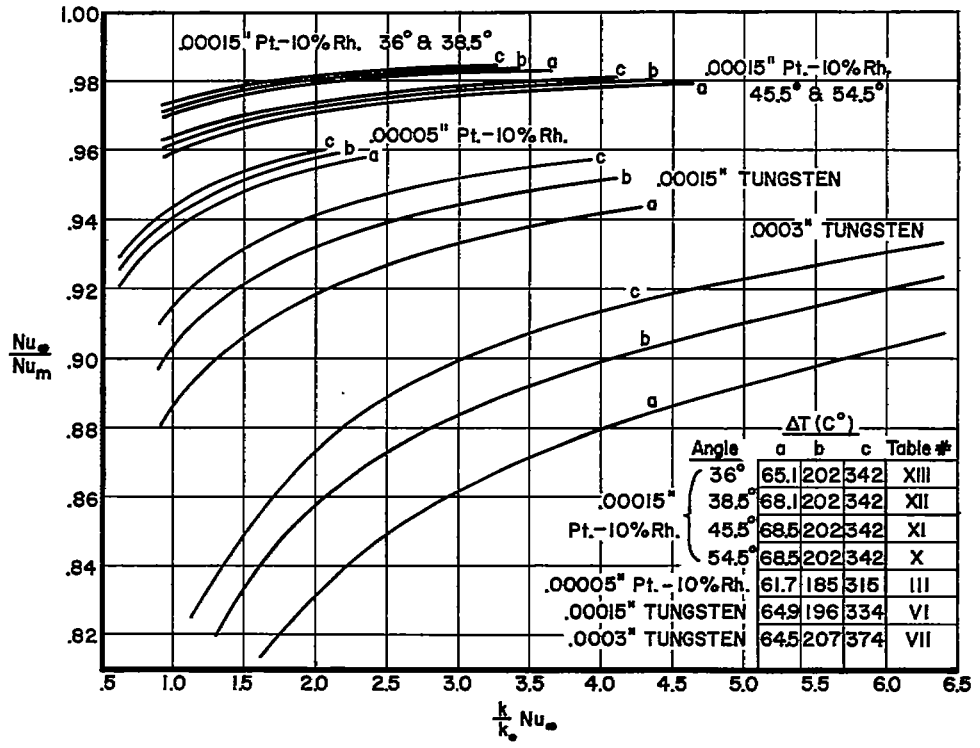

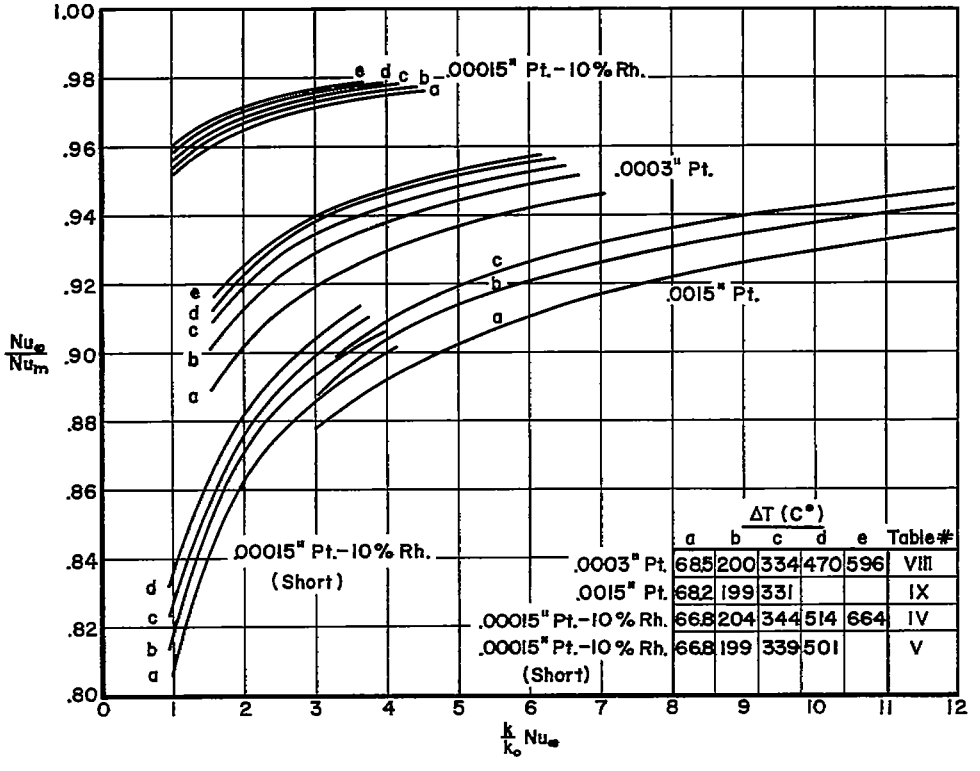

Figure 12.- End-loss correction factors.

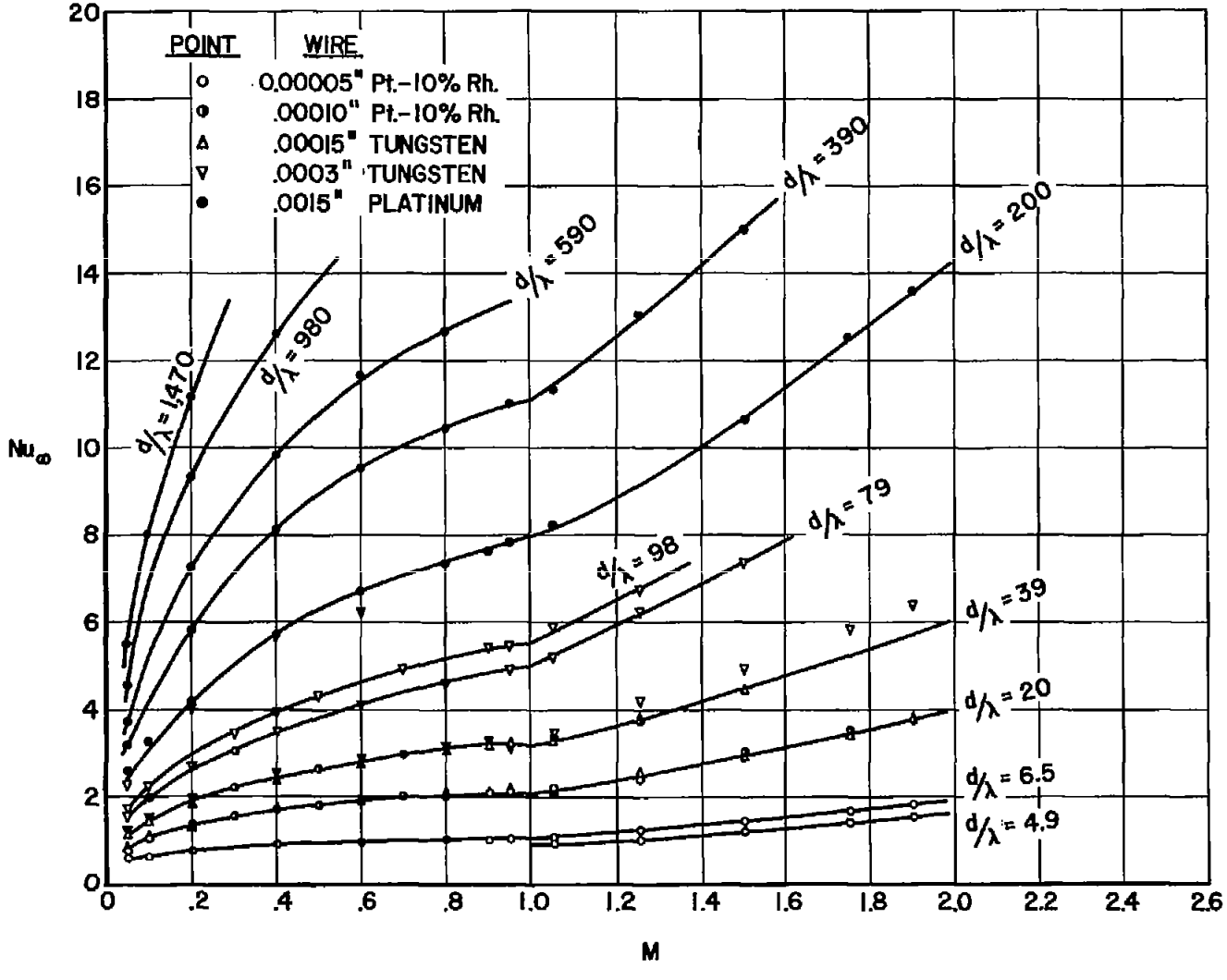

Figure 13.- Variation of Nusselt number with Mach number for infinitely long wires.

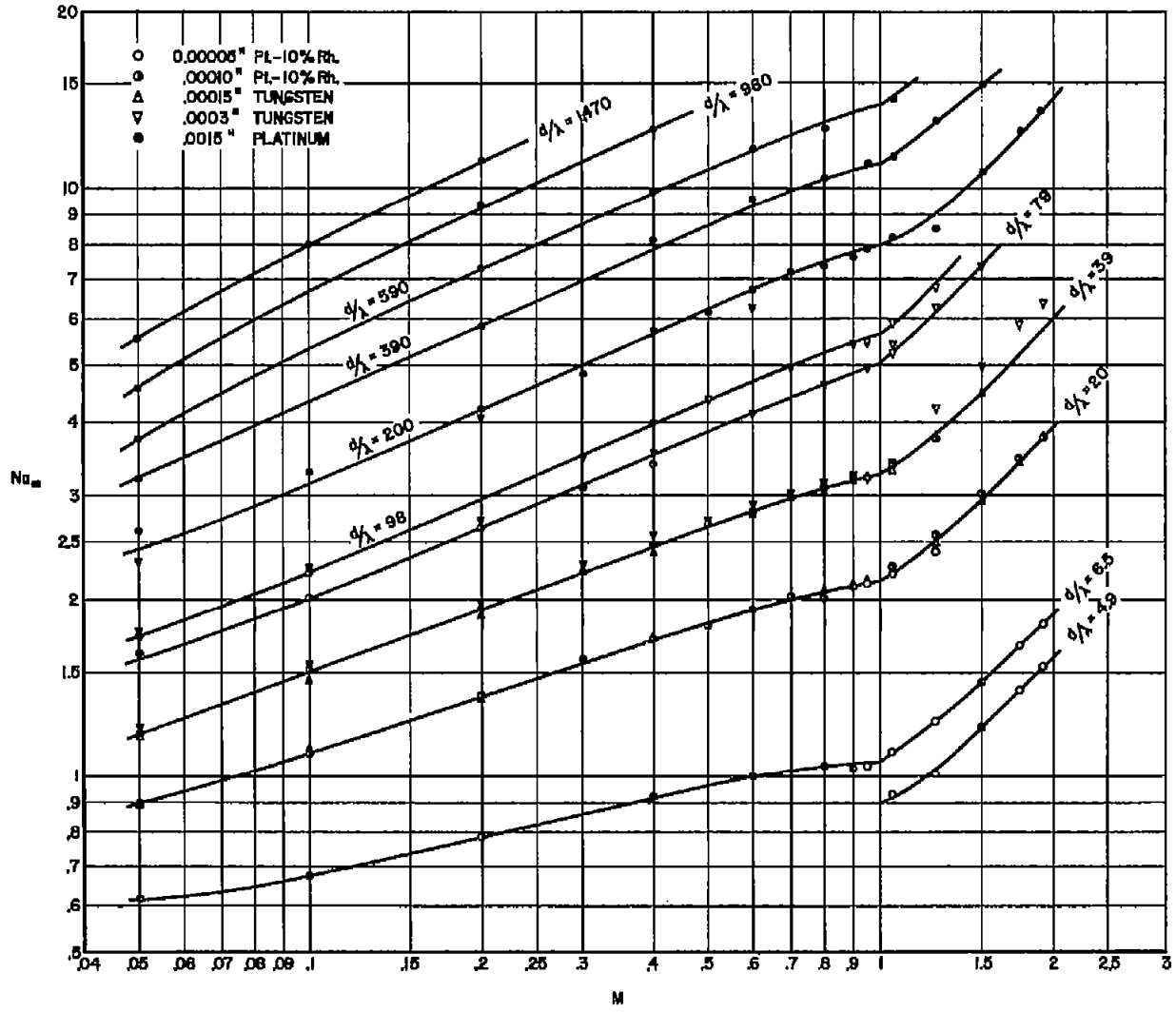

Figure 14.- Logarithmic variation of Nusselt number with Mach number for infinitely long wires.

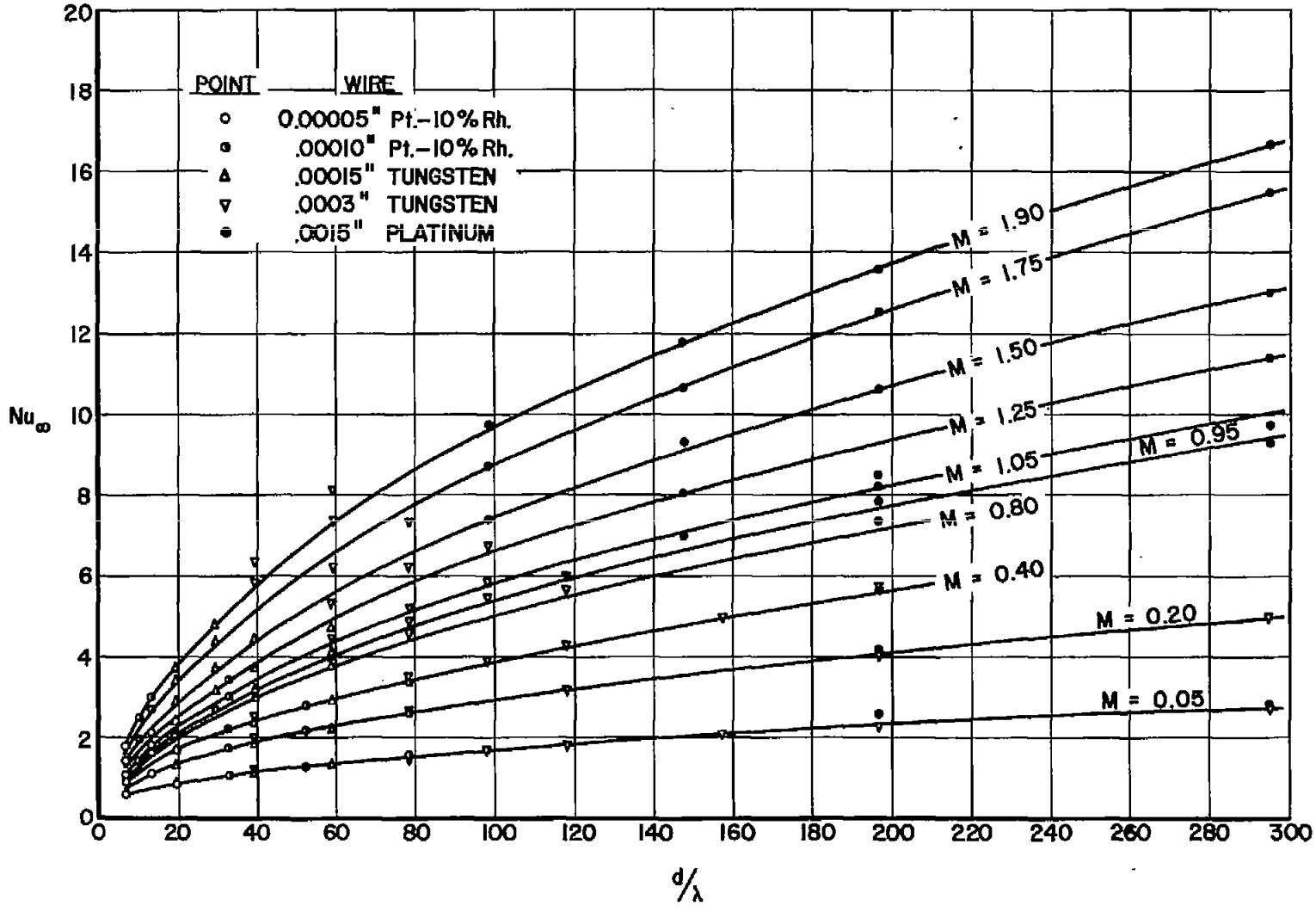

Figure 15.- Variation of Nusselt number with d/λ for infinitely long wires.

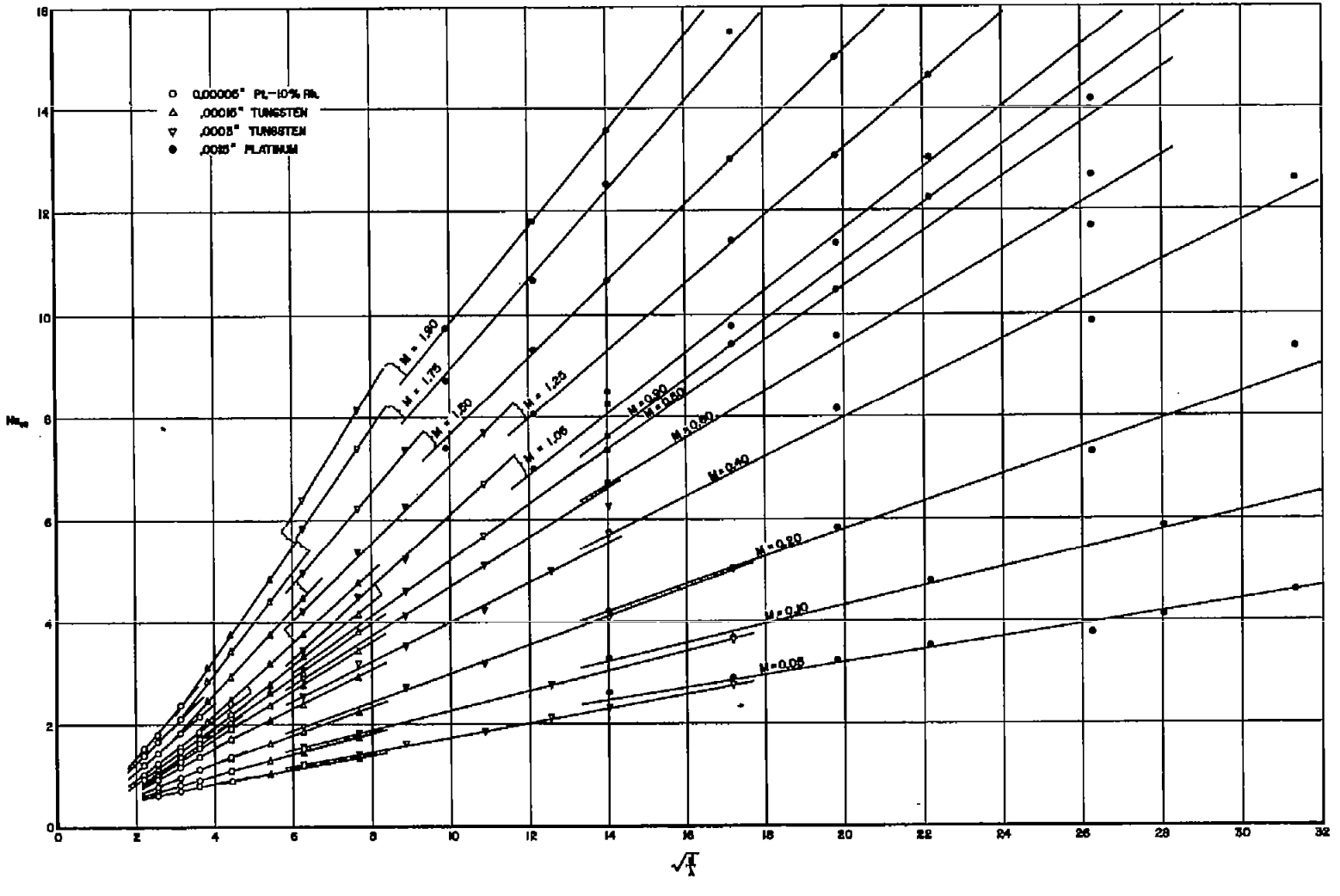

Figure 16.- Variation of Nusselt number with $\sqrt{d/\lambda}$ for infinitely long wires.

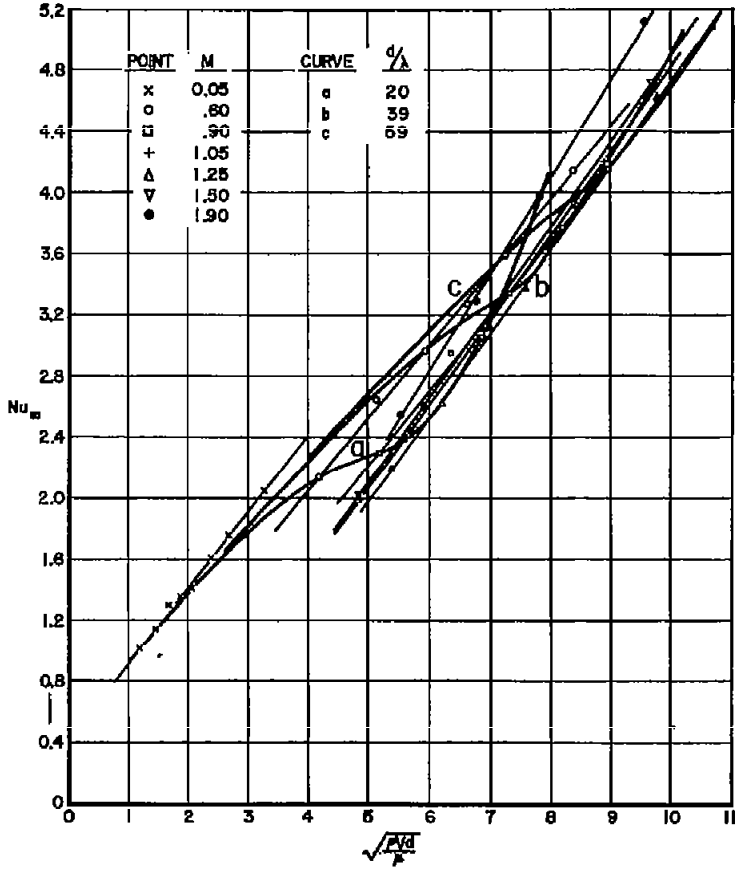

(a) All data computed at theoretical free-stream temperature.

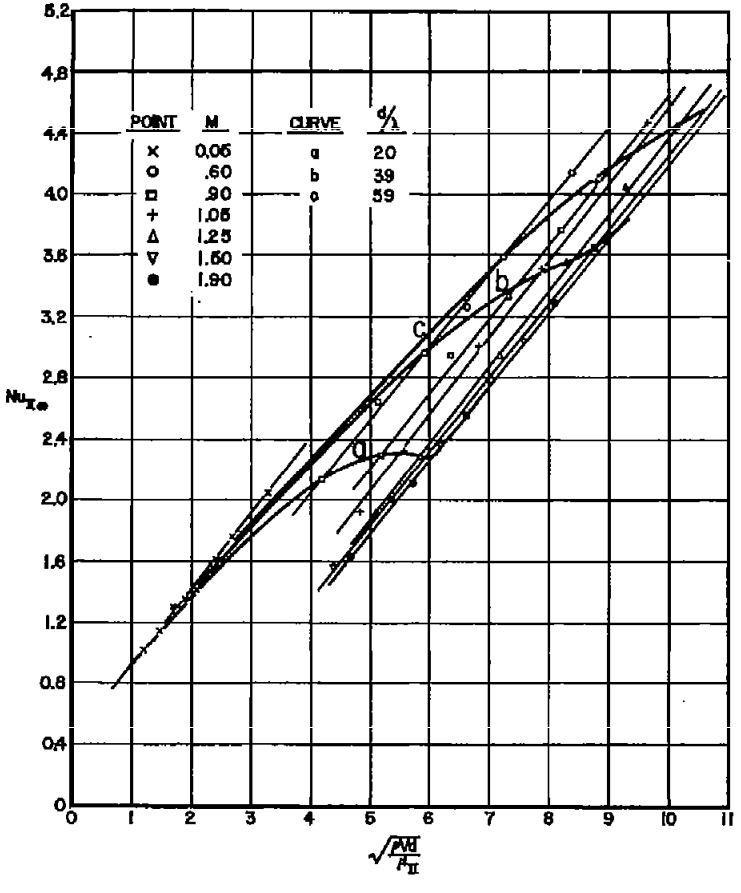

(b) Subsonic data computed at theoretical free-stream temperature; supersonic data computed at theoretical temperature behind normal shock.

Figure 17.- Dependence of Nusselt number on Reynolds number for 0.00015-inch-diameter platinum wire containing 10 percent rhodium. Wire with air conductivity and viscosity evaluated at assumed ambient conditions as indicated.

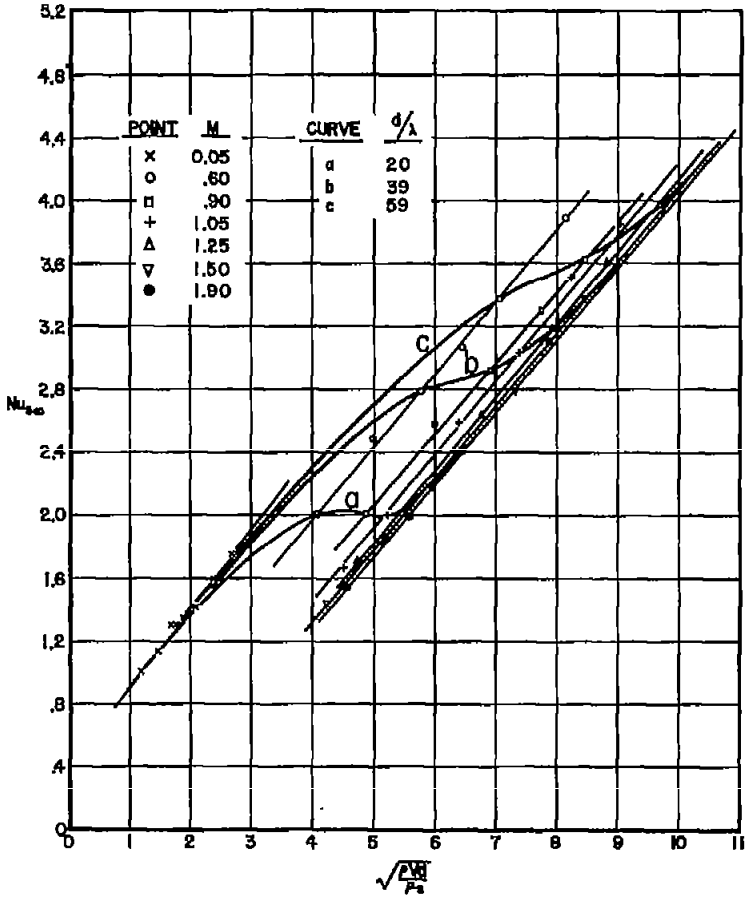

(c) All data computed at stagnation temperature.

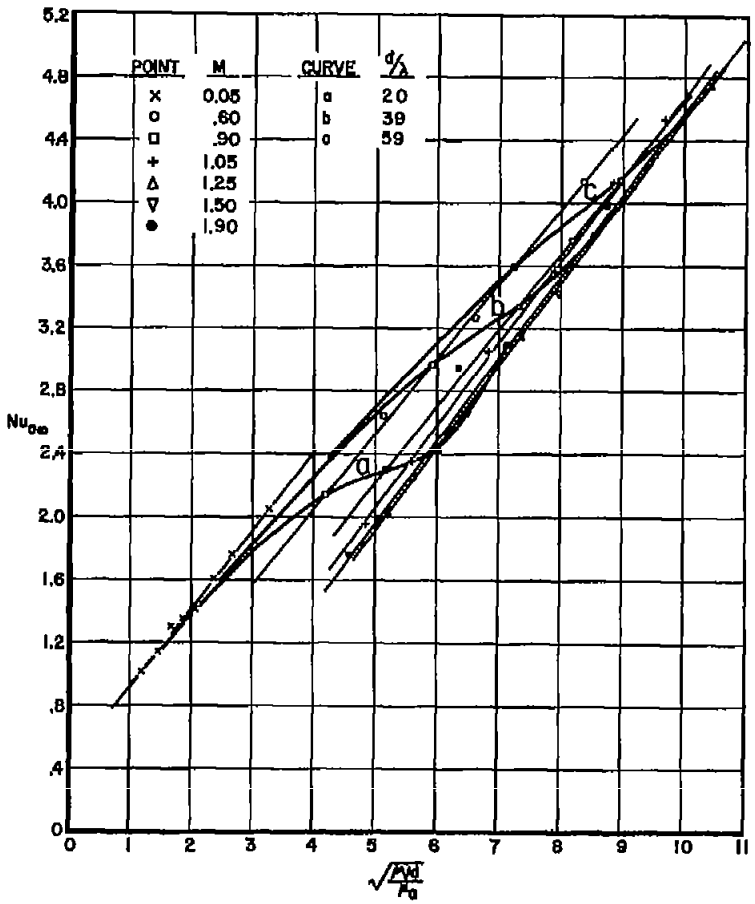

(d) Subsonic data computed at theoretical free-stream temperature; supersonic data computed at mean between theoretical free-stream temperature and temperature behind normal shock.

Figure 17.- Concluded.

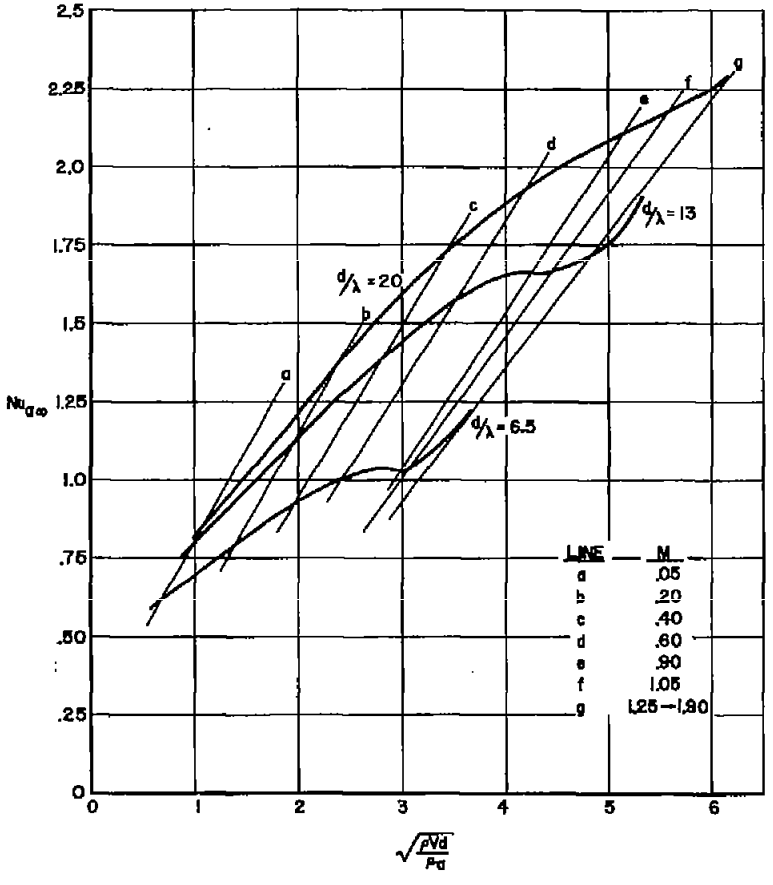

(a) 0.00005-inch-diameter platinum wire containing 10 percent rhodium.

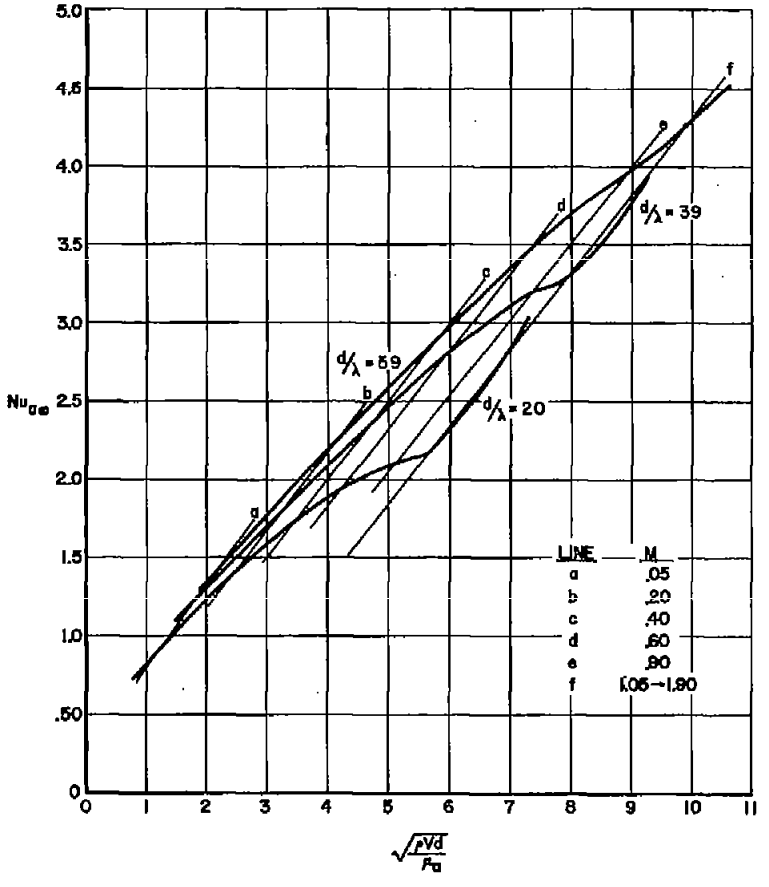

(b) 0.00015-inch-diameter tungsten wire.

Figure 18.- Variation of Nusselt number with Reynolds number for wires of various diameters. Subsonic data computed at theoretical free-stream temperature; supersonic data computed at mean between theoretical free-stream temperature and temperature behind normal shock.

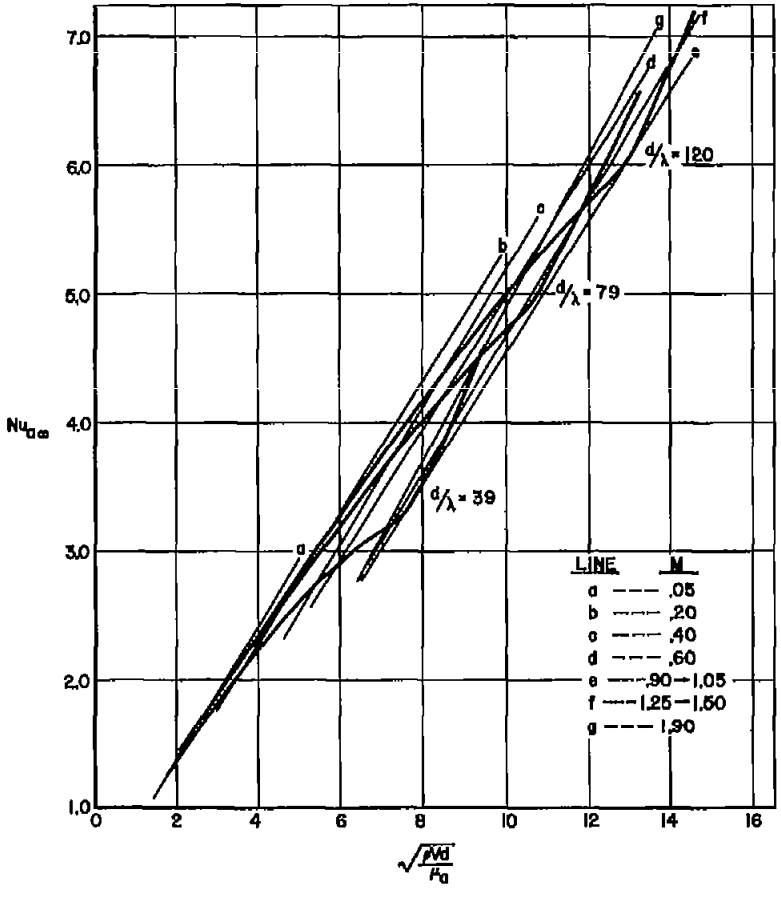

(c) 0.0003-inch-diameter tungsten wire.

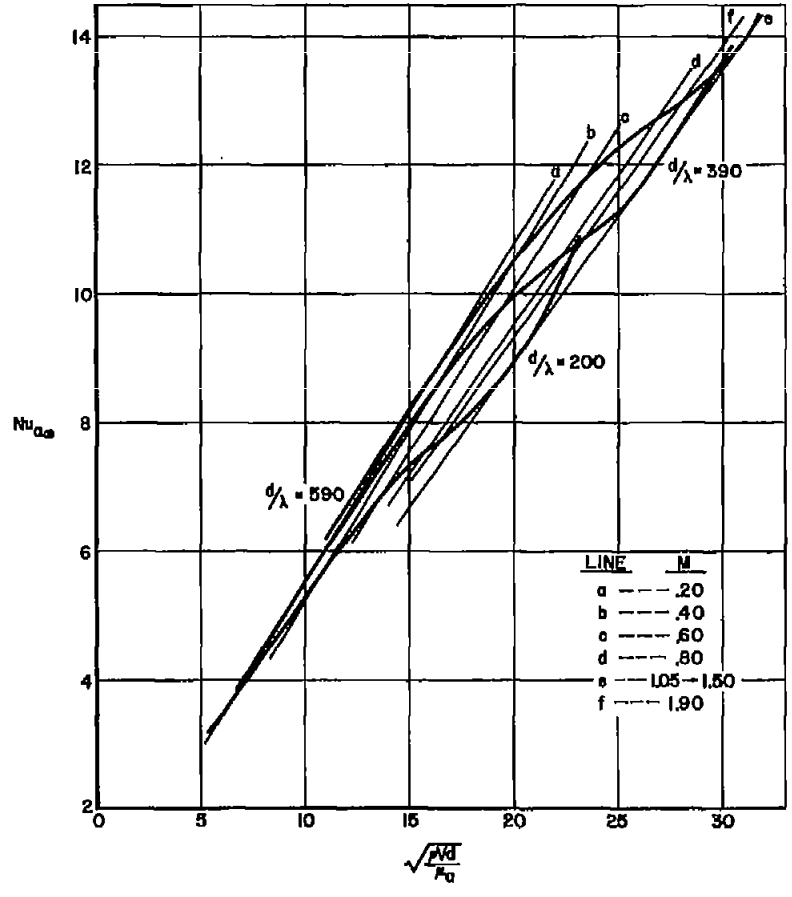

(d) 0.0015-inch-diameter platinum wire.

Figure 18.- Concluded.

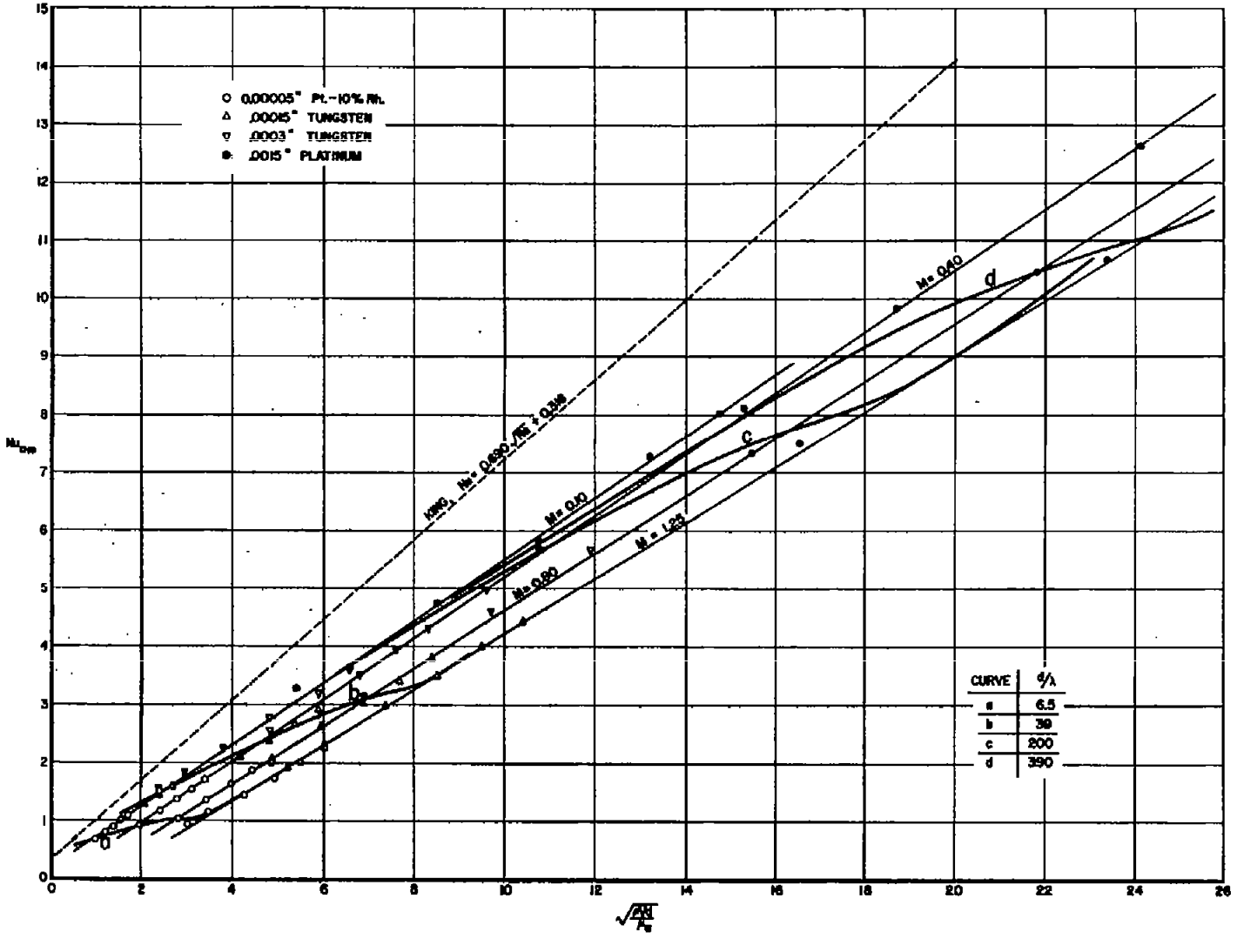

Figure 19.- Comparison of data for wires of several diameters with King's formula.

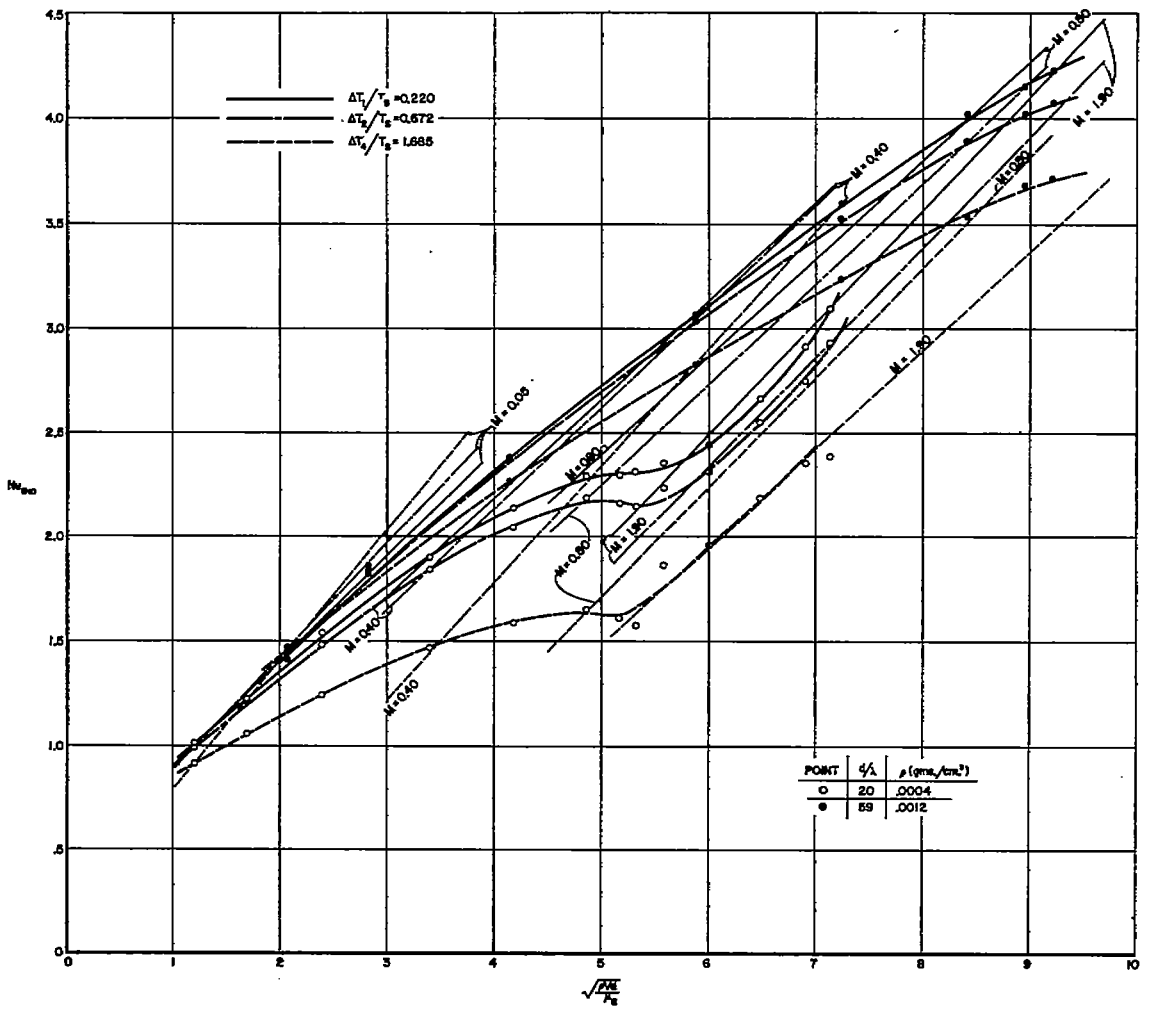

Figure 20.- Effect of temperature loading on Nusselt number at selected densities and Mach numbers. 0.00015-inch-diameter platinum wire containing 10 percent rhodium.

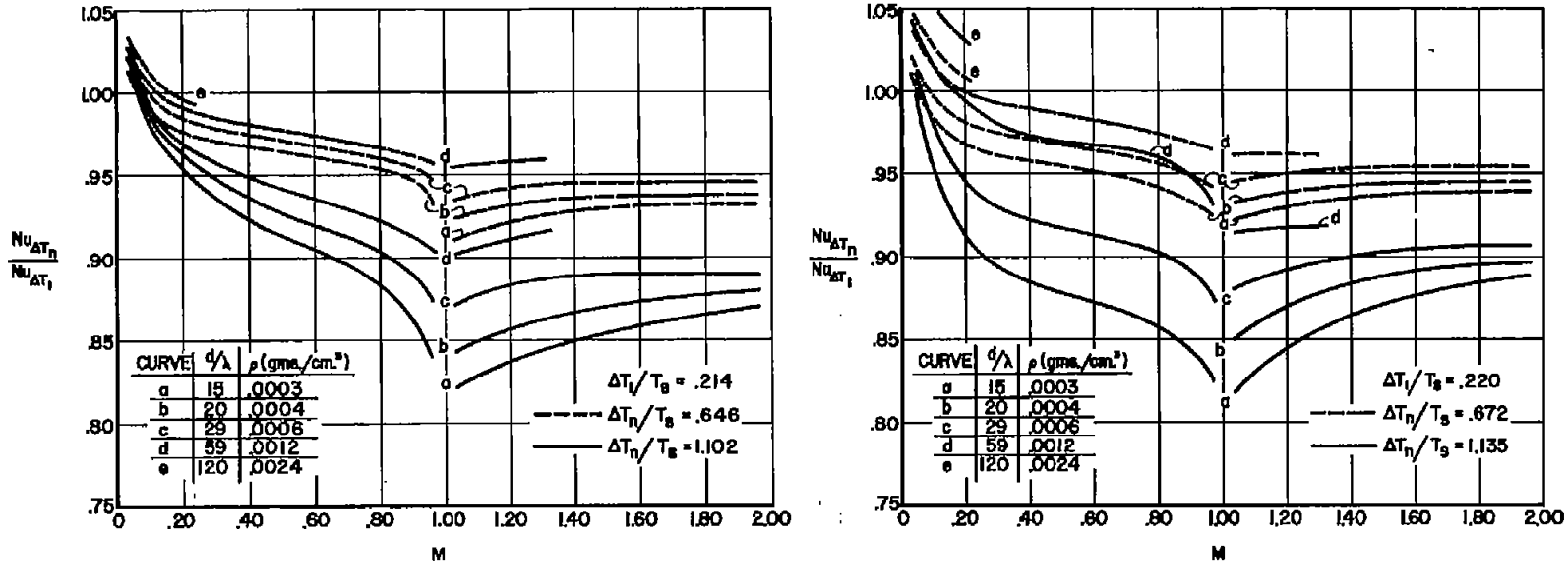

(a) 0.00015-inch-diameter tungsten wire.

(b) 0.00015-inch-diameter platinum wire containing 10 percent rhodium.

Figure 21.- Variation of Nusselt number with Mach number for several wire diameters at selected densities and temperature loadings.

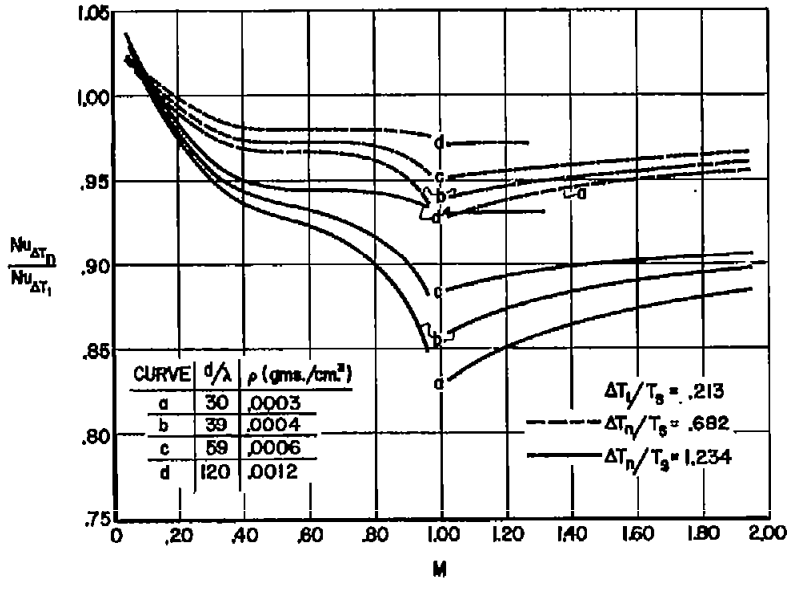

(c) 0.0003-inch-diameter tungsten wire.

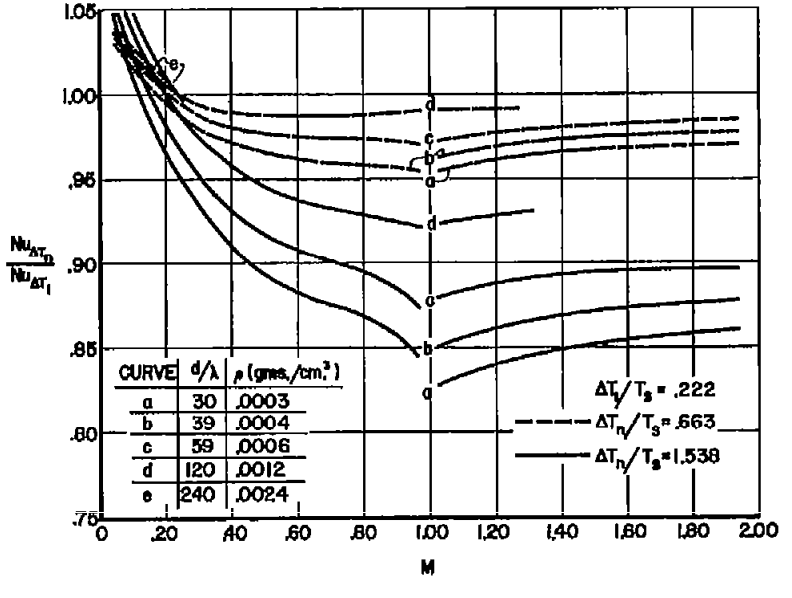

(d) 0.0003-inch-diameter platinum wire.

Figure 21.- Continued.

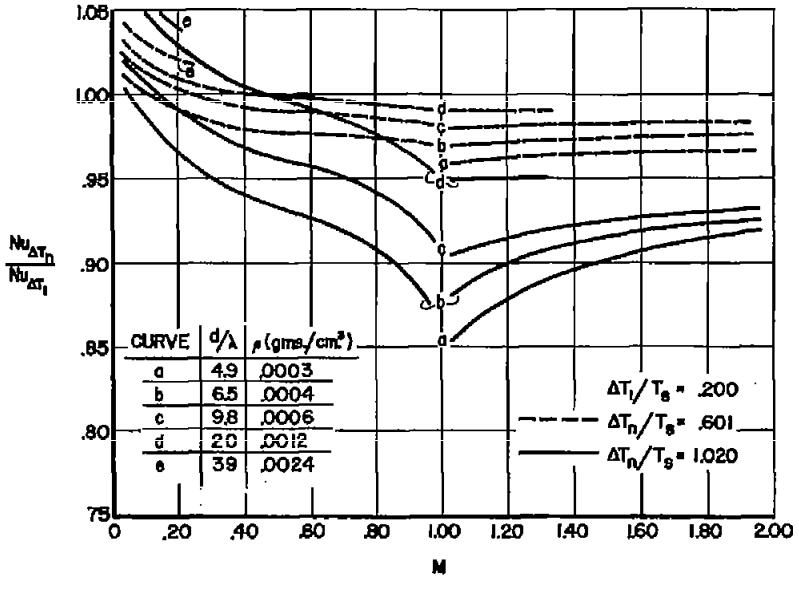

(e) 0.00005-inch-diameter platinum wire containing 10 percent rhodium.

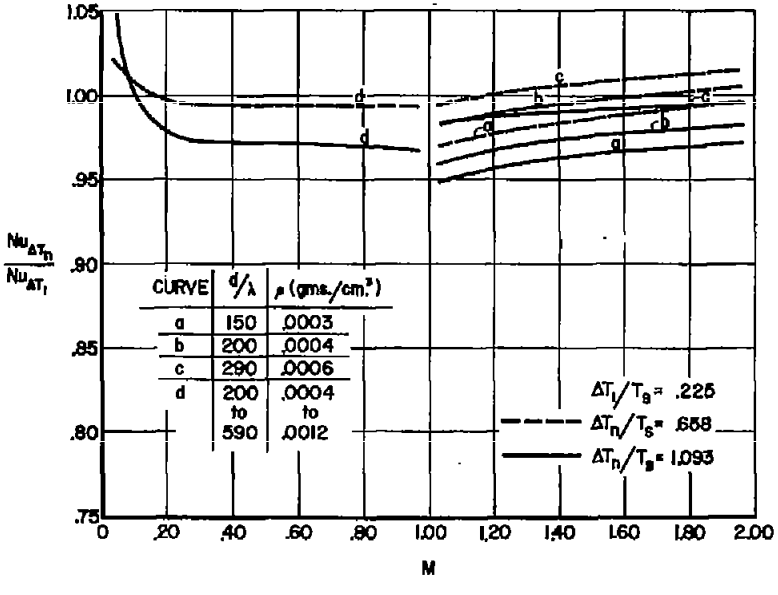

(f) 0.0015-inch-diameter platinum wire.

Figure 21.- Concluded.

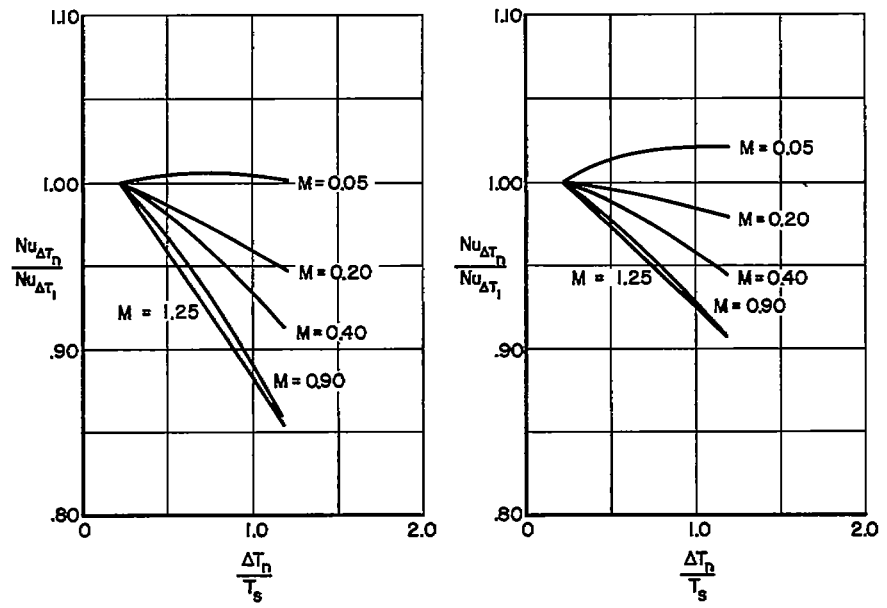

(a) 0.00015-inch-diameter tungsten wire; ρ = 0.0004 gram per cubic centimeter; d/λ = 20.

(b) 0.00015-inch-diameter tungsten wire; ρ = 0.0012 gram per cubic centimeter; d/λ = 59.

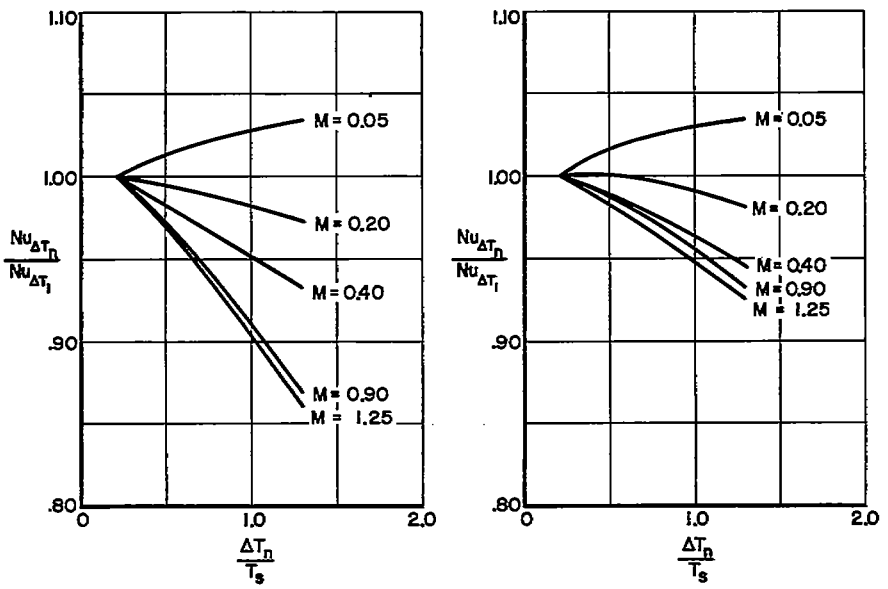

(c) 0.0003-inch-diameter tungsten wire; ρ = 0.0004 gram per cubic centimeter; d/λ = 39.

(d) 0.0003-inch-diameter tungsten wire; ρ = 0.0012 gram per cubic centimeter; d/λ = 120.

Figure 22.- Variation of Nusselt number with temperature loading for several wire diameters at selected densities and Mach numbers.

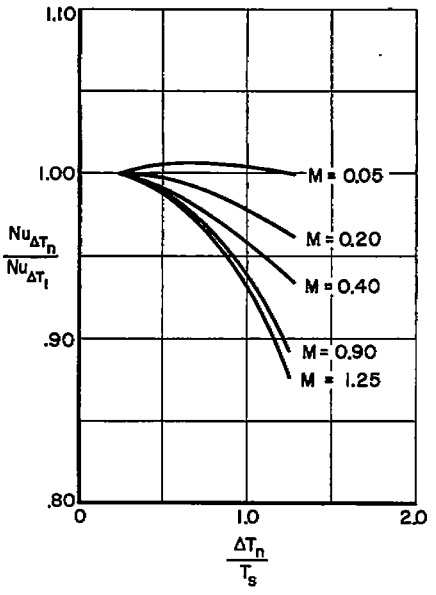

(e) 0.00005-inch-diameter platinum wire containing 10 percent rhodium; ρ = 0.0004 gram per cubic centimeter; d/λ = 6.5.

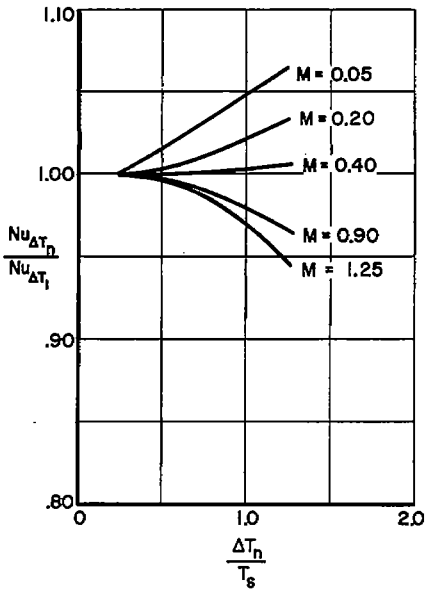

(f) 0.00005-inch-diameter platinum wire containing 10 percent rhodium; ρ = 0.0012 gram per cubic centimeter; d/λ = 20.

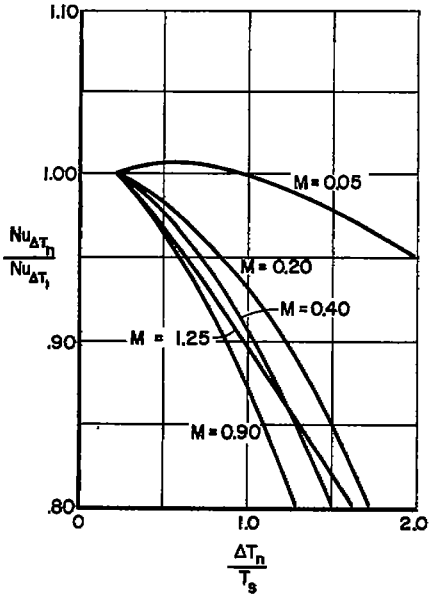

(g) 0.00015-inch-diameter platinum wire containing 10 percent rhodium; ρ = 0.0004 gram per cubic centimeter; d/λ = 20.

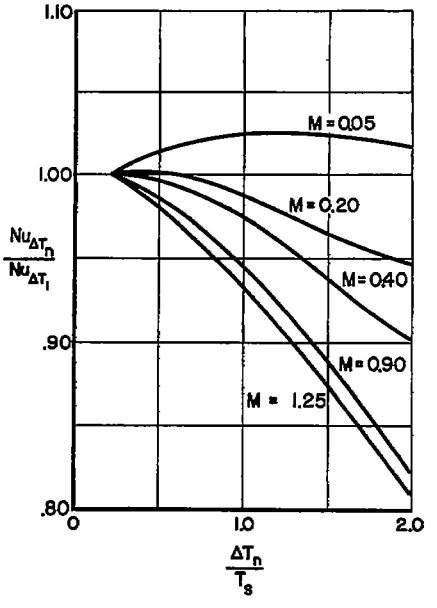

(h) 0.00015-inch-diameter platinum wire containing 10 percent rhodium; ρ = 0.0012 gram per cubic centimeter; d/λ = 59.

Figure 22.- Continued.

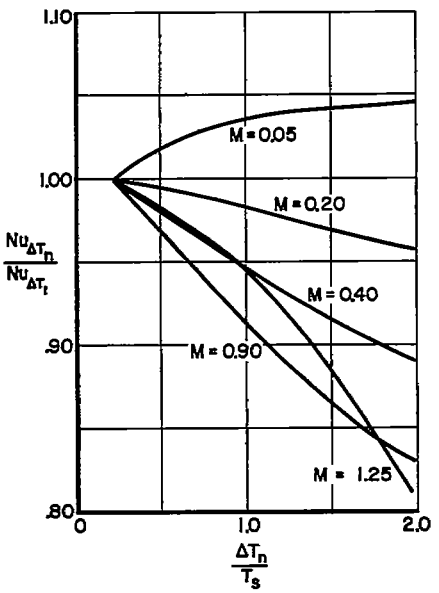

(i) 0.0003-inch-diameter platinum wire; ρ = 0.0004 gram per cubic centimeter; d/λ = 39.

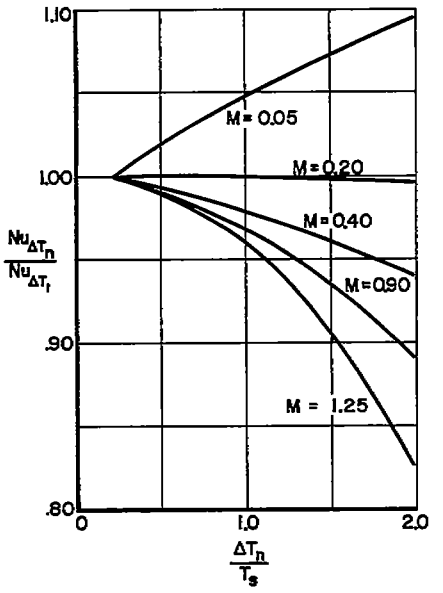

(j) 0.0003-inch-diameter platinum wire; ρ = 0.0012 gram per cubic centimeter; d/λ = 120.

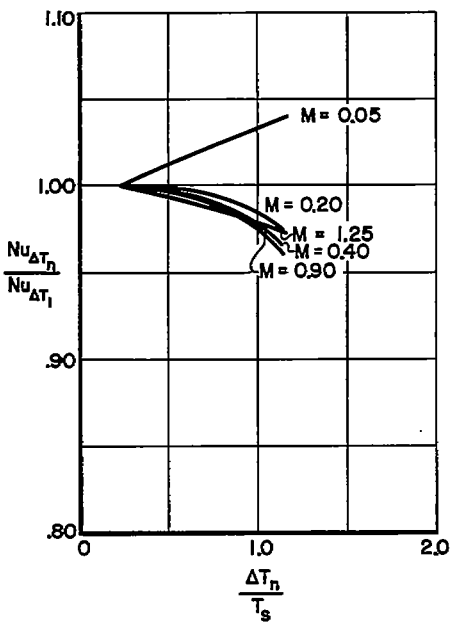

(k) 0.0015-inch-diameter platinum wire; ρ = 0.0004 gram per cubic centimeter; d/λ = 200.

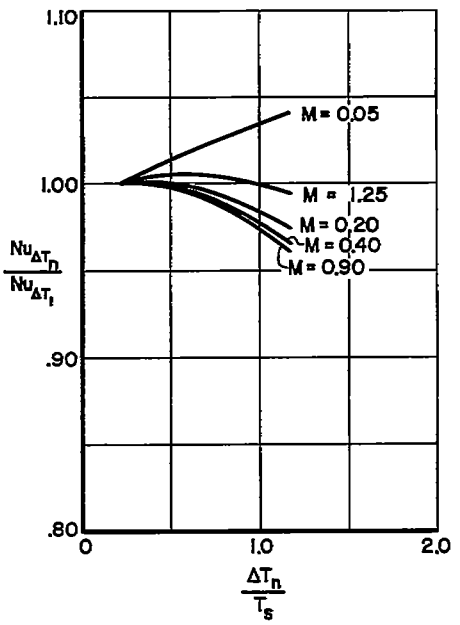

(l) 0.0015-inch-diameter platinum wire; ρ = 0.0012 gram per cubic centimeter; d/λ = 590.

Figure 22.- Concluded.

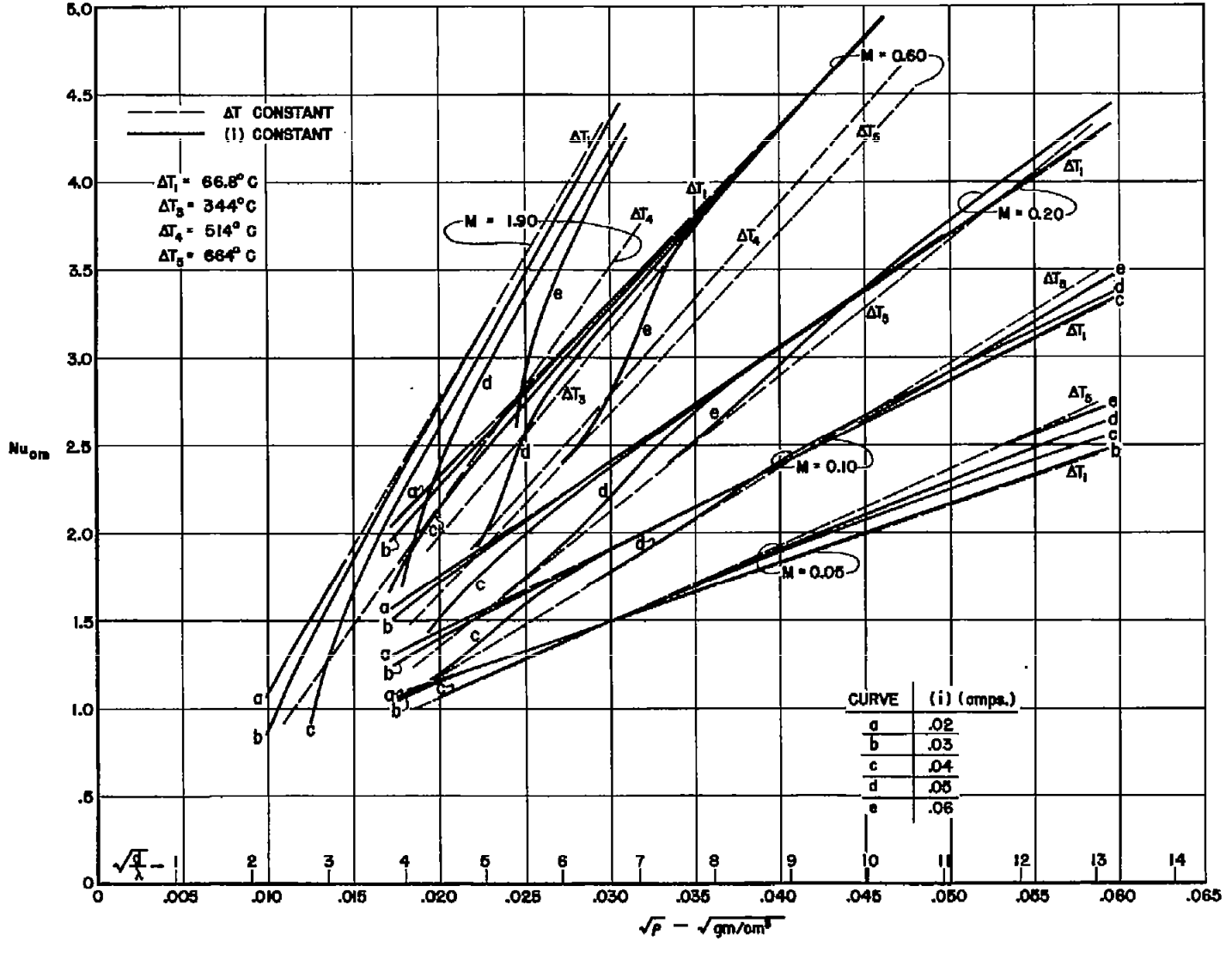

Figure 23.- Comparison of hot-wire calibrations with density variable under constant-temperature and constant-current operation. 0.00015-inch-diameter platinum wire containing 10 percent rhodium.

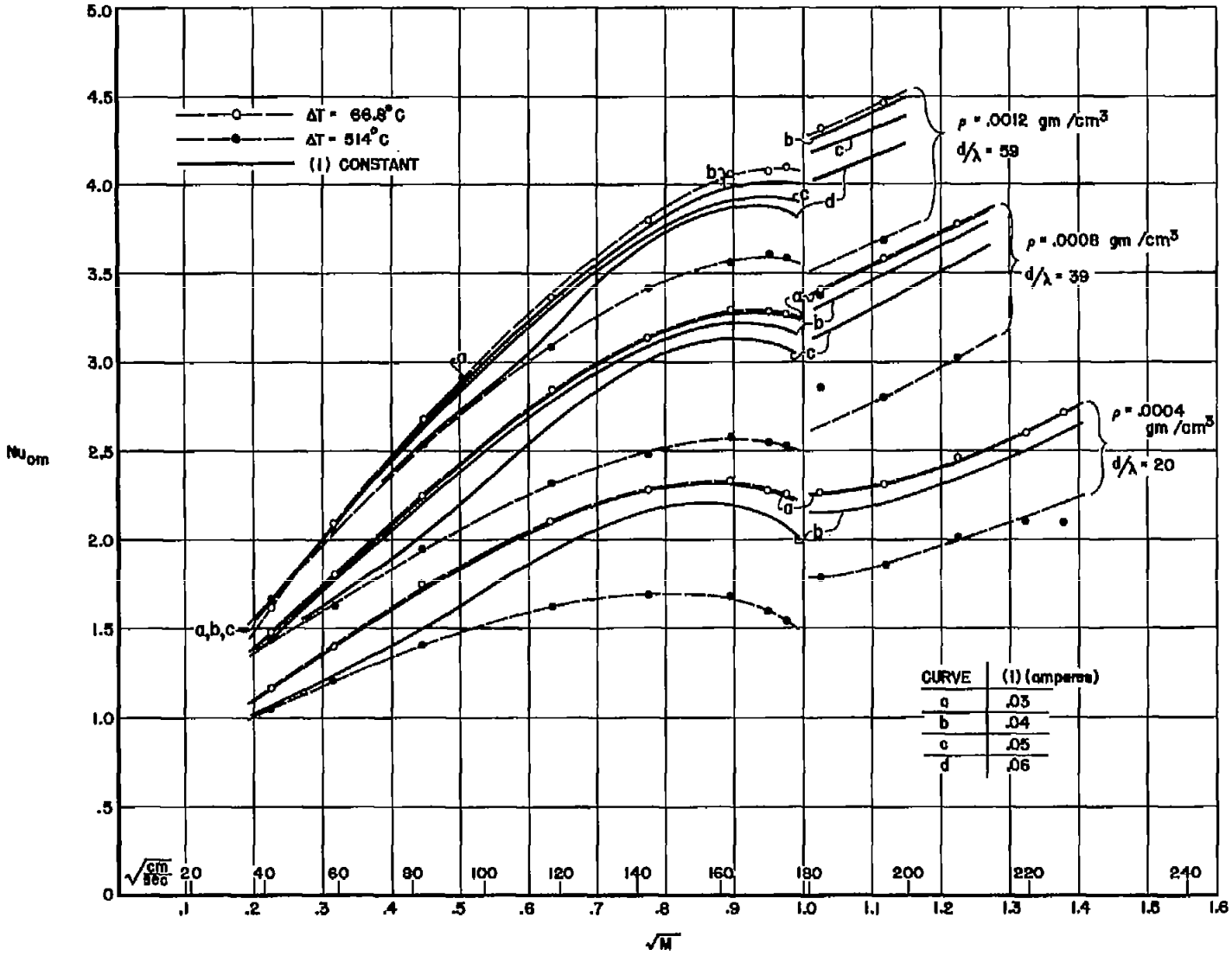

Figure 24.- Comparison of hot-wire calibrations with Mach number variable under constant-temperature and constant-current operation. 0.00015-inch-diameter platinum wire containing 10 percent rhodium.

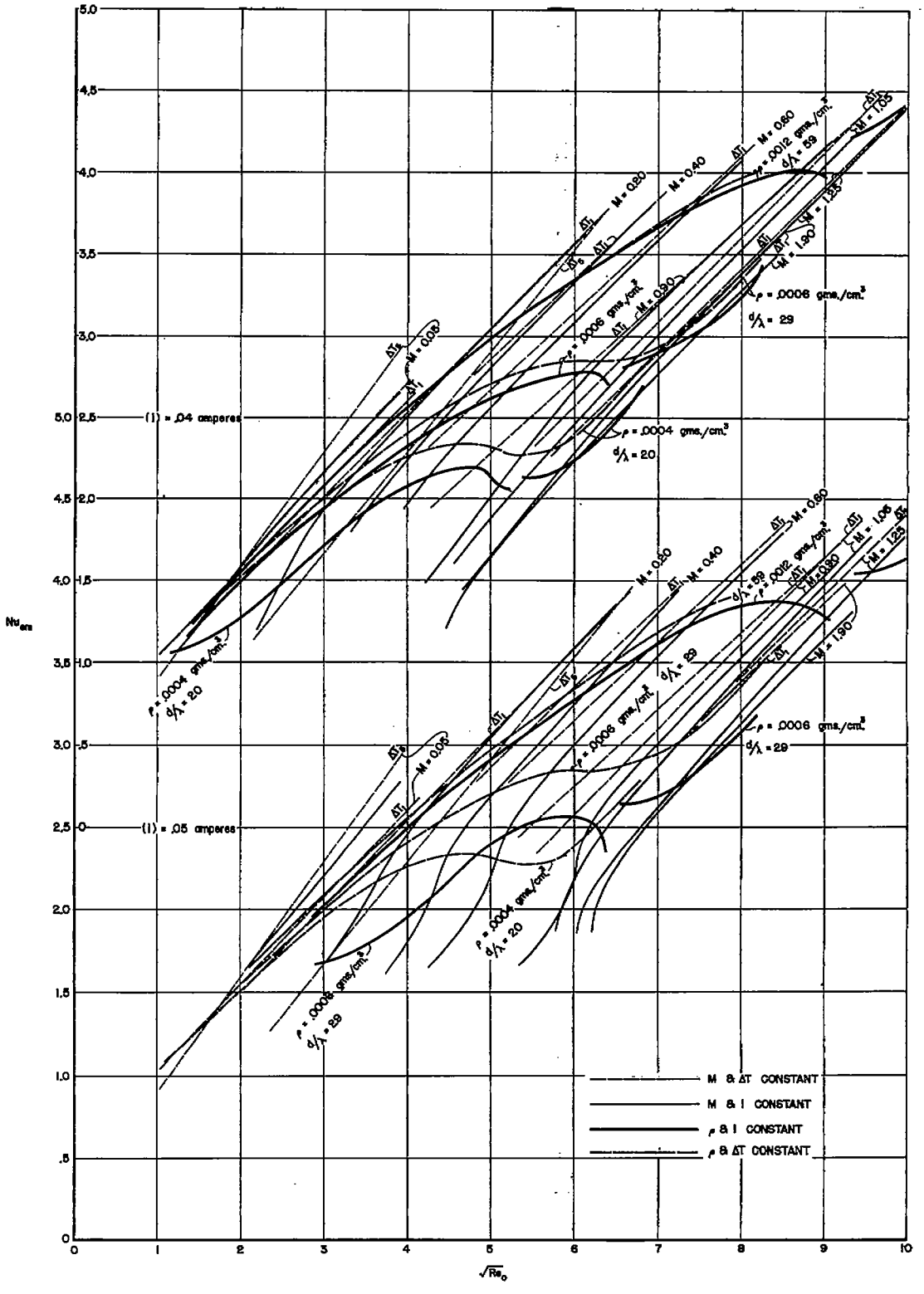

Figure 25.- Comparison of hot-wire calibrations with Reynolds number variable under selected conditions of constant Mach number, density, temperature loading, and current. 0.00015-inch-diameter platinum wire containing 10 percent rhodium. $\Delta T_1 = 66.8^\circ$ C; $\Delta T_5 = 664^\circ$ C.

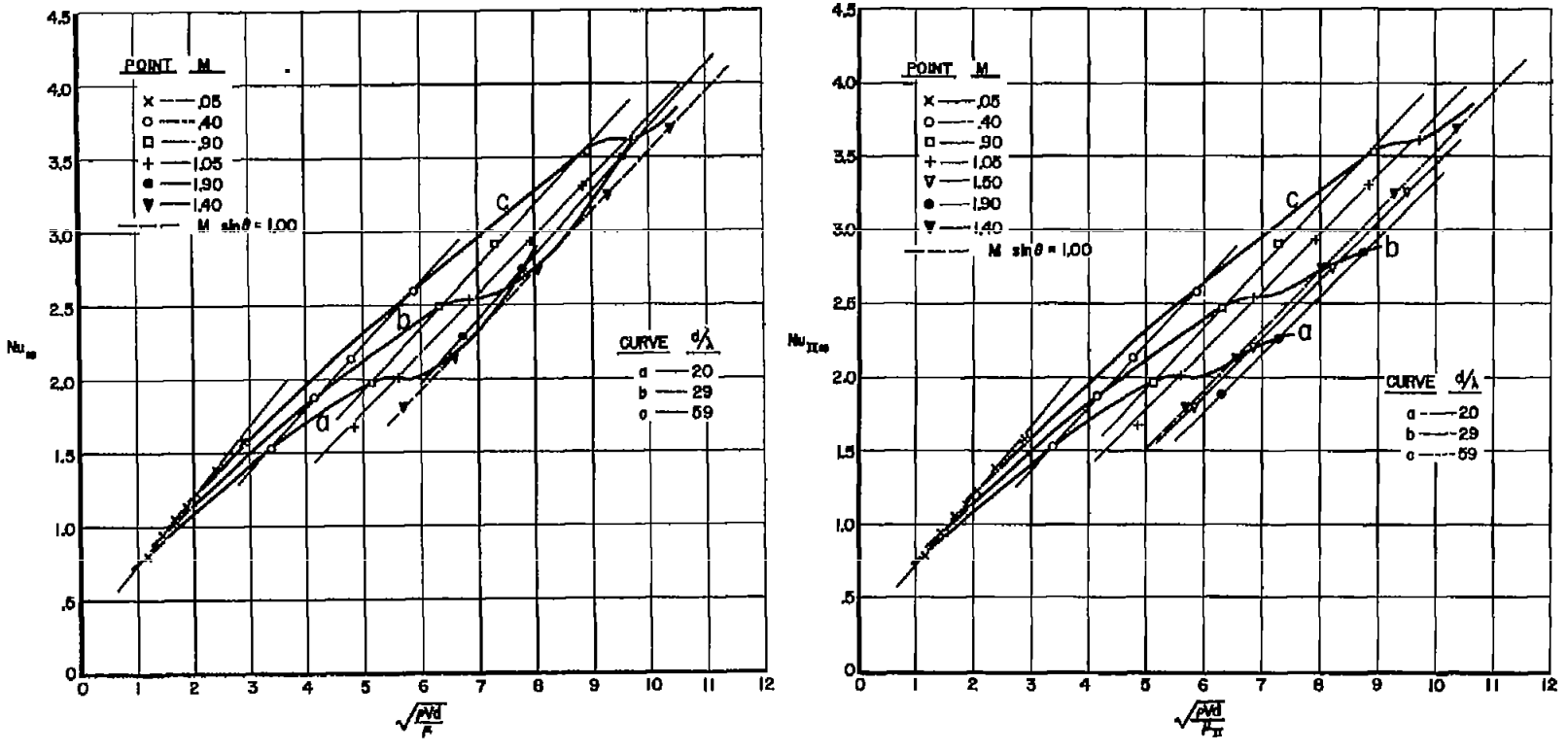

(a) All data computed at theoretical free-stream temperature.

(b) Subsonic data computed at theoretical free-stream temperature; supersonic data computed at theoretical temperature behind normal shock.

Figure 26.- Dependence of Nusselt number on Reynolds number for a swept wire with air conductivity and viscosity evaluated at assumed ambient conditions as indicated. 0.00015-inch-diameter platinum wire containing 10 percent rhodium; $\theta = 45.5^\circ$.

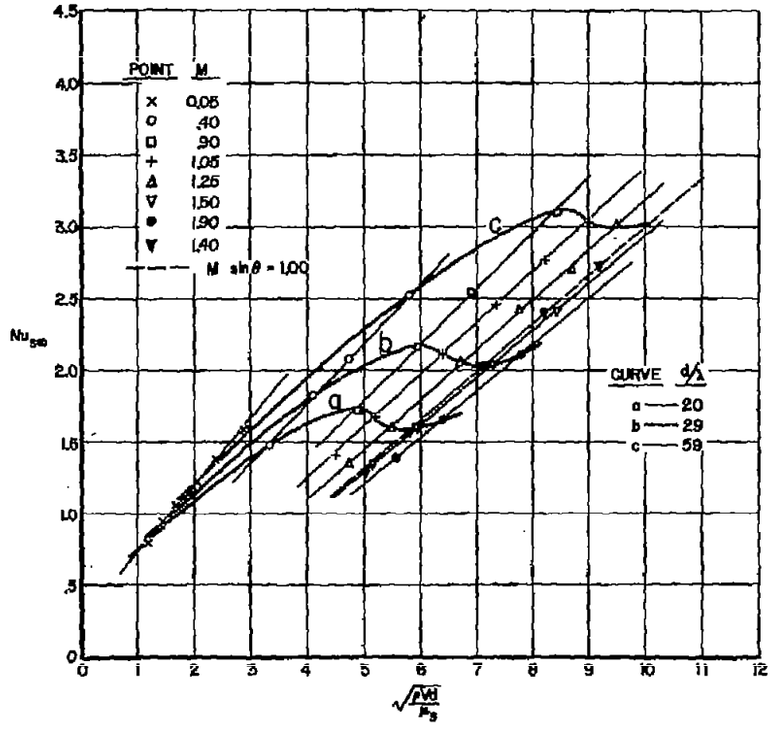

(c) All data computed at stagnation temperature.

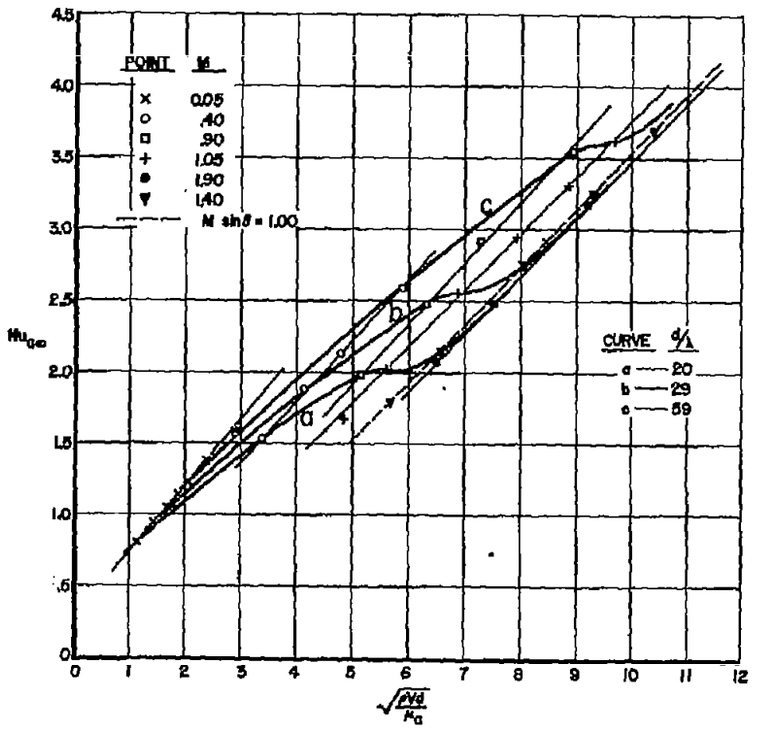

(d) Subsonic data computed at theoretical free-stream temperature; supersonic data computed at mean between theoretical free-stream temperature and temperature behind normal shock.

Figure 26.- Concluded.

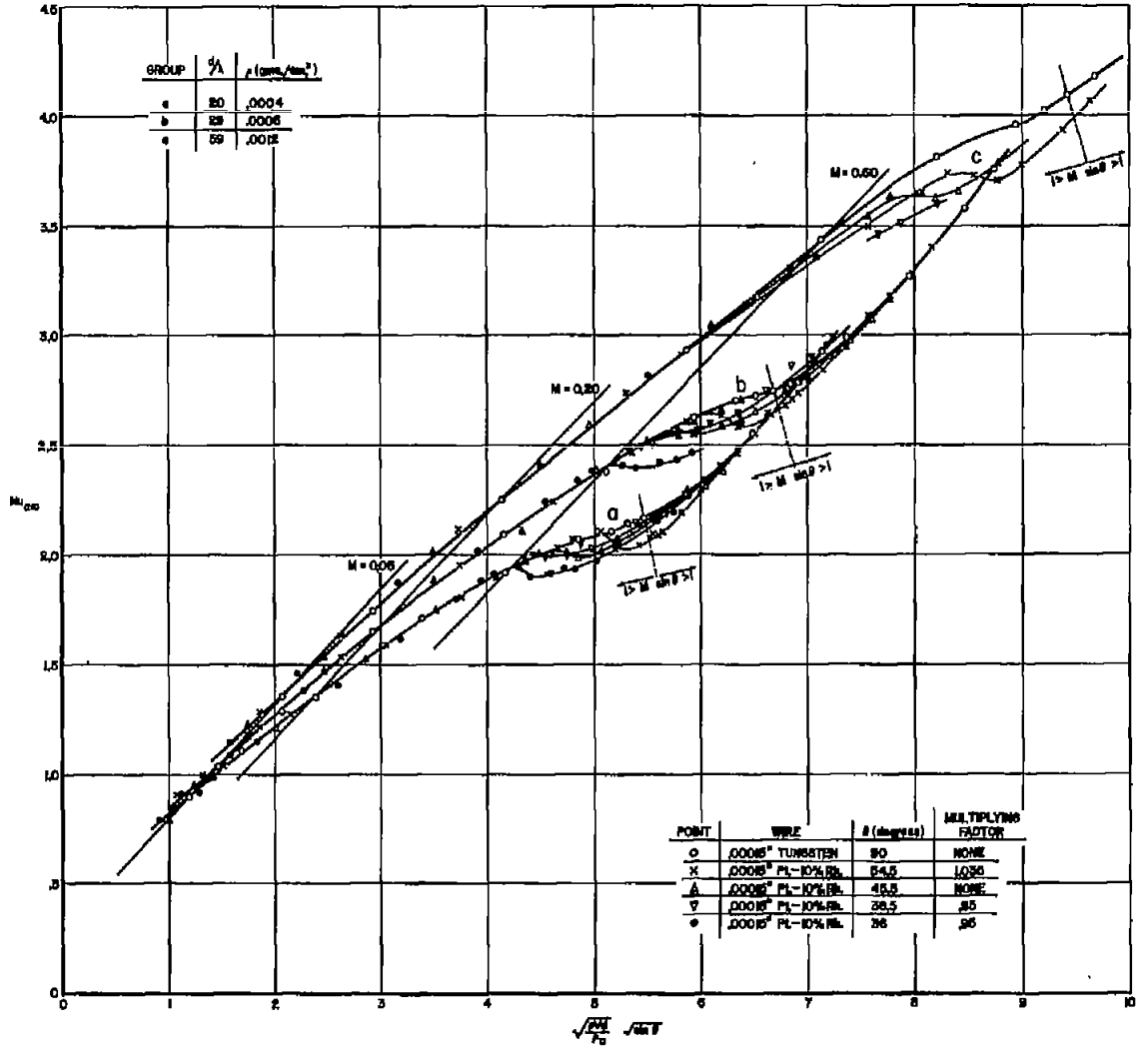

Figure 27.- Comparison of Nusselt numbers of several swept wires with Nusselt number of a normal wire at selected Mach numbers and densities.

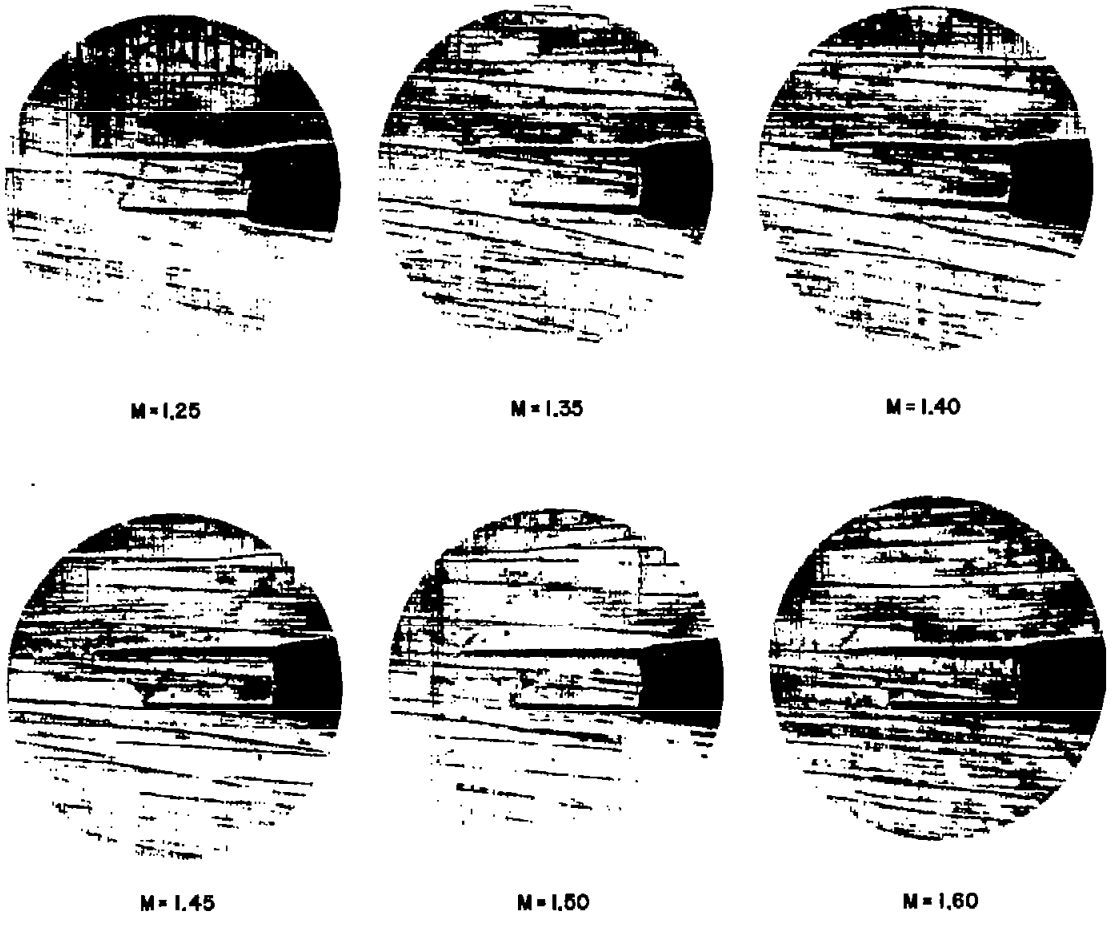

L-87570

Figure 28.- Schlieren photographs of swept wire in several supersonic flows. 0.00015-inch-diameter platinum wire containing 10 percent rhodium, ρ = 0.0006 gram per cubic centimeter, θ = 45.5°, and $1/\sin\theta$ = 1.4.

NACA-Langley - 5-13-55 - 1000